UNIVERSIDADE FEDERAL DE ALAGOAS – UFAL

INSTITUTO DE CIÊNCIAS BIOLÓGICAS E DA SAÚDE – ICBS

PROGRAMA DE PÓS-GRADUAÇÃO EM CIÊNCIAS DA SAÚDE – PPGCS

CARMELITA BASTOS MENDES

EXPRESSÃO DIFERENCIAL DE AQUAPORINAS 1 E 4 EM GLIOMAS HUMANOS E HORMÔNIOS TIREOIDEANOS COMO SEUS POSSÍVEIS CORREGULADORES: UMA ABORDAGEM DE BIOINFORMÁTICA.

MACEIÓ

2022

CARMELITA BASTOS MENDES

EXPRESSÃO DIFERENCIAL DE AQUAPORINAS 1 E 4 EM GLIOMAS HUMANOS E HORMÔNIOS TIREOIDEANOS COMO SEUS POSSÍVEIS CORREGULADORES: UMA ABORDAGEM DE BIOINFORMÁTICA

Dissertação de Mestrado apresentada ao Programa de Pós-Graduação em Ciências da Saúde da Universidade Federal de Alagoas para obtenção do título de Mestre em Ciências da Saúde.

Orientadora: Prof.ª Dr.ª Adriana Ximenes da Silva

MACEIÓ

2022

Catalogação na Fonte
Universidade Federal de Alagoas
Biblioteca Central
Divisão de Tratamento Técnico
Bibliotecário: Marcelino de Carvalho Freitas Neto – CRB-4 – 1767

M538e Mendes, Carmelita Bastos.
Expressão diferencial de aquaporinas 1 e 4 em gliomas humanos e hormônios tireoideanos com seus possíveis correguladores : uma abordagem de bioinformática / Carmelita Bastos Mendes. – 2022.
106 f. : il.

Orientadora: Adriana Ximenes da Silva.
Dissertação (mestrado em ciências da saúde) – Universidade Federal de Alagoas. Instituto de Ciências Biológicas e da Saúde. Programa de Pós-Graduação em Ciências da Saúde. Maceió, 2022.

Bibliografia: f. 66-74.
Apêndices: f. 74-106.

1. Glioma. 2. Aquaporina 1. 3. Aquaporina 4. 4. Biomarcadores. 5. Expressão gênica. 6. Biologia computacional. I. Título.

CDU: 577.175.2/.7

À minha mãe, Olga, por ser quem é e, assim sendo, não ter desistido de acreditar em mim e de quem eu sou.

DEDICO

AGRADECIMENTOS

À força que tudo criou, pelo dom da vida.

À minha mãe, Olga, por tudo: por ser quem é, por ter sempre me acolhido, pelo carinho e dedicação incondicionais a mim dedicados. Não existe folha de agradecimento que dê conta de agradecê-la. Nós duas sempre!

Ao meu tio Tiago e à minha tia Genilma; ao meu primo e às minhas primas, Tiago Filho, Gabriele e Graziele, pela torcida, apoio e por tornarem meus dias ruins mais leves desde sempre. Estarei sempre aqui para o que der e vier!

À minha tia Ana Bastos pela torcida fiel (sempre), pelos livros e por me apoiar tanto em todos os momentos.

Ao meu primo e às minhas primas Paulo Júnior, Cecília Ataíde, Anália Costa (minha comadre) por todo amor e companheirismo.

Ao meu tio e à minha tia Paulo Costa e Meire Gonçalves pelo incentivo e torcida. Ainda, agradeço ao meu afilhado Emmanuel por ser uma estrelinha muito especial em nossas vidas.

Ao meu irmão Matheus, à minha cunhada Beatriz e à minha sobrinha Marina (minha eterna orientadora particular), pelas caronas, alegrias e momentos de leveza. Eu amo vocês.

De forma especial, quero agradecer ao meu amiguinho de quase todas as tardes (sobrinho do coração) e à sua fiel escudeira, Humberto Neto e Silvinha Fradique. Novamente, agradeço à minha Marina, minha sobrinha. Vocês me convencem todos os dias, através da delicadeza inocente e da alegria, de que a vida vale a pena. Espero ajudá-los algum dia tanto quanto vocês me ajudam agora. Assim como o poeta, eu também fico com a pureza da resposta das crianças!

Ao Cristhian, meu parceiro, pelo incentivo e torcida sincera.

Às psicólogas Lúcia Cerqueira Bastos e Eliane Ferreira, pela disponibilidade e carinho. Sem vocês, eu não teria chegado tão longe na pós-graduação.

Ao Dr. Gustavo Omena, pela delicadeza e humanidade em suas condutas para comigo. Que sua postura sirva de exemplo para uma formação mais humana e resolutiva das futuras gerações médicas.

Aos meus avós maternos, Carmelita Bastos e Paulo Bastos (*in memoriam*), pela torcida verdadeira e preocupação de sempre. Eu tenho plena consciência de que onde quer que o meu avô esteja agora, ele está, de alguma forma, torcendo por mim.

À Renata Barbosa, professora de inglês incrível e que esteve comigo desde antes da seleção para a pós-graduação. Não tenho palavras para agradecê-la. Seu amor pelo conhecimento é inspirador!

À minha orientadora Professora Adriana Ximenes da Silva, por ter me acolhido em sua equipe, pela confiança e por ter me dado tantas oportunidades ao longo de minha permanência no laboratório. Foram quase sete anos de convivência intensa e, sem dúvida, de muito aprendizado. Muito obrigada e conte sempre comigo!

Aos Professores Emiliano Barreto e Carlos Fraga e à Professora Mykaella Andrade de Araújo, desde já, por terem aceitado o convite e por todas as sugestões, correções e atenção dispensadas a este trabalho.

Aos amigos que fiz no Laboratório de Eletrofisiologia e Metabolismo Cerebral (LEMC) e que foram essenciais nessa jornada da pós-graduação: Lanni Sarmento, Jaqueline, Rodrigo, Giselma Alcântara, Maísa de Araújo, Lucas Chagas e Cibelle Bastos, muito obrigada! Nossos momentos de confraternização ficaram na memória. Contem comigo e vamos em frente!

Ao meu amigo, Dr. José Clementino Neto pela torcida de sempre.

De maneira especial, gostaria de agradecer à Lanni Sarmento. Nos demos bem desde o início e seu apoio sincero, principalmente no mestrado (durante uma pandemia), foi muito importante para que eu chegasse até aqui. Você tem em mim uma amiga.

À Coordenação de Aperfeiçoamento de Pessoal de Nível Superior (CAPES) pela concessão da bolsa de mestrado durante os dois anos de trabalho.

Muito obrigada!

“Poucas tragédias podem ser maiores que a atrofia da vida, poucas injustiças mais profundas do que ser privado de batalhar ou até de ter esperanças, por um limite imposto de fora, falsamente identificado como interno.”

Stephen Jay Gould,

A falsa medida do homem

LISTA DE FIGURAS

LISTA DE GRÁFICOS

LISTA DE TABELAS

LISTA DE ABREVIATURAS E SIGLAS

AQP1 – Aquaporina 1

AQP4 – Aquaporina 4

AQPs - Aquaporinas

BHE – Barreira Hematoencefálica

D2 – Desiodase do tipo 2

D3 – Desiodase do tipo 3

DA – Doença de Azheimer

DNA – Ácido desoxirribonucleico

FDA – Food and Drug Administration

GBM - Glioblastoma

GFAP – *Glial fibrillary acidic protein*

HGG – *High grade-glioma*

HTs – Hormônios da tireoide

INCA – Instituto Nacional do Câncer

LGG – *Low grade-glioma*

MEC – Matriz extracelular

MHC – Complexo principal de histocompatibilidade

MRI – Imagem por ressonância magnética

OAPs – Arranjos ortogonais de partículas

OMS – Organização Mundial de Saúde

PET – Tomografia por emissão de pósitrons

RNA-seq – Sequenciamento de RNA

SNC – Sistema Nervoso Central

SNP – Sistema Nervoso Periférico

T3 – Triiodotironina

T4 - Tiroxina

TMZ - Temozolamida

VEGF - Fator de crescimento endotelial vascular

SUMÁRIO

RESUMO

Em 2016, a Organização Mundial da Saúde (OMS) incluiu marcadores moleculares (expressão genotípica) como importantes fatores preditivos para o diagnóstico de tumores cerebrais. No cérebro, a expressão e localização de transportadores de água, aquaporinas (AQPs), está substancialmente modificada em gliomas durante os processos de tumorigênese, migração celular, formação e resolução do edema cerebral. Dessa forma, hipotetizamos que as alterações moleculares associadas às *AQP1* e *AQP4* cerebrais podem ser potenciais alvos terapêuticos no câncer. Nosso grupo de pesquisa, por exemplo, já demonstrou uma ação moduladora da triiodotironina (T3), forma biologicamente ativa do hormônio tireoidiano, sobre a expressão da AQP4 durante o desenvolvimento do sistema nervoso central e sobre as células humanas de glioblastoma multiforme. Para testar esta hipótese, realizamos uma análise bioinformática a partir de dados gênicos públicos e disponíveis para download. Neste caso, analisamos os dados de *RNA-seq* como estratégia experimental e identificamos a expressão diferencial dos transcritos de *AQP1* e *AQP4* em tecidos de gliomas comparando-os com seus níveis em tecidos cerebrais saudáveis. Como esperado, os genes das AQPs estavam superexpressos em pacientes com glioma. Entre os subtipos moleculares dos gliomas, *AQP1* e *AQP4* estavam superexpressos em astrocitoma (glioma de baixo grau) e no subtipo clássico (glioma de alto grau). A análise de sobrevida global demonstrou que ambos os genes das AQPs podem ser usados como fator prognóstico para pacientes com glioma de baixo grau, confirmando os resultados de estudos anteriores e reforçando seus valores clínicos. Também observamos graus de correlação entre a expressão de genes envolvidos nas vias da tirosina e dos hormônios tireoidianos e as AQPs em questão. A saber: *PNMT, ALDH1A3, AOC2, HGDATP1B1, ADCY5, PLCB4, ITPR1, ATP1A3, LRP2, HDAC1, MED24, MTOR e ACTB1* (coeficiente de Spearman = ≥ 0,20 e p = ≤ 0,05). Essas vias moleculares e os genes *AQP1* e *AQP4* podem ser usados para estudar novas drogas antitumorais, além de ser úteis no diagnóstico molecular neste tipo de tumor, pois apresentam potencial como biomarcadores diagnósticos e terapêuticos em gliomas malignos.

Palavras-chave: glioma, AQP1, AQP4, biomarcador, expressão gênica, correlação, bioinformática

ABSTRACT

In 2016 the World Health Organization (WHO) included molecular markers (genotypic expression) as important predictive factors for diagnostic of brain tumors. In the brain, the expression and localization of water channel transporters, aquaporins (AQPs), are substantially modified in gliomas during tumorigenesis, cell migration, edema formation and resolution. Therefore, we hypothesized that molecular changes associated with AQP1 and AQP4 in the brain may be potential anticancer therapeutic targets. Our research group, for instance, has already shown a modulating action of triiodothyronine (T3), the biologically active form of thyroid hormone, on the AQP4 expression in the developing nervous system and on GBM cells. To test it, a bioinformatic analysis from publicly available data from international consortia was carried out. Here, we used RNA-seq as an experimental strategy and identified the differential expression of AQP1 and AQP4 transcripts numbers in gliomas tissue if compared to normal brain tissues. Indeed, the AQPs genes were overexpressed in glioma patients. Among gliomas subtypes, *AQP1* and *AQP4* were overexpressed in astrocytoma (low grade-glioma) and classical (high grade-glioma). The overall survival analysis demonstrated ~~us~~ both AQP genes can be used as a prognostic factor for patients with low grade-glioma, confirming the results of previous studies and reinforcing their clinical value. We also observed a correlation between the expression of genes involved in tyrosine and thyroid hormone pathways and AQPs. Namely: *PNMT, ALDH1A3, AOC2*, *HGDATP1B1, ADCY5, PLCB4, ITPR1, ATP1A3*, *LRP2*, *HDAC1, MED24, MTOR* and *ACTB1* (Spearman's coefficient = ≥ 0.20 and p-value = ≤ 0.05). These molecular pathways and AQP1 and AQP4 genes may be used to study new anti-tumor drugs and the molecular diagnosis of gliomas because showing potential as diagnostic and therapeutic biomarkers for malignant gliomas.

Keywords: glioma, AQP1, AQP4, biomarker, gene expression, correlation analysis, bioinformatics

1. INTRODUÇÃO

Tumores com origem sistema nervoso central (SNC) estão entre os 20 mais incidentes no mundo com, aproximadamente, 308.102 casos notificados nos últimos dois anos (FERLAY et al., 2021). Taxas relacionadas à mortalidade também preocupam com números de mortes iguais a 2,8 casos/100.00 habitantes (SUNG et al., 2021).

A Classificação de Tumores do Sistema Nervoso Central mais recente da Organização Mundial de Saúde (OMS) determina que os tumores cerebrais não devem ser diagnosticados apenas com base em seus fenótipos histológicos, mas também a partir de marcadores moleculares (classificações genotípicas) (LOUIS et al., 2016, MARTINEZ-LAGE; SAHM, 2018) a fim de evitar diagnósticos imprecisos, no sentido de aumentar as opções e a precisão do tratamento para os pacientes acometidos por esse tipo de câncer.

Apesar dos avanços nas variedades terapêuticas, o tripé composto por ressecção tumoral associada às quimioterapias e radioterapia, garante uma taxa de sobrevida de apenas 12-15 meses a partir do diagnóstico inicial e uma taxa de sobrevida relativa de 3-5% em 5 anos (FEDELE et al., 2019).

Um fator comum a tumores cerebrais é a formação de edema cerebral vasogênico e a modificação do padrão de expressão de várias moléculas que levam a alterações de junções comunicantes, resultando em danos a barreira hematoencefálica (BHE), resultando em redução significativa da qualidade de vida do paciente (SOLAR et al., 2022).

Aquaporinas (AQPs) são uma família de proteínas transmembranas de canais transportadores de água que desempenham um papel crucial na resposta às mudanças no ambiente osmótico (SAADOUN et al., 2002).

As AQP1 e AQP4 são consideradas os principais canais de água do SNC e têm um papel primordial na manutenção da homeostase hídrica e da integridade da BHE. Em virtude de seu local de expressão - processos perivasculares de células astrocitárias - a AQP4, por exemplo, é reconhecida por proporcionar um sistema bastante eficiente para o transporte de água entre o espaço perivascular e as células

gliais, além de ser considerada responsável pelo *clearence* do parênquima cerebral através do chamado sistema glinfático (MESTRE et al., 2018, SMITH et al., 2017).

A AQP4 também tem seu padrão de expressão aumentado em tumores gliais e participa de alguns processos da gênese do tumor, tais como migração celular e invasão, o que resulta em diversos mecanismos diretamente ligados aos diferentes graus de malignidade do tumor e mau prognóstico (LAN et al., 2017). A saber: formação de edema na região peritumoral, aumento da pressão intracraniana e episódios convulsivos (DUBOIS et al., 2014, MAUGERI et al., 2016).

Um inibidor de proteínas quinases ativadas por mitógeno p38 (p38-MAPK) regulou negativamente a expressão das AQP1 e AQP4 em roedores anteriormente submetidos à intoxicação por monóxido de carbono. Esta inibição resultou na facilitação do efluxo do edema cerebral formado (LI et al., 2019). Ainda, a forma biologicamente ativa do hormônio da tireoide, a triiodotironina (T3), teve sua ação sobre a expressão da AQP4 em células oriundas de glioblastoma humano e sobre o desenvolvimento do SNC de camundongos avaliada: em ambos os casos, o T3 foi capaz de modular o padrão de expressa desta proteína.

As AQPs foram validadas como importantes alvos para ação terapêutica, mas ainda não há um único medicamento que tenha sido aprovado com sucesso nas fases clínicas dos testes (HUANG et al., 2021) e a busca por um regulador em potencial (inibidor ou agonista) para este processo continua válida.

No âmbito de algumas patologias, especialmente àquelas que têm alterações genéticas como base, como os gliomas, por exemplo, algumas condições podem ser inferidas a partir de estudos de dados genômicos e análise de redes gênicas (YANG et al., 2014). Diversas análises *in silico*, a exemplo da simulação de dinâmica molecular, expressão diferencial e análise mutacional, podem determinar os fatores que afetam a progressão do tumor, como o padrão de expressão de um gene e sua proteína. O desenvolvimento de uma terapia em potencial a partir destes achados, pode proporcionar a identificação de fatores preditivos que tornem possível os diagnóstico e tratamento precoces desse tipo de patologia (KAMARAI; PUROHIT, 2014, WANG et al., 2019).

2. REVISÃO BIBLIOGRÁFICA

2.1 Células gliais e tumores gliais

O sistema nervoso dos mamíferos é constituído, basicamente, por células neuronais e não-neuronais (JÄKEL; DIMOU, 2017). Dentre as últimas citadas, as células gliais são consideradas emergentes em importância terapêutica e diagnóstica desde o reconhecimento de seu papel para além do suporte neuronal (ASSINCK et al., 2017, GOMES et al., 2013). Até o momento, quatro linhagens diferentes de células da glia foram identificadas: astrócitos, oligodendrócitos, células ependimárias e a micróglia; diferindo-se em função e distribuição ao longo do sistema nervoso central (SNC) e sistema nervoso periférico (SNP) (KOVACS, 2018).

Tendo sua descoberta atribuída a Rudolf Virchow, Santiago Ramón y Cajal e Pío del Río-Hortega, em meados de 1800 (JÄKEL; DIMOU, 2017), essa linhagem celular vem ganhando notoriedade por sua participação direta na homeostasia cerebral; desde a manutenção da integridade da barreira hematoencefálica (BHE), secreção de fatores tróficos e migração neuronal, à recaptação e metabolismo do neurotransmissores para controle da neuroexcitabilidade (excitotoxidade) e reutilização deste para as células neuronais (PEKNY el al., 2016, PELLERIN et al., 1998, HUANG et al., 2020, MASON, 2017).

Os astrócitos, as células mais abundantes do SNC e, também, a classe de maior interesse neste trabalho, têm papel crucial nas funções mantenedoras da fisiologia desse sistema citadas anteriormente; especialmente as que estão diretamente relacionadas à integridade da medula espinal e do encéfalo (VOSKUHL et al.,2009)

Um estudo *in vivo* conduzido por TOGNATTA et al (2020), evidenciou que astrócitos presentes na medula espinal são cruciais para a viabilidade de oligodendrócitos maduros e do processo de mielinização durante o os primeiros sete dias de vida de roedores, bem como na idade adulta destes animais.

Estudos das últimas duas décadas têm destacado um processo unicamente desencadeado por células astrocitárias reativas conhecido como gliose reativa ou astrogliose (WURM et al., 2019, MOULSON et al., 2021) Esse processo é caracterizado por uma mudança na morfologia e metabolismo dessas células (Figura

1), tornando-as reativas em função da instalação e consequente reconhecimento de um acometimento patológico sobre o SNC, a exemplo de traumatismos, acidente vascular cerebral (AVC) e tumores (PEKNY; PEKNA, 2014; WURM et al., 2019).

O papel primordial da astrogliose é contribuir para a neuroproteção através de alguns processos já bem elucidados. Como, por exemplo, a alteração do seu perfil transcricional quando comparado com astrócitos normais, como as proteínas do complexo principal de histocompatibilidade (MHC classe II) apresentadoras de antígeno interagindo com células T auxiliares e desencadeando um processo de inflamação local. (MOULSON et al., 2021**;** O'BRIEN; HOWARTH; SIBSON, 2013).

Figura 1- Representação esquemática do processo de astrogliose

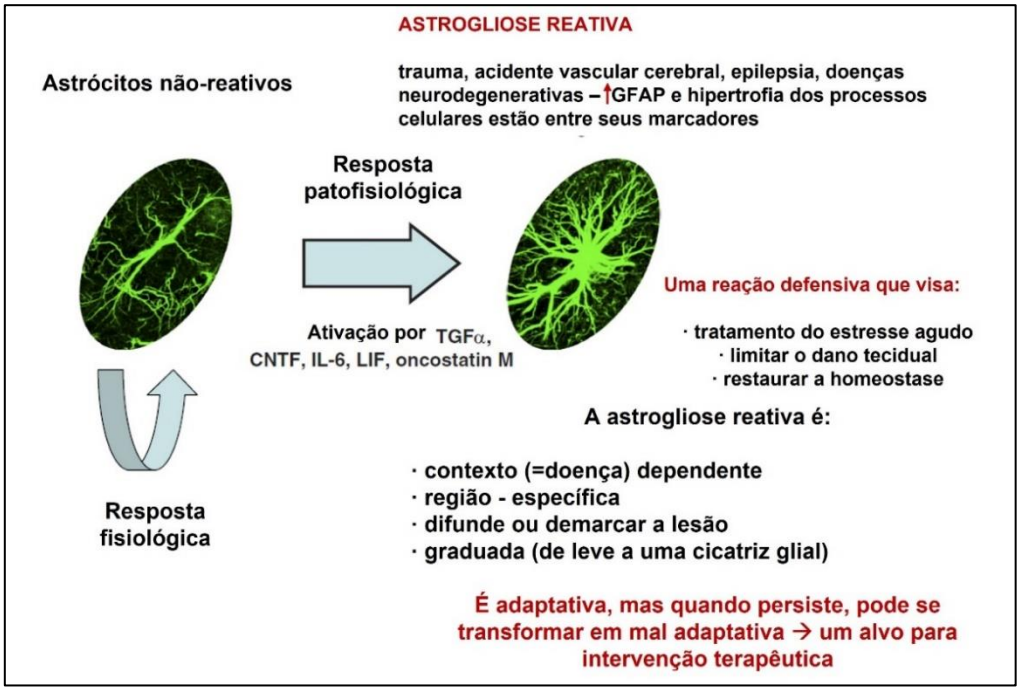

Fonte: Adaptado de PEKNY; PEKNA, 2014.

Experimentos *ex vivo* a partir de modelos murinos da doença de Alzheimer (DA), nos quais os astrócitos reativos sofreram ablação, resultaram em acentuação do déficit de memória, diminuição de marcadores sinápticos e aumento de citocinas pró-inflamatórias (neuroinflamação) (KATSOURI et al., 2020). Fortalecendo, dessa forma, o argumento de que os astrócitos desempenham papeis de neuroproteção e de promoção da plasticidade sináptica, fatores de extrema importância para a homeostasia de células nervosas (DAVIS et al., 2021).

Por outro lado, experimentos com animais e humanos têm demonstrado uma função dúbia relacionada aos astrócitos reativos: células astrocitárias também exercem importantes funções na etiologia e progressão de alguns tumores cerebrais a exemplo dos gliomas e meduloblastomas (CHENG et al., 2020).

Astrócitos próximos à massa tumoral (não necessariamente derivados do tumor) podem estar envolvidos na repressão da função imunológica antitumoral, bem como na secreção de fatores pró-oncogênicos (O'BRIEN; HOWARTH; SIBSON, 2013, WURM et al., 2019).

Os gliomas, um dos objetos de estudo do presente trabalho, são neoplasias malignas de origem celular glial e os tipos mais frequentes de tumores do SNC (LOUIS et al., 2016), representando aproximadamente 80% de todos os tumores malignos intracranianos (OSTROM et al., 2014).

Estes tumores estão subdivididos em astrocitoma, ependimoma, oligodendroglioma, oligoastrocitoma e glioblastoma (GBM), sendo este último seu tipo mais agressivo e letal. Fatores tais como sua localização, irregularidade de borda e capacidade infiltrativa os tornam quase sempre inoperáveis e de difícil manejo clínico, diminuindo drasticamente a qualidade de vida e as chances de sobrevivência dos pacientes (SINGH et al., 2021).

2.1.1 Epidemiologia atual no Brasil e no mundo

Na última década, têm-se observado um aumento significativo do número de casos de câncer diagnosticados em todo o mundo: 19.292.789 novos casos em 2020 (FERLAY et al., 2020). O continente asiático compreende quase metade (48,4%) da totalidade de casos. A Europa, por sua vez, comporta 23,4%, seguida da América do Norte com 13,2%, América Latina e Caribe (7,8%) e África (5,8%).

A Agência Internacional para a Pesquisa sobre Câncer, órgão/entidade que responde à Organização Mundial de Saúde (OMS), expõe que países como a China, Estados Unidos da América, Índia, Japão, Alemanha, Brasil, Federação Russa, França, Reino Unido e Itália ocupam os dez primeiros lugares no ranking das maiores incidências da doença no mundo (SUNG et al., 2020; FERLAY et al., 2021).

Tumores relacionados ao encéfalo e, ao SNC como um todo, estão entre os 20 mais incidentes no planeta terra. Aproximadamente 308.102 casos foram notificados

nos últimos dois anos (FERLAY et al., 2021). Dados relacionados à mortalidade também indicam que esses tumores ocupam posição de destaque - 12ª posição dentre os 36 tipos de tumores observados -, com taxa de mortalidade igual a 2,8 casos/100.00 habitantes (SUNG et al., 2021).

Dados epidemiológicos dos últimos 9 anos também revelaram uma tendência crescente no número total de casos de neoplasias malignas e de tumores do encéfalo em todo o território brasileiro (Gráfico 1).

Gráfico 1 – Tendência de ocorrência do número de casos de neoplasias malignas gerais e do encéfalo no Brasil entres os anos de 2013 e 2021.

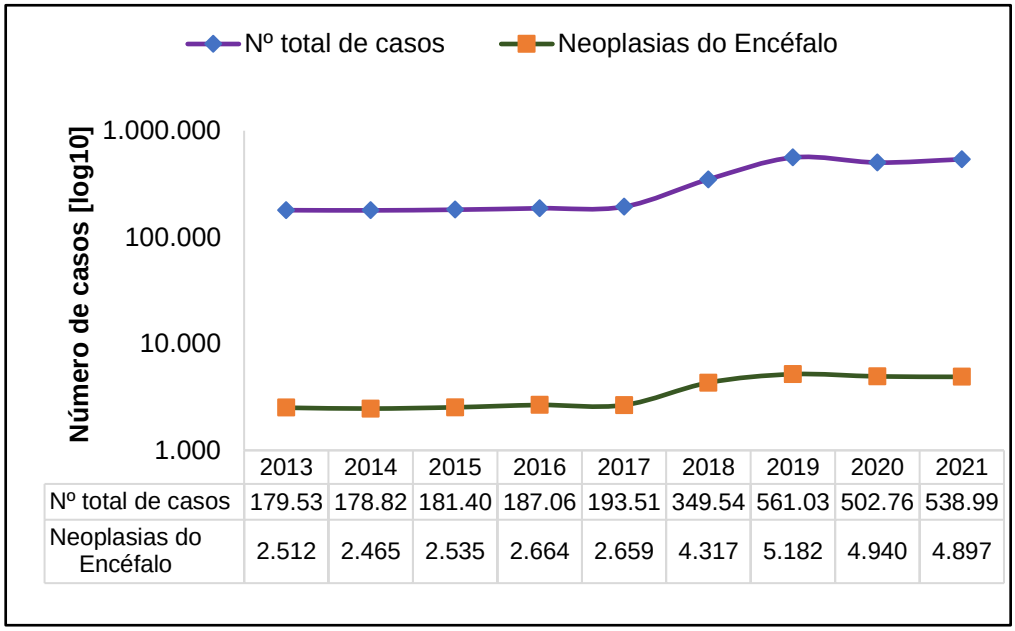

	2013	2014	2015	2016	2017	2018	2019	2020	2021
Nº total de casos	179.53	178.82	181.40	187.06	193.51	349.54	561.03	502.76	538.99
Neoplasias do Encéfalo	2.512	2.465	2.535	2.664	2.659	4.317	5.182	4.940	4.897

Nota: Cada losango azul (linha roxa) e quadrado coral (linha verde) representa o número total de casos de câncer ou de diagnóstico específico para neoplasias do encéfalo segundo ano de diagnóstico entre 2013 e 2021. Não há dados disponíveis para os anos anteriores a 2013. Fonte: Elaborado pela própria autora. Brasil, Ministério da Saúde. Banco de dados do Sistema Único de Saúde-DATASUS. Disponível em http://www.datasus.gov.br [Acesso em 13 de junho de 2022].

No que diz respeito à distribuição dos números totais dos casos de câncer e dos casos somente relacionados ao SNC dentre as regiões do Brasil, as Tabelas 1 e 2 mostram o valor percentual da última década para cada região, respectivamente. Em ambas as análises, as regiões Sul, Sudeste e Nordeste ocupam os três primeiros lugares em diagnóstico.

O Instituto Nacional do Câncer (INCA) estima, para o Brasil, um total de 11.090 novos casos de tumores cerebrais para cada ano do triênio de 2020 – 2022. Segundo essa estimativa, pouco mais de 50% destes casos estão e estarão relacionados a indivíduos do sexo masculino. Em valores de risco correspondentes, estes números representam um risco de 5,61 casos novos a cada 100 mil homens e de 4,85 casos novos a cada 100 mil mulheres (INCA, 2019).

Tabela 1 - Distribuição percentual do número total de casos de neoplasias malignas segundo região do Brasil (2013 – 2022)

Região	Número de casos	(%)
Norte	88.075	3,86
Nordeste	534.991	23,40
Sudeste	1.002.495	43,83
Sul	513.432	22,46
Centro-oeste	147.797	6,47
Total	**2.286.790**	**100**

Fonte: Brasil, Ministério da Saúde. Banco de dados do Sistema Único de Saúde-DATASUS. Disponível em http://www.datasus.gov.br [Acesso em 13 de junho de 2022]. Sistema de Informação Ambulatorial (SIA), através do Boletim de Produção Ambulatorial Individualizado (BPA-I) e da Autorização de Procedimento de Alta Complexidade; Sistema de Informação Hospitalar (SIH); Sistema de Informações de Câncer (SISCAN). Data de atualização dos dados: 23/05/2022.

Tabela 2 - Distribuição percentual do número total de casos de neoplasias malignas no encéfalo segundo região do Brasil (2013 - 2022)

Região	Número de casos	(%)
Norte	1.579	4,83
Nordeste	6.298	19,28
Sudeste	13.705	41,93
Sul	7.937	24,29
Centro-oeste	3.162	9,68

Total	**32.681**	**100**

Fonte: Brasil, Ministério da Saúde. Banco de dados do Sistema Único de Saúde-DATASUS. Disponível em http://www.datasus.gov.br [Acesso em 13 de junho de 2022]. Sistema de Informação Ambulatorial (SIA), através do Boletim de Produção Ambulatorial Individualizado (BPA-I) e da Autorização de Procedimento de Alta Complexidade; Sistema de Informação Hospitalar (SIH); Sistema de Informações de Câncer (SISCAN). Data de atualização dos dados: 23/05/2022.

Ainda segundo o INCA, alterações adquiridas ao longo do tempo por predisposição genética ou por exposição aos fatores de risco, são as principais responsáveis pelo desenvolvimento de neoplasias malignas relacionadas ao sistema nervoso. Fatores tais como exposição prévia à radiação ionizante, deficiência do sistema imunológico, exposições ambientais (arsênio, chumbo e mercúrio), exposições ocupacionais (a exemplo de trabalhadores da indústria petroquímica, de borracha, plástico e gráfica) e obesidade, são listados como riscos para o desenvolvimento desses tipos de tumores (INCA, 2019).

2.1.2 Abordagem terapêutica atual para pacientes com gliomas

A partir do ano 2007, a OMS passou a classificar os tumores de origem glial em gliomas de baixo grau (graus I e II) e gliomas de alto grau (graus III e IV) (LOUIS et al., 2007). Até 2016, estes eram categorizados e classificados segundo grau de agressividade com base somente em seus fenótipos histológicos: alta atividade mitótica, atipias nucleares, fragilidade vascular e necrose (LIMA et al., 2012, PERRY; WESSELING, 2016).

Mais recentemente, porém, Classificação de Tumores do Sistema Nervoso Central da OMS, estabeleceu que os tumores cerebrais não devem ser diagnosticados apenas com base em seus fenótipos histológicos, mas também em marcadores moleculares, tais como IDH- 1/2, 1p/19q, MGMT, ATRX, TERT, H3, EGFR, BRAF e Ki67 (LOUIS et al., 2016, MARTINEZ-LAGE; SAHM, 2018, SOLDATELLI et al., 2022) a fim de evitar diagnósticos imprecisos, no sentido de aumentar as opções e a precisão do tratamento para os pacientes acometidos por esse tipo de câncer.

A despeito dos avanços nas variedades terapêuticas, o tripé composto por ressecção tumoral (cirurgia neurológica) associada às quimioterapias e radioterapia,

garante uma taxa de sobrevida de apenas 12-15 meses a partir do diagnóstico inicial e uma taxa de sobrevida relativa de 3-5% em 5 anos (FEDELE et al., 2019).

Da mesma forma, o tratamento quimioterápico padrão ouro para o GBM, a temozolamida (TMZ), um agente alquilante do DNA (WESOLOWSKI; RADJEV; MUKHERJI, 2016), ainda permite uma taxa significativa de recorrência tumoral e confere resistência ao tratamento quando associados às outras drogas (STROBEL et al., 2019) devido à sua baixa especificidade e capacidades limitadas para atravessar a BHE (UMANS; SONTHEIMER, 2018).

Por ter a célula cancerígena uma grande capacidade de invadir tecidos adjacentes ao centro do tumor, o uso de anti-angiogênicos é um comum no tratamento de canceres como forma adjuvante (CARMELIET; JAIN, 2011). Dadas as suas características de alta proliferação endotelial, hiperpermeabilidade e expressão do fator de crescimento pró-angiogênico (VEGF) associadas aos gliomas de alto grau, principalmente, ao GBM, esse tipo de abordagem tornou-se uma opção no tratamento contra esse tipo de tumor. No entanto, sua interferência sobre a distribuição e a eficácia do quimioterápico principal, a TMZ, era desconhecida até então (GERSTNER et al., 2019).

Um ensaio clínico utilizando uma combinação de técnicas de imagens de tomografias por emissão de pósitrons (PET) e de ressonâncias magnéticas (MRI), avaliou as alterações vasculares desencadeadas pelo Bevacizumabe (medicamento de ação antiangiogênica) em pacientes com GBM recorrente e como isso impactou de forma negativa sobre o poder de ação da TMZ (GERSTNER et al., 2019).

Os pacientes do estudo foram submetidos aos exames de imagem em três momentos diferentes: antes da primeira dose com o Bevacizumabe, um dia após a primeira dose e antes da terceira dose (GERSTNER et al., 2019). Os resultados mostraram que dentro de todo o volume do tumor com realce de contraste (marcador de fluxo da TMZ), tanto a captação do quimioterápico padrão quanto a permeabilidade vascular diminuíram após o início da administração do antiangiogênico.

Os autores do estudo destacaram que em sub-regiões tumorais onde a permeabilidade vascular era baixa e a integridade da BHE não estava comprometida,

o aumento da perfusão foi diretamente proporcional ao aumento da captação da temozolomida.

Outro agente quimioterápico, assim como a TMZ também aprovado pela agência reguladora norte-americana *Food and Drug Admnistration* (FDA) entre 2003 e 2005, o comercialmente denominado Gliadel® (ASHBY; SMITH; STEA, 2016), tem sido utilizado de forma secundária no tratamento de pacientes com gliomas. O Gliadel® trata-se de discos copolímeros biodegradáveis impregnados com o agente alquilante do DNA carmustina (1,3-bis(2- cloroetil)-1-nitrosurea) e implantado localmente na massa tumoral, através de neurocirurgia (ASHBY; SMITH; STEA, 2016).

A revisão sistemática conduzida por ASHBY; SMITH; STEA (2016) mostrou que uso combinado e sequencial de Gliadel®, radiação padrão (60y) e TMZ foi benéfico nos casos de pacientes com gliomas recém-diagnosticados e/ou recorrentes: acréscimo de 3 a 4 meses de vida quando comparado com a terapia isolada com qualquer um dos dois quimioterápicos citados. Os eventos adversos mais comumente relatados foram mielossupressão, déficit neurológico e anormalidades de cicatrização.

Um estudo prospectivo conduzido por CHAMPEAUX; WELLER (2020) avaliando os anos 2010 – 2018 na França corrobora os resultados benéficos dessa utilização combinada e sequencial. No entanto, chamam atenção para os riscos aumentados de infecção do sítio de incisão da cirurgia, o que pode resultar na volta do paciente para o centro cirúrgico. Além disso, há também um alto custo financeiro da técnica.

2.2 Hormônios da tireoide e câncer: uma relação terapêutica em potencial?

Ao longo de todo o período de vida de um ser humano os hormônios produzidos e secretados pela glândula tireoide (HTs), o 3,5,3',5'-tetraiodo-L-tironina (T4) e o 3,5,3'-triiodo-L-tironina (T3), forma biologicamente ativa destes hormônios, têm ganhado notoriedade por sua ampla ação sobre diversos sistemas biológicos tanto em contextos fisiológicos como patológicos; a exemplo destes últimos: os distúrbios psiquiátricos, os distúrbios de desenvolvimento e o câncer (SUDAH, et al., 2017).

Sobre o SNC, as ações destes hormônios afetam significativamente a morfologia cerebral através do estímulo de processos de mielinização, proliferação e

diferenciação de células gliais, além do desenvolvimento de conexões sinápticas e ramificações dendrítica e axonal (NAUMAN, 2015; NODA, 2015).

É consenso que há uma estreita relação entre os sistemas endócrino e nervosos (central e periférico) e a biodisponibilidade de T3 para o cérebro em desenvolvimento bem como o adulto, que são dela dependentes. Essa relação é controlada de maneira rigorosa por mecanismos que regulam a secreção de THs, a fração livre não ligada às globulinas de ligação à tiroxina (TBG), as atividades dos transportadores de monocarboxilato (MCTs) e das desiodases, enzimas responsáveis pelo metabolismo e, consequentemente, pela ativação e inativação desses hormônios (HAINFELD et al., 2019).

As células astrocitárias exercem função primordial no metabolismo dos HT's: convertem o T4 sérico em T3, em virtude da atividade da isoforma 3 das desiodases (D3), expressa nessa linhagem celular neural. O que, consequentemente, garante o aporte ideal deste hormônio aos tecidos nervosos (CICATIELLA; GIROLAMO; DENTICE, 2018).

Uma revisão elaborada por TALHADA et al (2019) nos traz que após a fase aguda do acidente vascular cerebral, o tecido cerebral acometido apresenta capacidade, ainda que reduzida, de reparo e recuperação de funções neurológicas. Os HTs foram identificados como moduladores da expressão de diversos genes que podem estimular a neuroplasticidade endógena e, portanto, facilitar o processo reparativo. Demonstrou-se também que eles foram capazes de modular a transcrição de genes de filamentos intermediários, neurofilamentos (Nefh e Nefm), e GFAP em astrócitos maduros.

Um estudo de base populacional (KRASHIN et al., 2022) avaliou a relação dos níveis de TSH e T4 livre com o risco global para o desenvolvimento de câncer, bem como o risco para alguns tipos específicos de câncer: câncer de próstata, melanoma, câncer de tiroide, câncer de cólon, câncer de pulmão e câncer uterino. Pacientes com hipertireoidismo e com menos de 50 anos de idade, apresentaram maiores chances para o desenvolvimento de câncer. De forma contrária, pacientes 50 anos ou mais, apresentaram menor risco para desenvolver a doença. O que pode evidenciar que ação dos HTs e sua influência em condições de doença não está somente relacionada ao estado puramente biológico do indivíduo.

Ainda dentro do campo da oncologia, uma revisão publicada em 2019, reuniu estudos que permitiram aos autores concluírem que condições clínicas relacionadas à superprodução/disponibilidade (hipertiroidismo) ou à produção/ação insuficiente (hipotiroidismo) dos HTs podem ser peças chaves para a eficácia no tratamento e no prognóstico de pacientes oncológicos (LIU; YEH; LIN, 2019)

Segundo LIU; YEH; LIN (2019), o hipotireoidismo clínico, por exemplo, estava associado ao atraso no crescimento/progressão do câncer. No entanto, o hipertireoidismo estava correlacionado com a prevalência de câncer em vários tipos de tumores, incluindo câncer de mama, tireoide, pulmão, cérebro, fígado e colorretal, corroborando os resultados de outros estudos, tais como o estudo de base populacional citado anteriormente.

Como potenciais (cor)reguladores, os HTs parecem apresentar vantagem farmacodinâmica em relação às outras moléculas sintéticas quaisquer: a passagem através da BHE não parece ser um grande problema, visto que há uma produção local destes hormônios no cérebro e que os astrócitos são fundamenteis neste processo.

2.3 Aquaporinas e gliomas humanos: o que sabemos?

É neste contexto de busca contínua por novos alvos e agentes terapêuticos que surgem as aquaporinas (AQPs), uma família de proteínas transmembranas de canais transportadores de água que desempenham um papel crítico na resposta às mudanças no ambiente osmótico (SAADOUN et al., 2002).

Esses canais facilitam principalmente o transporte de água, embora alguns membros desta família proteica possam transportar outras pequenas moléculas, tais como glicerol, ureia, gases e alguns íons (WAN; RAN; JIANG, 2014). No sistema nervoso central, oito membros da família do canal de água são expressos. A saber: AQP1, AQP3, AQP4, AQP5, AQP6, AQP8, AQP9 e AQP11 (MAUGERI et al., 2016, YANG, 2017).

As AQP1 e AQP4 são consideradas os principais canais de água no SNC e têm um papel primordial na manutenção da homeostase hídrica e da integridade da barreira hematoencefálica (BHE). As AQPs são proteínas que têm uma estrutura tetramérica e estão dispostas na membrana celular em arranjos ortogonais de

partículas (OAPs) (Figura 2) (YANG; BROWN; VERKMAN, 1996, NESVERONA; TÖRNROTH-HORSEFIELD, 2019).

Por causa da sua localização nos processos perivasculares de células astrocitárias a AQP4, por exemplo, é reconhecida por fornecer um sistema eficiente para o transporte de água entre o espaço perivascular e as células gliais, além de ser considerada responsável pelo *clearence* do parênquima cerebral através do chamado sistema glinfático (MESTRE et al., 2018, SMITH et al., 2017).

Além disto, um corpo de evidências tem destacado uma ampla participação das AQPs em processos celulares que, à primeira análise, parecem não ter ligação alguma com sua função precípua de transportar moléculas de água entre os ambientes intra e extracelulares em função de um gradiente osmótico. Sua interação com outras proteínas presentes na membrana ou mesmo fatores de transcrição que, por sua vez, modulam a progressão do ciclo celular ou regulam a biossíntese de vias de componentes estruturais celulares, por exemplo, retratam esses processos (GALÁN-COBO; RAMÍREZ-LORCA; ECHEVARÍA, 2016).

A expressão dessas proteínas pode ser regulada de acordo com alterações nas funções metabólicas, o volume do fluido extracelular, por exemplo, e em distúrbios que produzem disfunções da BHE e edema cerebral (DENG *et.al*., 2014; SAADAUN *et.al*., 2002 e NOELL *et.al*., 2012).

Alguns trabalhos têm reportado o envolvimento, especificamente, das AQP1 e AQP4, em numerosas doenças de origem nervosa, onde seus padrões de expressão estão substancialmente alterados: doença de Alzheimer (HUBBARD; SZU; BINDER, 2018), epilepsia (ISOARDO et al., 2012), hidrocefalia, acidente vascular cerebral (SAADOUN et al., 2002, SADANA et al., 2012), toxicidade cerebral (MADER; BRIMBERG, 2019, XIMENES-DA-SILVA, 2016), bem como tumores de células gliais ou células precursoras da glia (COSTA et al., 2019, DING et al., 2011).

A AQP4 está superexpressa em gliomas e está envolvida nos processos da gênese do tumor, ou seja, migração celular, invasão e mudança funcional do tecido

circundante. Isto resulta em diferentes mecanismos subjacentes relacionados aos graus de malignidade do câncer (LAN et al., 2017): formação de edema na região

peritumoral, aumento da pressão intracraniana e episódios de convulsões (DUBOIS et al., 2014, MAUGERI et al., 2016).

Nosso grupo de pesquisa, por exemplo, conseguiu demonstrar que a administração da forma biologicamente ativa do hormônio da tireoide, a triiodotironina (T3) foi capaz de modular a expressão da AQP4 em, pelo menos, dois contextos biológicos diferentes (COSTA et al., 2019): 1) regulação negativa da AQP4 durante diferentes fases de desenvolvimento do sistema nervoso em camundongos. Neste experimento, camundongas fêmeas foram tratadas com T3 durante a fase final da gestação e avaliação foi feita a partir do tecido cerebral da prole, a fim de obtermos informações sobre o padrão de expressão da proteína no momento imediato ao nascimento; além disto, tratamos com T3 camundongos adultos (60 dias de vida) e jovem adultos (30 dias de vida). Os tecidos cerebrais destes animais também foram avaliados por meio de imuno-histoquímica por fluorescência.

Em outro experimento, tratando-se do segundo contexto biológico, a expressão da AQP4 foi analisada em células humanas de GBM previamente expostas ao T3 quando comparadas a astrócitos saudáveis e células tumorais não tratadas.

Figura 2 - Estrutura geral de aquaporinas e a localização de seus sítios de fosforilação individuais

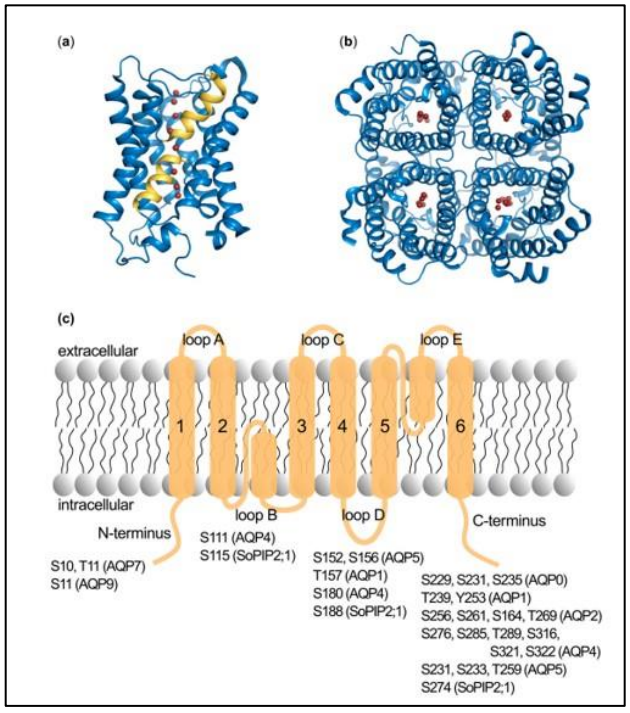

Fonte: NESVERONA; TÖRNROTH-HORSEFIELD, 2019.

Vários estudos *in vitro* e *in vivo* relataram redução da capacidade invasiva e migração em tumores após a deleção ou desregulação da AQP4 (DING et al., 2011, DING et al., 2010, CHENG et al.,2017). Suas isoformas M1 e M23 demonstraram alterar o estado de agregação/desagregação das OAPs e da viabilidade das células oriundas de glioma. Um estudo revelou que a isoforma M23 reduziu a invasão e proliferação de células tumorais, submetendo-as ao processo de morte celular programada (apoptose) (SIMONE et al., 2019).

Li et al. (2019) também demonstraram que o inibidor de proteínas quinases ativadas por mitógeno p38 (p38-MAPK) regulou negativamente a expressão das AQP1 e AQP4, e que isto facilitou o efluxo de edema cerebral após envenenamento agudo por monóxido de carbono. Além disso, camundongos com melanoma e *null* para o gene da AQP1 exibiram crescimento celular, migração e angiogênese reduzidos (SAADOUN et al., 2005).

Dessa forma, uma via de modulação comum entre AQP1 e AQP4 pode ser especulada, pois há trabalhos que demonstram que a homeostase da pressão do líquido cefalorraquidiano (LCR) não foi alterada pela inibição alternativa de nenhuma das proteínas em questão (TRILLO-CONTRERAS, et al., 2019).

No que diz respeito aos edemas cerebrais, vale ressaltar que podem ser classificados em dois tipos principais: 1) citotóxico e 2) vasogênico. O citotóxico é resultado do acúmulo de líquido intracelular desencadeado por traumas físicos ou isquemia. Este ocorre sem qualquer dano à BHE. O vasogênico, comum em tumores, por sua vez, resulta do escape do conteúdo plasmático capilar: com danos à BHE. Ambos podem representar um processo contínuo, sendo o o segundo a evolução clínica do primeiro (GU et al., 2022).

Nas duas situações a AQP4 pode exercer suas funções de maneira bifásica: no edema citotóxico, a ausência desta proteína proporciona a resolução do edema. Isso ocorre porque a taxa de entrada de água pela AQP4 compreende uma etapa limitante da taxa de fluxo de água do sangue para o SNC; logo, a AQP4 faz parte da formação do edema. No edema vasogêncio, a presença da AQP4 é que tem efeito resolutivo, pois as forças hidrostáticas conduzem a água e solutos do sangue através da BHE danificada para o espaço extracelular independente da AQP4. Ou seja, a AQP4 não

influencia na formação do edema, mas participa de sua absorção/clearence. (PAPADOPOULOS *et.al*., 2004). Em suma, o comportamento funcional das AQPs vai depender da etiologia da doença que afeta o SNC.

Figura 3 - Distribuição da AQP4 e GFAP em seções do córtex cerebral (5 µm de espessura) usando imunofluorescência

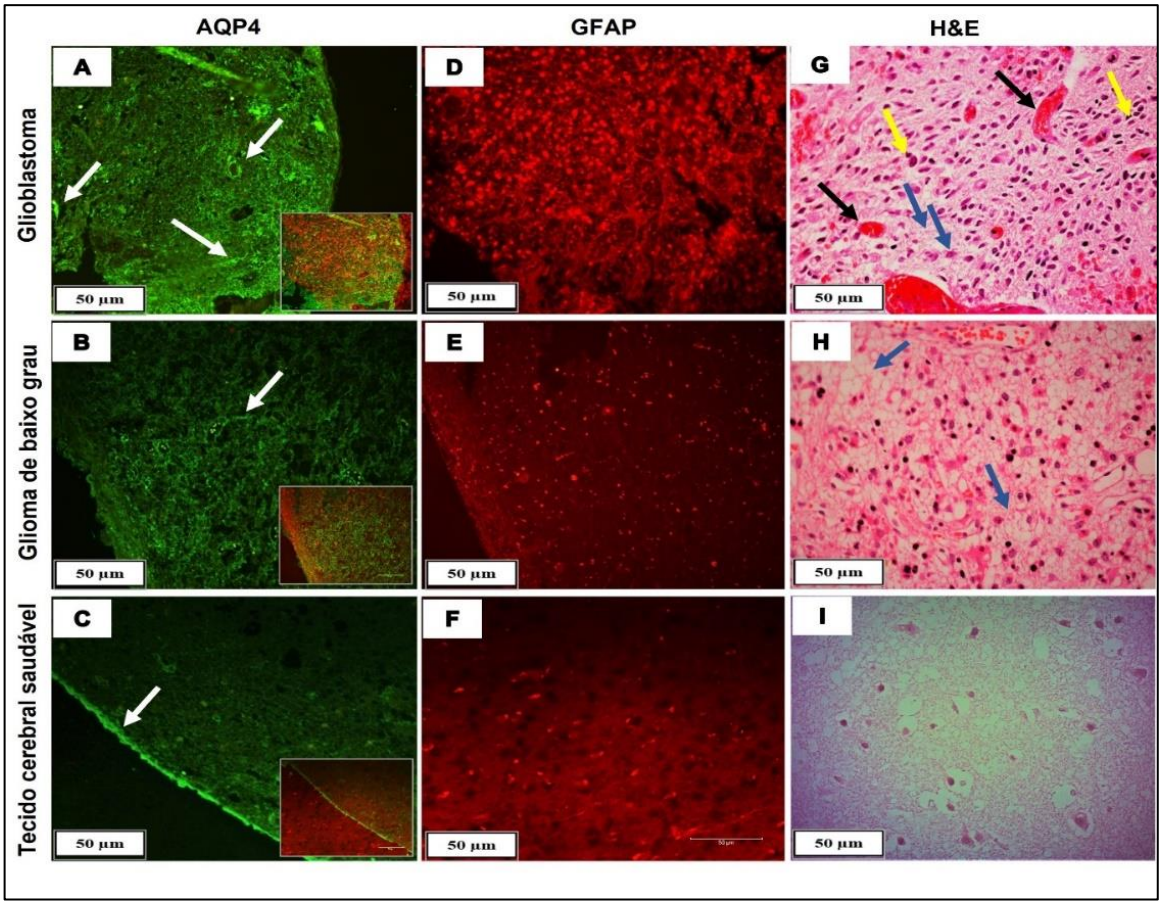

Nota: Na fluorescência AQP4: setas brancas indicam a distribuição AQP4 despolarizada em A) glioblastoma, B) glioma de baixo grau e polarizada em C) tecido cerebral saudável. Em B – F, temos a marcação por fluorescência de proteína ácida fibrillar glial (GFAP); esta aumenta em intensidade de marcação à medida que o grau de malignidade tumoral aumenta, indicando, também, a presença de astrócitos reativos no tecido. A marcação com hematoxilina e eosina (H&E): em G e H, as setas pretas indicam endotélio vascular espessado; e setas azuis, o fundo fibrilar em ambos os graus de malignidade dos gliomas.

Fonte: Autora, 2020.

As AQPs foram validadas como importantes alvos para ação terapêutica, mas ainda não há um único medicamento que tenha sido aprovado com sucesso (HUANG

et al., 2021). Sabendo que tanto a regulação da expressão quanto da disposição/distribuição das AQPs são fosforilação-dependentes, a busca por um inibidor ou agonista deste processo continua válida.

2.4 Bioinformática e Câncer

A bioinformática, como ciência, surgiu nos anos de 1960: a molécula de DNA acabara de ser descoberta e o genoma ainda não havia sido mapeado (GAUTHIER et al., 2019). Como é possível supor, seu avanço se dá em paralelo ao avanço de outras ciências; ou seja, métodos mais robustos e precisos da biologia celular e molecular e manipulação da molécula de DNA a partir destes e, ainda, ao avanço de potência dos computadores: hardwares e softwares capazes de executar tarefas para atender a demanda cada vez maior de perguntas científicas, bem como o armazenamento do grande volume de dados produzidos nas bancadas dos laboratórios científicos, um fenômeno conhecido como Big Data (Figura 4) (GAUTHIER et al., 2019).

Não à toa, a própria etimologia do nome atribuído a este campo das ciências da vida já nos traz a ideia de interdisciplinaridade, pois, a partir dela, áreas para além da biologia/saúde e de tecnologia da informação passaram a se interessar e colaborar na construção desta história. Profissionais da física, matemática e engenharia, por exemplo, são muito requisitados (BARLLET; LEWIS; WILLIAMS, 2016).

A bioinformática também tem se destacado como importante ferramenta na pesquisa translacional; a modelagem de fármacos, o desenho de novas moléculas e a predição de suas respectivas interações com receptores e o desenvolvimento de vacinas, por exemplo, já são realidades (XIA, 2016, HERWIG, 2014).

Uma de suas vantagens é a disponibilidade gratuita dos dados. Base de dados como os projetos *The Cancer Genome Atlas program* (TCGA) e *Genotype-Tissue Expression* (GTEx) (LONSDALE et al.,2013) são bons exemplos. Estes, frutos de um esforço mútuo para a construção de bases científicas onde seja possível estudar a expressão e regulação de genes de forma específica e em grande escala. Somente o TCGA, por exemplo, já tornou público mais de 2,5 petabytes de dados genômicos, epigenômicos, transcriptômicos e proteômicos (WEINSTEIN et al.,2013).

Figura 4 - Quantidade total de sequências nos bancos de dados NCBI GenBank e Whole Genome Shotgun ao longo do tempo.

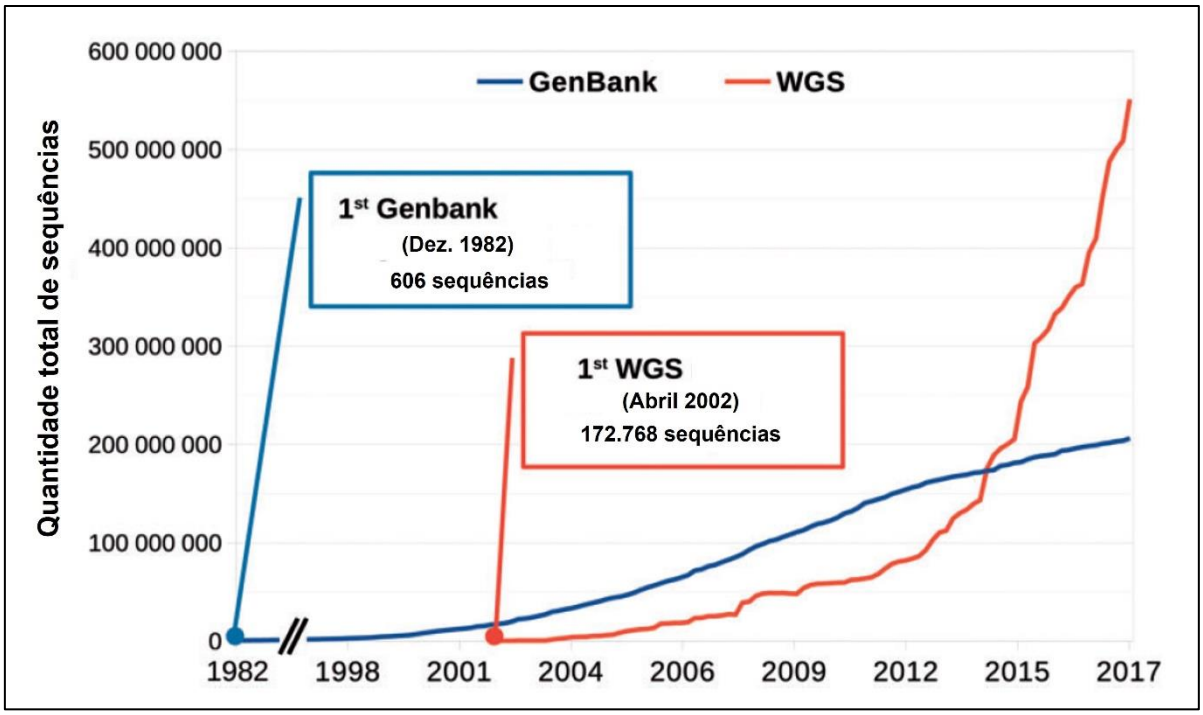

Nota: O número de genomas rascunhos/incompletos excedeu a quantidade de sequências genômicas completas em junho de 2014, e continua a crescer exponencialmente. Fonte: https://www.ncbi.nlm.nih.gov/genbank/statistics/.

Fonte: adaptado de GAUTHIER et al. (2019).

MA et al (2021) destacam que os métodos tradicionais da biologia não seriam suficientemente capazes de identificar, compreender e produzir características de genoma e proteínas, diagnóstico clínico, mecanismos patogênicos e desenvolvimento de medicamentos e vacinas antivirais, respectivamente, contra um patógeno desconhecido, como o caso novo coronavírus para lidar com a pandemia da COVID-19. Segundo os autores, utilizando a tecnologia de sequenciamento de próxima geração (NGS) e sequenciamento de terceira geração (TGS), tanto o agente etiológico da doença pôde ser detectado, como o genoma do vírus pôde ser obtido rapidamente.

Alterações genéticas causadoras de doenças podem ser inferidas a partir de estudos abrangentes de dados genômicos e análise de redes gênicas (YANG et al., 2014). O câncer, por exemplo, é uma dessas doenças. CHINNAPPAN et al (2021),

por exemplo, a partir de uma análise integrativa de bioinformática (bancos de dados e ferramentas online publicamente disponíveis), avaliaram e investigaram o mecanismo de ação da Nitroglicerina, um medicamento comumente utilizado em problemas de origem cardiovascular, por meio da identificação de seus genes-alvos em diversos tipos de tumores. Diversas análises *in silico*, a exemplo da simulação de dinâmica molecular e análise mutacional, podem determinar os fatores que afetam a progressão do câncer permitindo, assim, o desenvolvimento de uma terapia medicamentosa em potencial (KAMARAI; PUROHIT, 2014, WANG et al., 2019).

.

3 OBJETIVOS

Objetivo geral

Identificar os genes presentes no microambiente tumoral que potencialmente regulam e/ou estão correlacionados com a expressão das AQP1 e AQP4 em gliomas humanos.

Objetivos específicos

Analisar a expressão diferencial das AQP1 e AQP4 em amostras de gliomas humanos oriundos de bases de dados de RNAseq;

Analisar as chances de sobrevivência relacionadas a cada uma das aquaporinas nos diferentes graus de malignidade de gliomas humanos; (analisar a expressão de cada aquaporina como fatores de risco...)

Identificar vias de sinalizações moleculares alteradas em gliomas a partir dos genes diferencialmente expressos no tumor;

Identificar potenciais reguladores ou correguladores das AQP1 e AQP4 no tumor.

4 RESULTADOS

Thyroid hormones as possible coregulators of aquaporins 1 and 4 in human gliomas: a pilot study using a bioinformatics approach.

Carmelita Bastos Mendes [a] and Adriana Ximenes da Silva [a]

[a] Instituto de Ciências Biológicas e da Saúde, Universidade Federal de Alagoas, Alagoas, Maceió, Brazil

Number of words: 4690

Corresponding author:

Adriana Ximenes-da-Silva, PhD

E-mail: aximenes@ccbi.ufal.br

Phone: + 55-82-3214-1127

Keywords: glioma, AQP1, AQP4, biomarker, gene expression, correlation analysis,

Abstract

The expression and localization of the water channel transporters, aquaporins (AQPs), in the brain are substantially modified in gliomas during tumorigenesis, cell migration, edema formation, and resolution. We hypothesized that the molecular changes associated with AQP1 and AQP4 in the brain may potentially be anticancer therapeutic targets. To test this, a bioinformatics analysis of publicly available data from international consortia was performed. We used RNA-seq as an experimental strategy and identified the number of differential AQP1 and AQP4 transcript expressions in glioma tissue compared to normal brain tissue. Our results demonstrated that AQPs genes are overexpressed in patients with glioma. Among the glioma subtypes, *AQP1* and *AQP4* were overexpressed in astrocytoma (low-grade glioma) and classical (high-grade glioma). Overall survival analysis demonstrated that both AQP genes can be used as prognostic factors for patients with low-grade glioma. Additionally, we observed a correlation between the expression of genes involved in the tyrosine and thyroid hormone pathways and AQPs. Namely: *PNMT, ALDH1A3, AOC2*, *HGDATP1B1, ADCY5, PLCB4, ITPR1, ATP1A3*, *LRP2*, *HDAC1, MED24, MTOR* and *ACTB1* (Spearman's coefficient = ≥ 0.20 and p-value = ≤ 0.05). These findings indicate that the thyroid hormone pathways and AQPs 1 and 4 are potential targets for new anti-tumor drugs and therapeutic biomarkers for malignant gliomas.

1. Introduction

Gliomas are the most common central nervous system tumor type (Louis et al., 2016), accounting for approximately 80% of all malignant intracranial tumors with high episodes of recurrence (Ostrom et al.,2014).

Depending on the cell type of origin, they can be classified or subdivided into astrocytomas, ependymomas, oligodendrogliomas, oligoastrocytomas, and glioblastoma multiforme (GBM) (Ostrom et al., 2014).

Glioblastoma is the most aggressive brain tumor owing to its high invasiveness. Despite advances in therapeutic modalities (tumor resection combined with chemotherapy and radiotherapy), the overall patient survival rate is 12–15 months from the initial diagnosis, with only 5% of patients reaching a 5-year survival rate (Fedele et al.,2019).

Likewise, the standard first-line treatment for GBM, temozolomide (TMZ), a DNA alkylating agent, has a significant tumor recurrence rate and confers drug resistance (Strobel et al.,2019) due to its low specificity and limitations in crossing the blood-brain barrier (BBB).

Persistent headaches, neurological and behavioral deficits, seizures, cognitive deficits, drowsiness, dysphagia, confusion, aphasia, motor deficits, fatigue, dyspnea, and mood changes are common symptoms in patients diagnosed with glioblastoma (Bienkowski et al., 2017, Maugeri et al., 2016; IJzerman-Korevaar et al., 2018). Usually, its localization, size, and grade make it inoperable and difficult to treat, dramatically decreasing the quality of life of patients with glioma (Fedele et al.,2019).

Many symptoms are derived from neurological findings such as increased intracranial pressure and brain herniation. Edema around the tumor causes hypoxia (lack of oxygen supply) (Solar et al., 2022; Koenig, 2018), resulting in long-term disability, psychiatric disorders, substance abuse, or self-harm (Huang et al., 2021).

A clinical study carried out by Wu et al. (2015) showed that within the identification of peritumoral edema during the preoperative period in patients with glioblastoma, factors such as necrosis and edema extent were independent factors for poor outcome and overall survival (OS).

Aquaporins (AQPs), a family of transmembrane water channel proteins, play a critical role in responding to changes in the osmotic environment. Eight members of the water channel family are expressed in the central nervous system (Maugeri et al.,2016, Saadoun et al.,2002, Yang, 2017). AQP1 and AQP4 are the major water channels in the brain and play a pivotal role in water homeostasis and the maintenance of BBB integrity (Galán-Cobo et al., 2016).

Brain AQPs are distributed primarily in astroglial membranes, especially in perivascular astrocyte foot processes and glia limitans, near the brain fluid compartments (Wolburg et al.,2012, Verkman et al.,2014) and ependymal cells, providing an efficient system to promote water and solute transport between the perivascular space and glial cells, and to support brain parenchymal clearance through the glymphatic system (Mestre et al., 2018, Smith et al., 2017; Lohela et al., 2022).

AQP4, an orthodox AQP type, is upregulated in gliomas and is involved in the tumorigenesis process, that is, cell migration, invasion, and functional changes in the surrounding tissue. AQP4 distribution has been hypothesized to underlie mechanisms related to the degree of malignancy (Lan et al., 2017), edema formation in the peritumoral region, increased intracranial pressure, and seizure episodes (Dubois et al., 2014, Maugeri et al.,2016).

Several *in vitro* and *in vivo* studies have reported reduced invasive capacity and migration in tumors after AQP4 depletion or downregulation (Ding et al., 2011, Ding et al., 2010, Cheng et al., 2017) by decreasing water permeability, which in turn upregulates transmembrane water fluxes during tumor or healthy astroglial cell movement (Huang et al., 2021).

In contrast, AQP1 (also considered a classic aquaporin) is predominantly expressed in the circumventricular brain and areas associated with cerebrospinal fluid production. Its expression is altered in the human brain under pathological conditions (Satoh et al., 2007) such as cancer. In brain tumors, AQP1 and AQP4 expression is upregulated with the malignancy grade (Saadoun et al.,2002).

Inhibition of tumor growth and suppression of vasculogenic mimicry formation were observed following *AQP1* silencing *in vivo*, which could be related to reduced tumor aggressiveness, malignancy, and metastasis (Yang et al., 2018).

More recently, the newly updated WHO Classification of Tumors of the Central Nervous System classifies brain tumors based on their histological appearance (Lima et al., 2012, Perry and Wesseling, 2016) and molecular markers (genotypic classifications). Namely: isocitrate dehydrogenase (IDH) mutation, 1p/19q codeletion, and O-6-methylguanine-DNA methyltransferase (MGMT) methylation, (Martinez-Lage and Sahm, 2018; Zhang et al., 2020; Zhang et al., 2020) avoiding imprecise diagnosis, thereby significantly influencing in the selection of treatment options for patients.

Because of the role of molecular markers in the early diagnosis of gliomas, we hypothesized that AQP1 and AQP4, as homeostatic brain proteins, could act as potential anticancer therapeutic targets.

In this study, we aimed to characterize the expression patterns of genes encoding AQP1 and AQP4 proteins and to identify the genes present in the cancerous microenvironment that potentially regulate or correlate with their expression in human gliomas. Our findings, from a bioinformatic approach, allowed us to conduct a wide and diversified scale analysis and provided evidence for the role of these proteins and other related genes, thus paving the way for the development of potential biomarker candidates for the diagnosis and therapeutic targets of glioma for future research.

2. Materials and Methods

2.1 Experimental Design

This *in silico* study was executed using publicly available data from international consortia. In this study, RNA-seq was used as the experimental strategy. Differential expression analysis was performed using Bioconductor statistical packages with R software (version 4.1). Human cancer samples originated from The Cancer Genome Atlas (TCGA) and healthy tissue of the Genotype-Tissue Expression (GTEx) project.

We used web tools to assess the variables beyond differential expression. Correlation analysis was performed using Gene Expression Profiling Interactive Analysis (GEPIA2) (Tang et al., 2019) (http://gepia2.cancer-pku.cn), survival analysis, and Tumor IMmune Estimation Resource (TIMER) (Li et al., 2020) (http://timer.cistrome.org/). In addition, we used the Atlas of Human Pathology (https://www.proteinatlas.org/) to visualize the distribution pattern of AQP1 and AQP4 proteins in healthy brain and cancer tissues.

The database annotation, visualization, and integrated discovery (DAVID) web server (Sherman et al., 2021) (https://david.ncifcrf.gov/) was used to identify a network of related genes in altered pathways in the tumor microenvironment (functional enrichment analysis). The same analysis was performed using PathfindR package (Ulgen et al., 2019).

In a short time, the genes involved in the pathways of our choice were evaluated by the degree of correlation with *AQP1* and *AQP4* expression in glioma tissues, both low-grade glioma (LGG) and GBM, to find similarities in expression profiles and suggest some degree of co-regulation.

Clinical data from patients regarding brain tumor location were not accessed and were not included in this study.

2.2 Transcriptional expression of *AQP1* and *AQP4*

Normal and solid primary tumor tissues for the two types of cancer were downloaded from TCGA (https://gdc-portal.nci.nih.gov) using TCGAbiolinks R package version 2.12.6.

A dataset composed of 2,080 RNA-seq of both tumor stages (LGG and GBM, N = 671) and healthy patient samples (N = 1,409) from TCGA and GTEx projects was used. Data were derived from the Illumina HiSeq RNA-Seq platform. The transcript levels of orthodox AQPs (*AQP1* and *AQP4*) in tumor and non-tumor tissues were evaluated. All data were processed and standardized using R software version 4.1.0.

The GEPIA2 web-based tool was used to build graphs to better visualize the results. One-way analysis of variance (ANOVA) was used for the assessment of the disease state: tumor, N = 518 (LGG) and N = 163 (GBM), or normal brain cortex, N = 207, as the variable for calculating the differential expression. The expression data were first transformed using the formula log2 (TPM + 1).

The fold change (log2FC) was defined as the difference in the median value between the normal and tumor samples. Genes with $P \leq 0.05$ and $|\log_2 \text{fold change (FC)}| \geq 1.0$ were considered differentially expressed genes (DEGs). The same analysis was performed for glioma subtypes. All the results are presented in table and box plot forms.

The values were calculated using the corresponding formula:

$$log2FC = log2(B) - log2(A)$$

Where B and A are representative of the median values of the genes expressed in the tumor and median values of the expressed genes in normal tissue, respectively.

2.3 Survival Analysis

We sought to assess whether our search goal genes in this study may have survival advantages and, thus, establish possible prognostic markers, confirming their clinical significance.

Patients with glioma were divided into high- or low-level groups based on the median value of genes, and OS rates were evaluated using Kaplan–Meier analysis. The TIMER tool used the log-rank test (Mantel-Cox test) for the hypothesis evaluation. The Cox proportional hazard ratio (HR) and 95% confidence interval (CI) were used as parameters in the Kaplan–Meier survival analysis. Statistical significance was set at $P < 0.05$.

2.4 Functional enrichment analysis

Kyoto Encyclopedia of Genes and Genomes (KEGG) is an integrated database resource for biological interpretation of genome sequences and other high-throughput data. KEGG analyses are available in the DAVID database (https://david.ncifcrf.gov/), a data resource composed of an integrated biology knowledge base and analysis tools to extract meaningful biological information from large quantities of gene and protein collections. Dysregulated pathway identification analysis was performed on differentially expressed genes using the DAVID web tool. The DEG analysis showed 4,820 genes in glioma samples (see supplementary material) that were divided into two groups of lists: upregulated and downregulated genes (logFC > 1 and logFC < 0). Subsequently, these lists were submitted separately to DAVID and the results were generated.

2.5 Analysis of Correlation using the GEPIA2 tool

A pairwise gene Spearman correlation analysis between AQP*1 or AQP4* and the expression of other preselected genes was performed using GEPIA2.

GEPIA data are presented as a log-scale axis and a non-log scale was used for calculation; the strength of the correlation was determined using the following guide for

the absolute value: ≤0.2 (weak), 0.21–0.50 (moderate), 0.51–0.80 (strong), and 0.81–1.0 (very strong). Spearman's coefficients >0 indicate a positive correlation, and a coefficient less than zero indicates a negative correlation. Spearman's coefficient ≥ 0.20 and *p* - values ≤ 0.05 were considered significant in the current study.

3. Results

3.1 *AQP1* and *AQP4* genes are overexpressed in gliomas compared to normal brain samples.

The expression pattern of AQP1 and AQP4 in brain cancers is a controversial question, mostly with respect to the degree of several tumors or tumor subtypes**.** To characterize gene expression, differential expression analysis from TCGA and GTEx datasets was performed using the R software. This analysis revealed a list of 4,819 genes. Among these, five *AQPs* family members were identified: *AQP1, AQP4, AQP5, AQP7*, and *AQP8*.

As expected, both *AQP1* and *AQP4* mRNAs were overexpressed in glioma samples (logFC = 1.42 x 10+14 and 1.02 x 10+14; P-value = 1.66E-40 and 8.82E-26, respectively) compared to the healthy brain samples (Table 1, Figures 1C and 1D).

Histological samples of tumor and normal brain tissues from the Human Protein Atlas database show the distribution of AQP1 and AQP4 proteins. In summary, the staining intensity of both proteins increased with the degree of tumor malignancy. Figures 3A, B, and C show AQP1 staining, while Figures 3E, D, and F show AQP4 staining.

In addition, both AQP1 and AQP4 showed a significant difference in expression pattern if compared to tumor markers/antigens in gliomas that are consensually used in clinical practice to establish degrees of malignancy and prognosis (Soldatelli et al., 2022). For instance: TP53, ATRX, TERT, IDH1, EGFR and GFAP (Figure 4).

These results revealed a pivotal role of these genes in the gliomagenesis process.

3.2 *AQP1* and *AQP4* seem to play substantial roles in the molecular glioma subtype.

In a complementary manner, Figure 2 shows the differential expression of AQP1 *and* AQP4 in glioma subtypes*. A* and B represent the expression patterns in the

LGG subtypes (astrocytoma, oligoastrocytoma, and oligodendroglioma). In this case, AQP1 showed an increased number of transcripts in astrocytomas compared to oligodendroglioma tumors (*p ≤ 0.05) (Figure 2A). AQP4 mRNAs levels were not significant in these LGG samples (Figure 2B).

Regarding the GBM subtypes (classical, mesenchymal, neural, and proneural), only AQP4 presented considerable variation in its expression between classical and proneural subtypes, being more expressed in the classical case (*p ≤ 0.05) (Figure 2D).

These results indicate that the aquaporins in question most likely have an oncogenic role only in cells of astrocytic origin.

3.3 *AQP1* and *AQP4* could be potential risk factors and prognostic indicators for low-grade glioma patients

One of the factors in assigning clinical importance to a therapeutic target is the probability of increasing the chances of patient survival. Kaplan–Meier analysis revealed that OS was lower in patients with LGG who had high *AQP1* (HR = 1.458; log-rank = 0) and *AQP4* (HR:1.191; log-rank = 0.003) expression (Figure 5B and D). In the GBM patient groups, there was no difference between the high and low expression groups of these selected genes (Figure 5A and C).

Our findings suggest that high expression of *AQP1* and *AQP4* may be a risk factor for poor prognosis in patients with LGG because they are significantly associated with reduced survival.

3.4 Functional enrichment analysis

Understanding the functional impact of a disease data set is a crucial step in this line of work as we are looking for potential regulators of AQPs in gliomas only.

The DAVID tool analysis generated two lists of dysregulated pathways from upregulated and downregulated genes in the glioma microenvironment. A list of genes with LogFC ≥ 1.0 revealed 64 altered pathways (Table 1 supplementary) and, among them, 31 presented statistical significance ($p < 0.05$). Sixty-six pathways were identified in genes with negative LogFC values (Table 2). Among them, 30 were considered to be statistically significant.

PathfindR analysis, in turn, showed 113 pathways over-represented according to glioma differential expression (Table 3 supplementary).

Based on our previous study (Costa et al., 2019), we chose tree-specific pathways in the downregulated list of the functional enrichment analysis: hsa00350 (Tyrosine metabolism [9 genes]); hsa04918 (Thyroid hormone synthesis [15 genes]); and hsa04919 (Thyroid hormone signaling pathway [7 genes]) (Table 3 supplementary). It is worth noting that choosing the genes from downregulated pathways was timely to antagonize the overexpression of AQPs as well as our experimental benchtop background (*in vivo* and *in vitro*). In total, we identified 31 genes from the cellular pathways identified in the enrichment analysis.

3.5 Spearman's correlation

We hypothesized that the expression of both AQP1 and AQP4 could be modulated by genes involved in thyroid function. Here, we attempted to identify potential regulators that could interfere with some degree of regulation of the disposition and function of AQP1 and AQP4 in tumor cells. (Tables 2, 3 and 4)

Within the tyrosine metabolism pathway, five genes were correlated with AQP1 and AQP4, although only four met the statistical requirements already established: *PNMT, ALDH1A3, AOC2*, and *HGD* (Table 2).

In the thyroid hormone synthesis pathway, six genes were statistically significant (Table 3): *ATP1B1, ADCY5, PLCB4, ITPR1, ATP1A3*, and *LRP2*. Only four genes involved in the thyroid hormone signaling pathway (Table 4) were within the statistical inclusion criteria described in Subsection 2.5: *HDAC1, MED24, MTOR*, and *ACTB1*. All these genes are also listed and have potential actions on AQPs, as summarized in Table 5. Our data refer to the number of transcripts using Spearman's correlation analysis (AQP1 and AQP4 vs. genes selected from the functional enrichment analysis). Thus, we can consider them regulators at the translational level.

4. Discussion

In this study, we aimed to identify the expression pattern of AQP1 and AQP4 genes in human gliomas, as well as to point out their regulatory potential within the cancer microenvironment.

Here, we used RNA-seq as an experimental strategy to identify the differential expression of AQP1 and AQP4 transcripts in glioma tissues compared to normal brain tissues. Indeed, AQPs genes are overexpressed in glioma patients. Among the glioma subtypes, *AQP1* and *AQP4* are overexpressed in astrocytoma (LGG) and classical glioma (GBM). OS analysis showed that both AQP genes can be used as prognostic factors for patients with LGG, confirming the results of previous studies and reinforcing their clinical value. We also observed a correlation between the expression of genes involved in the tyrosine and thyroid hormone pathways and AQPs.

Emerging evidence suggests a positive relationship between AQP1 and AQP4 expression and histological tumor grade. Poor neurological prognosis has also been reported (Suzuki et al., 2018; Warth et al., 2007). Our results are supported by these findings, as aquaporin expression patterns increased when compared to the molecular subtypes of gliomas: AQP1 is improved in other subtypes of LGG classification (astrocytoma); in turn, AQP4 is increased only in the classical subtype GBM.

AQP4 isoforms, known as M1 and M23, have been shown to change the aggregation/disaggregation state into orthogonal arrangements of particular (OAPs) and glioma cell survival. One study revealed that the isoform M23 reduced the invasion and proliferation of glioma cells to promote their apoptosis (Simone et al., 2019).

Some endogenous factors such as hormonal and metabolic changes also modulate AQP4 expression in human gliomas (Lan et al., 2017). Likewise, an increase in *AQP1* expression was observed during central necrosis and hypoxia, which are characteristics of GBM tumors (HayashI et al., 2007, Honasoge; Sontheimer, 2013)

Gene expression is orchestrated by several endogenous and exogenous factors, such as DNA-binding transcription factors, regulatory proteins, and profile hormones (BATH; HONSON;GUTTMAN, 2021).

A study conducted by Nauman et al. (2004) evaluated the cellular concentrations of thyroxine (T4) and triiodothyronine (T3) in non-thyroidal illness syndrome (NTIS) patients with gliomas, where the TSH serum concentration was within the normal range and T4/T3 levels were lower than normal. They demonstrated that thyroid hormone levels were significantly lower in glioma tissues than in healthy tissues. In addition, both iodothyronine deiodinases (types 2 and 3) were higher in tumor tissues than in non-glioma tissues.

Some studies showed that hypothyroidism is a risk factor for metastatic cancer progression in patients with brain cancer. A cohort study (Berghoff et al, 2020) identified a beneficial role on OS in patients with brain metastasis, nearly doubling the life expectancy from the diagnosis of primary and metastatic cancer.

In contrast, the results of clinical research showed that almost 40% of the evaluated patients presented with overt or sub-clinical hypothyroidism, and 31% needed hormone replacement (Faghih-Jouybari et al. 2018).

In pediatric patients, an important probability of developing thyroid dysfunction was found post-treatment with surgery, chemotherapy, and radiotherapy (Cosnarovici et al., 2020; Jin et al., 2018); besides, abnormalities in thyroid function were found in patients with AQP4 antibody–seropositive optic neuritis (Zhao et al.,2016).

We previously identified a negative modulator of AQP4 protein and demonstrated that triiodothyronine (T3) treatment of GBM-95 line cells resulted in a slight reduction in cell migration (Costa et al., 2019); other studies have also evaluated the modulatory action of this hormone on the expression of AQP4 in stroke animal models (Sadana et. al., 2015 e Vella et.al., 2016).

Therefore, according to our results, we suggest two new hypotheses: 1) as all patient data are post-mortem (including data other than this one), it is possible that standard cancer treatment led to hypothyroidism and subsequently downregulated the thyroid hormone pathways. This could result in the overexpression of AQP1 and AQP4 in the more aggressive glioma subtypes (astrocytoma (LGG) and classical, respectively (GBM)), as we present in the differential expression results; and 2) hypothyroidism would already be a clinical risk condition for the development of glioma; patients diagnosed early with the tumor would present a sub-clinical pattern of thyroid gland dysfunction. This condition would be accentuated by the anticancer therapeutic approach, and these patients would have the same outcome, genetic, and molecular profile as mentioned in hypothesis 1.

Additional studies to clarify the specific inhibitors or promoters of these pathways, as well as transcription factors and post-transcription/translation modification methods, will help identify the most appropriate therapeutic targets for AQP1 and AQP4 modulation, relationships between genes, and signaling pathways in gliomas.

To the best of our knowledge, this is the first study to suggest a modulatory interaction between the gene encoding AQP1 and pathways related to thyroid hormones.

5. Limitations

The brain tissue is substantially plastic and heterogeneous. Factors such as age and sex can influence their genetic constitution. Glial tumor characteristics may also change depending on the topographic region of the brain where the tumor occurs. The non-separation of categorical patient groups based on the aforementioned factors is a limitation of this study. Single-cell analysis from different glioma patient groups would help us confirm the oncogenic role of the AQPs studied here, as well as their modulation by thyroid hormones.

6. Conclusion

To the best of our knowledge this study is the first to show a strong potential functional relationship between AQP1 and thyroid hormone pathways in brain tumors. The expression of AQP1 and AQP4 is significantly associated with a worse prognosis in patients with LGG. The molecular pathways and AQP1 and AQP4 genes identified here may be useful for the molecular diagnosis of gliomas and for screening new anti-tumor drugs for these malignant tumors.

Abbreviations

ANOVA	Analysis of variance
AQP	Aquaporin
BBB	Blood-brain barrier
CI	Confidence interval
CNS	Central nervous system
CSF	Cerebrospinal fluid
DEG	Differentially expressed gene
GBM	Glioblastoma
GTEx	The Genotype-Tissue Expression
HR	Hazard ratio
KEGG	Kyoto Encyclopedia of Genes and Genomes
LGG	Low-grade glioma
NCBI	National Center for Biotechnology Information
NTIS	Non-thyroidal illness syndrome
OS	Overall survival
TCGA	The Cancer Genome Atlas

TIMER Tumor IMmune Estimation Resource

Author Contribution

Conceptualization, CBM and AXS; methodology, CBM; formal analysis, CBM; writing—preparation of the original draft, CBM; writing – proofreading and editing, CBM and AXS.; supervision, AXS; funding acquisition, AXS. All authors have read and agreed to the published version of the manuscript.

Acknowledgements

To the Coordination for the Improvement of Higher Education Personnel (CAPES) for granting a master's scholarship (CBM). The results shown here are in part based on data generated by TCGA Research Network: https://www.cancer.gov/tcga.

The Genotype-Tissue Expression (GTEx) Project was supported by the Common Fund of the Office of the Director of the National Institutes of Health and by NCI, NHGRI, NHLBI, NIDA, NIMH, and NINDS. The data used for the analyses described in this manuscript were obtained from the GTEx Portal on 08/12/2022.

Conflict of Interest

All authors declare that they have no conflicts of interest.

Funding

This research received no external funding.

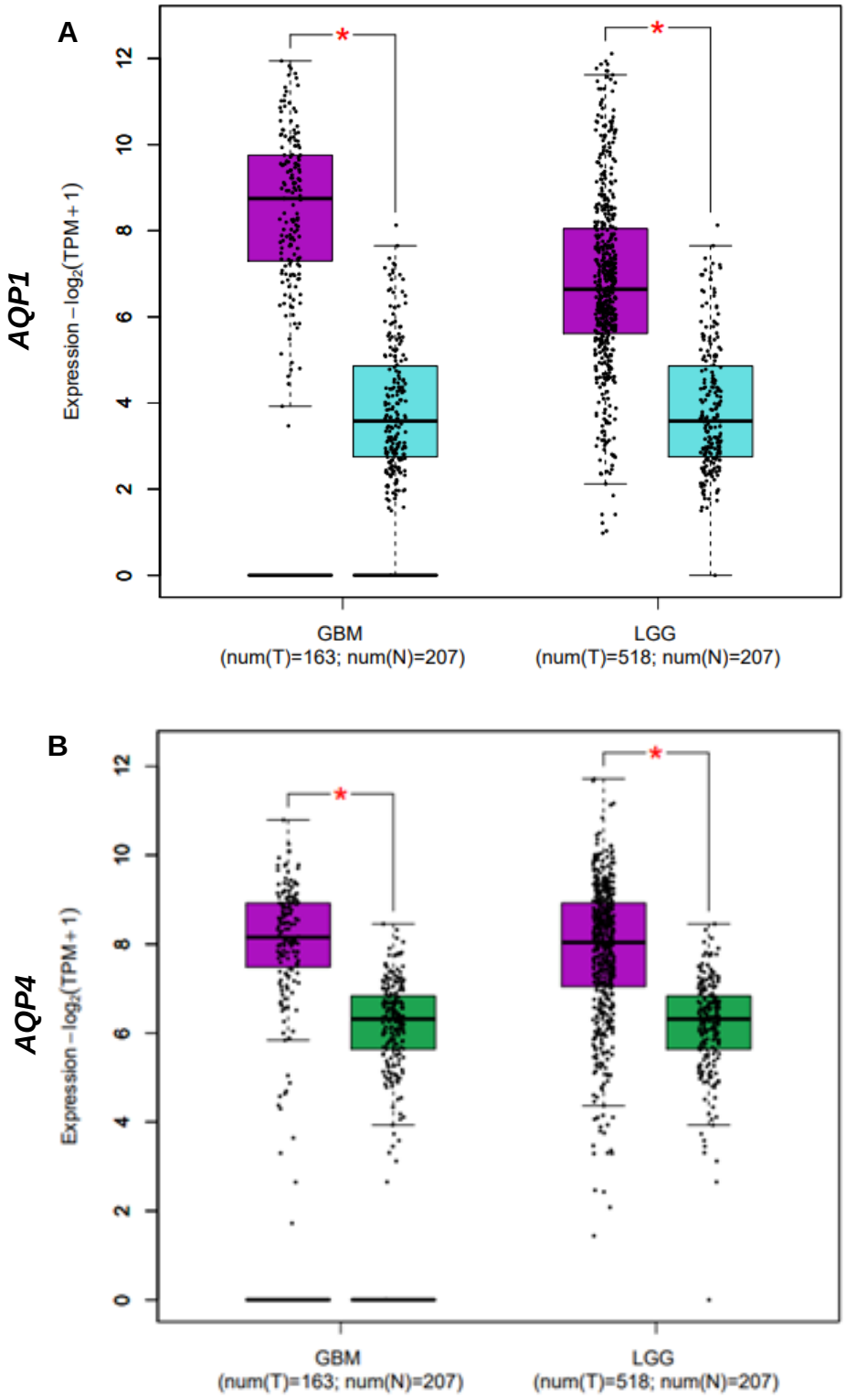

Figure 1 - AQPs mRNAs in gliomas samples from TCGA and GTEx dataset. AQP1 and AQP4 genes in normal (N=163; blue box for AQP1 data and green box for AQP4 data) and tumor (N=207; purple box) samples. Tumor samples are divided into LGG and GBM groups (X axis of both graphs). TPM: transcripts per kilobase million; LGG: low-grade glioma; GBM: glioblastoma multiforme. *$p < 0.05$. Graphs A and B were derived by the GEPIA2 webserver in January 2021.

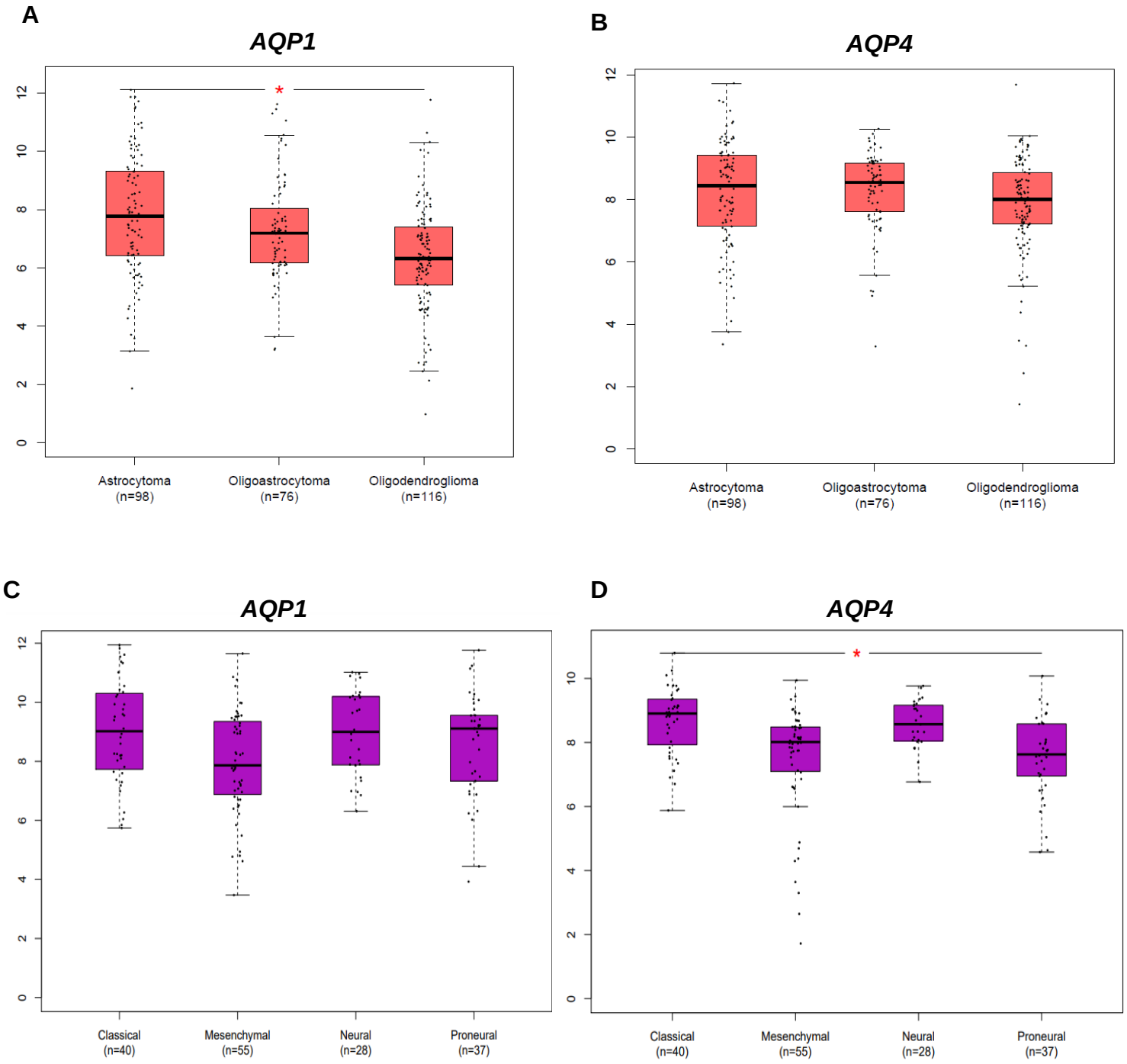

Figure 2 - AQPs mRNAs in gliomas samples from TCGA and GTEx dataset. *AQP1* and AQP4 genes. Tumor samples are divided into LGG and GBM subtypes groups. **A** and **B** represented both AQP1 and AQP4 profiles of expression in LGG subtypes. **C** and **D** represented both AQP1 and AQP4 profiles of expression in GBM subtypes. LGG: low-grade glioma; GBM: glioblastoma multiforme. *$p < 0.05$. All graphs were derived by the GEPIA database in January 2021

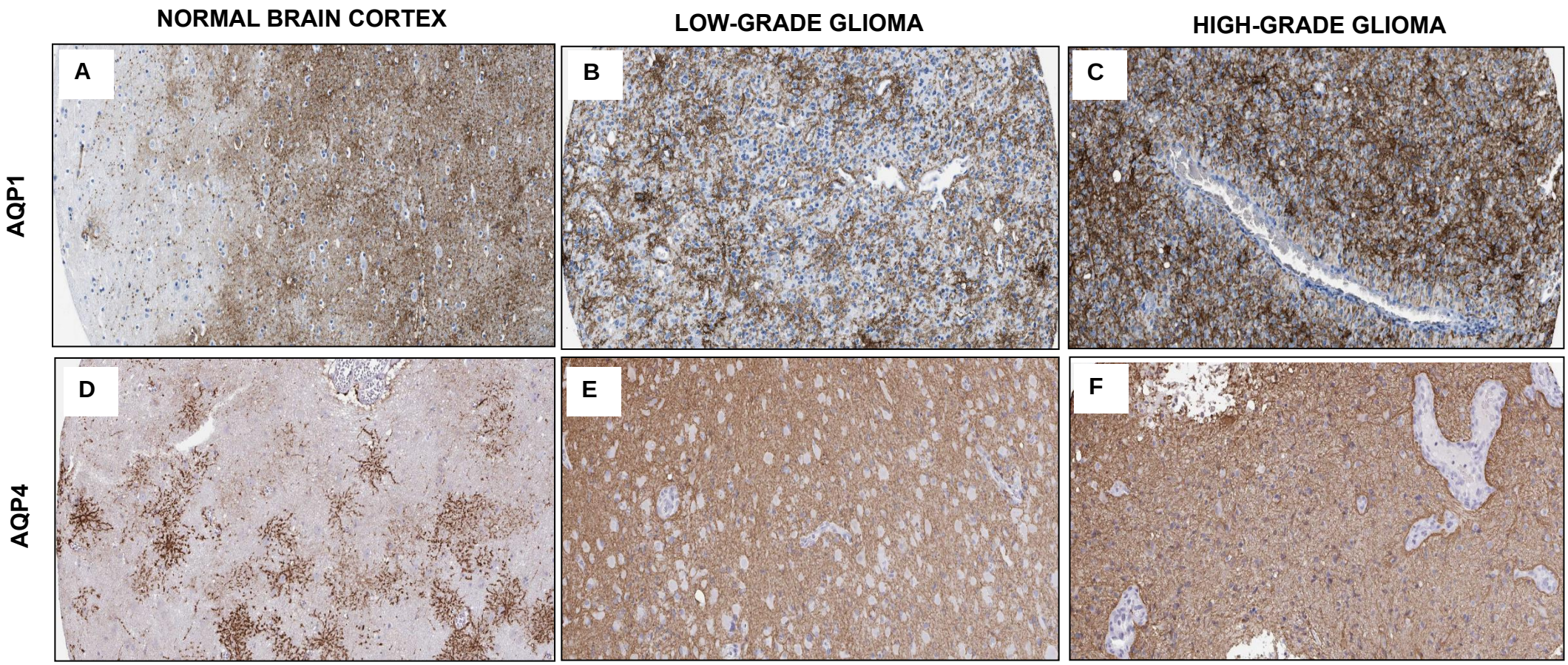

Figure 3 - Representative immunohistochemical staining distribution of AQP1 and AQP4 expressions in normal and glioma patient samples. Plates A-F were captured in 100 µm. All data were extracted from The Human Protein Atlas (https://www.proteinatlas.org/).

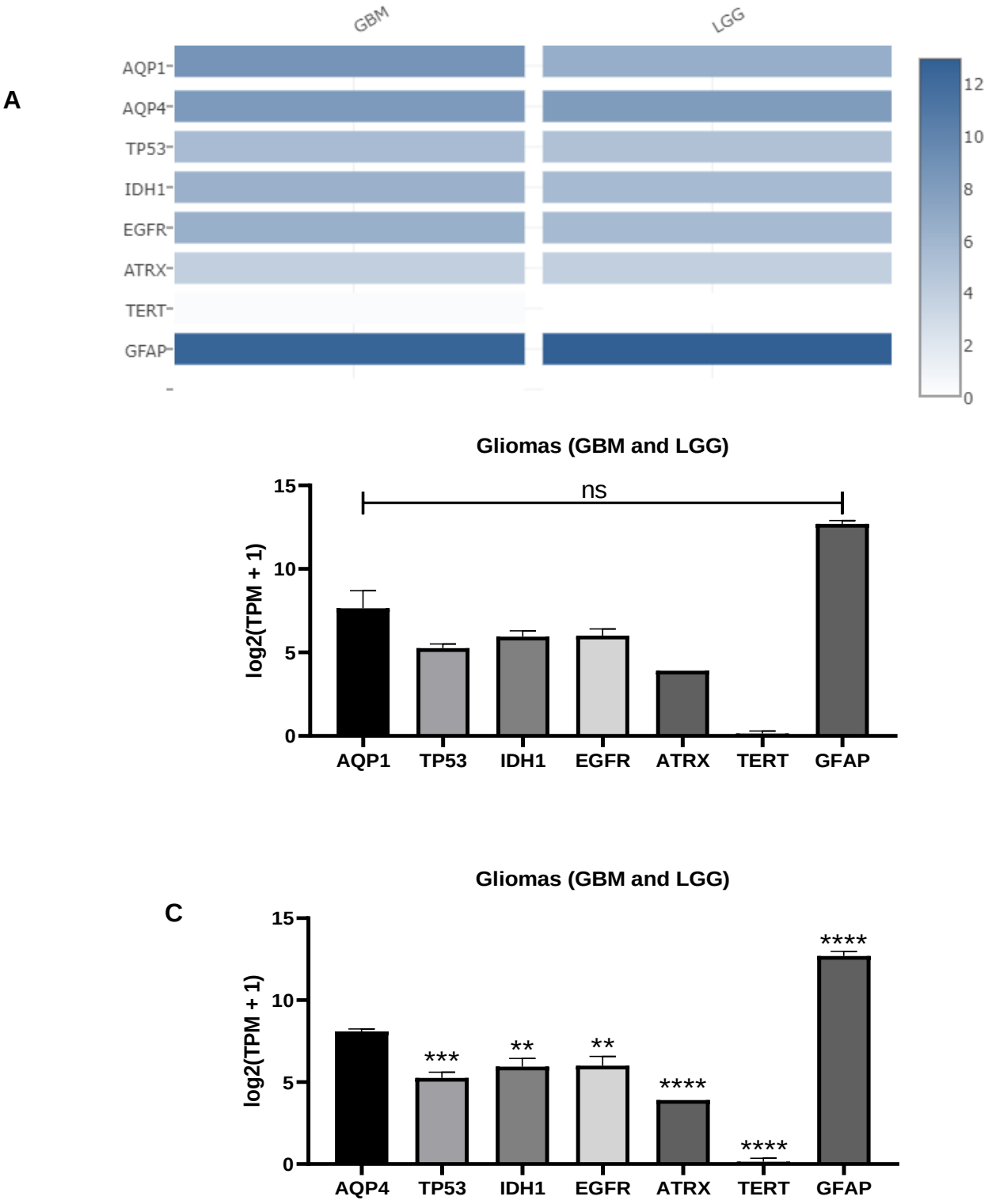

Figure 4 – Expression matrix graphs based on a list of genes considered biomarkers of glioma and AQP1 and AQP4. A) Heat Map derived from GEPIA2. The color density in each block represents the median value of gene expression in tumor tissue (GBM and LGG, separately) normalized by the maximum median value of the expression in all blocks. These data were transformed for plotting (linear to log2(TPM + 1)). Graphs B and C were created from the values provided by the heat map for each gene with a subsequent comparison with both AQP1 and AQP4, respectively. For this, one-way ANOVA was performed followed by Tukey's multiple comparisons tests using GraphPad Prism version 8.0. p-value < 0,05 *; p< 0,01 **; p< 0,001 *** and p< 0,0001 ****. **TP53**: Tumor Protein P53, **IDH1**: Isocitrate Dehydrogenase (NADP(+)) 1, **EGFR**: Epidermal Growth Factor Receptor, **ATRX**: ATRX Chromatin Remodeler, **TERT**: Telomerase Reverse Transcriptase, and **GFAP**: Glial Fibrillary Acidic Protein.

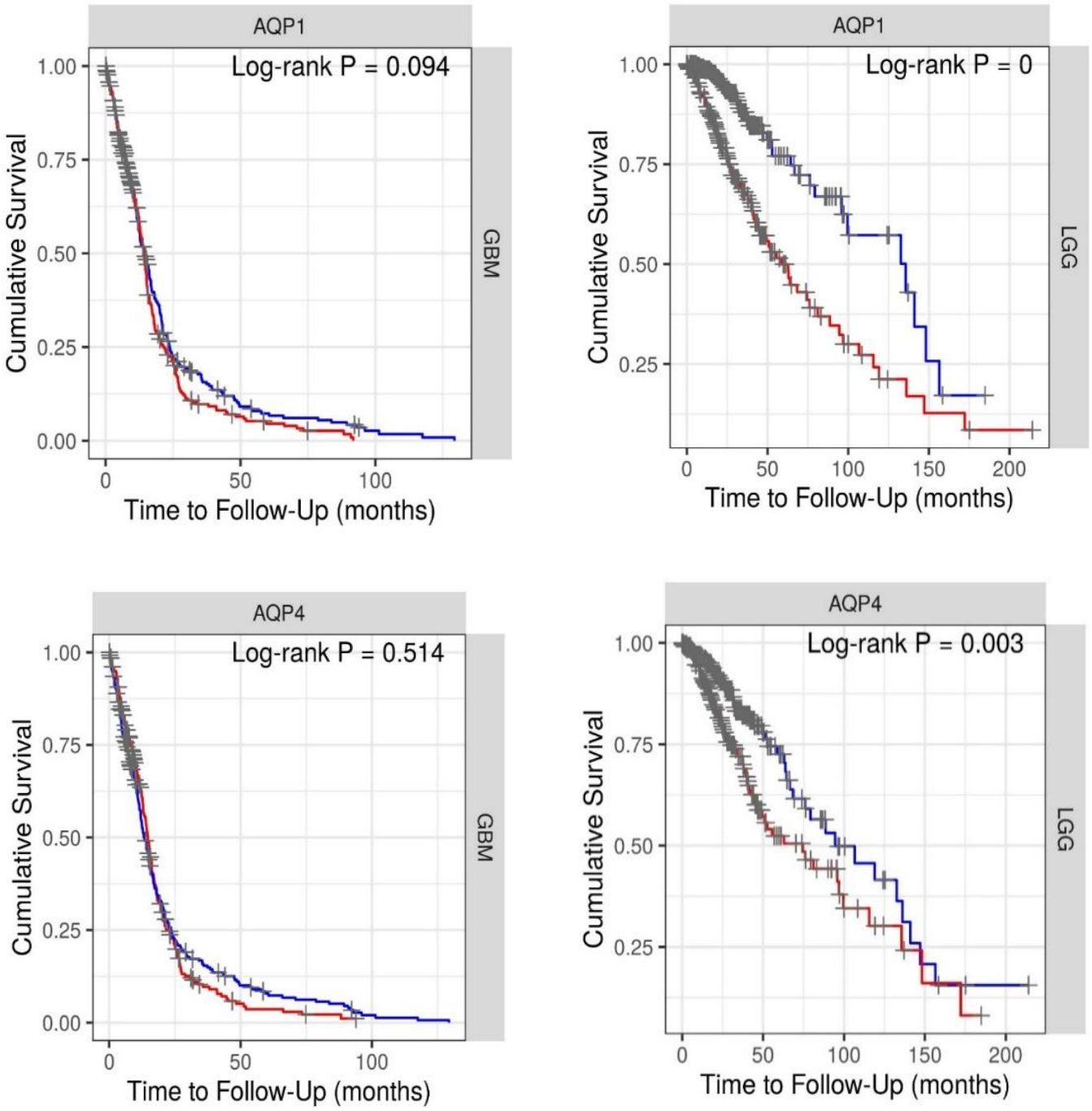

Figure 5 – Kaplan–Meier survival analysis. (**A** and **C**) patients with GBM and (**B** and **D**) patients with LGG. The Cox proportional hazard ratio (HR) and the 95% confidence interval were used in the Kaplan–Meier survival analysis. GBM, N = 523 patients with 448 dying. LGG, N = 514 patients with 125 dying. Log-rank P values ≤ 0.05 were considered statistically significant. All graphs were derived by the TIMER database in September 2021.

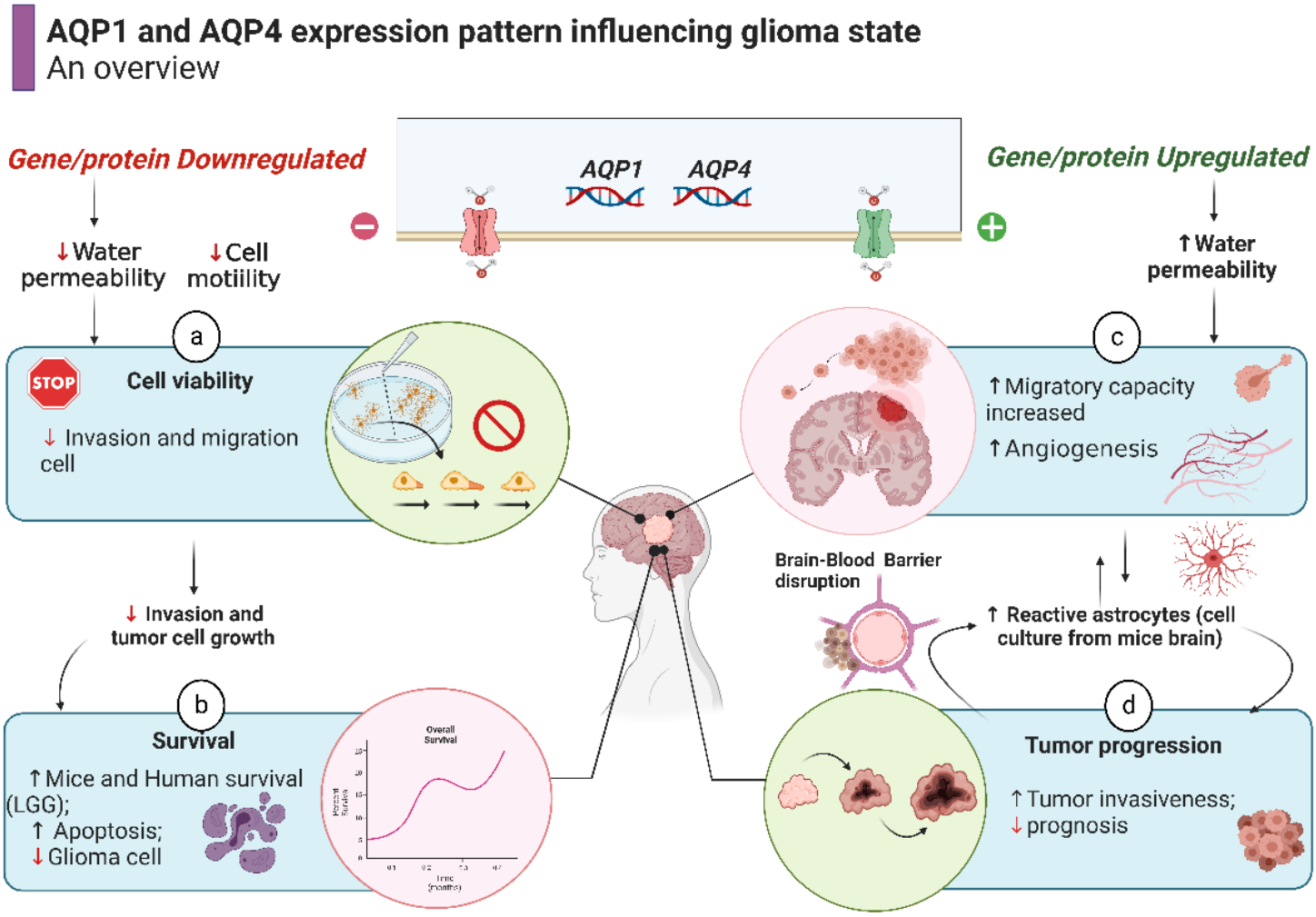

Figure 6 -. Schematic representation of cell processes involving AQPs activity in glioma state (already demonstrated by prior studies), resulting in better or worse outcome for a patient. The overall survival in human patient with LGG is shown in Figure 5.

7. References

1. Jäkel S, Dimou L. Glial Cells and Their Function in the Adult Brain: A Journey through the History of Their Ablation. Front Cell Neurosci. v. 11, n. 24, 2017.
2. Pekny M, Pekna M, Messing A, Steinhäuser C, Lee JM, Parpura V, Hol EM, Sofroniew MV, Verkhratsky A. Astrocytes: a central element in neurological diseases. Acta Neuropathol. 2016 Mar;131(3):323-45. doi: 10.1007/s00401-015-1513-1. Epub 2015 Dec 15. PMID: 26671410.
3. Zhangsen Huang, Lik-Wei Wong, Yixun Su, Xiaomin Huang, Nan Wang, Hui Chen, Chenju Yi, Blood-brain barrier integrity in the pathogenesis of Alzheimer's disease, Frontiers in Neuroendocrinology, Volume 59, 2020, 100857, ISSN 0091-3022, https://doi.org/10.1016/j.yfrne.2020.100857.
4. Tognatta, Reshmi et al. "Astrocytes Are Required for Oligodendrocyte Survival and Maintenance of Myelin Compaction and Integrity." *Frontiers in cellular neuroscience* vol. 14 74. 2 Apr. 2020, doi:10.3389/fncel.2020.00074.
5. Wurm, Julian et al. "Astrogliosis Releases Pro-Oncogenic Chitinase 3-Like 1 Causing MAPK Signaling in Glioblastoma." *Cancers* vol. 11,10 1437. 26 Sep. 2019, doi:10.3390/cancers11101437.
6. Moulson, Aaron J et al. "Diversity of Reactive Astrogliosis in CNS Pathology: Heterogeneity or Plasticity?" *Frontiers in cellular neuroscience* vol. 15 703810. 26 Jul. 2021, doi:10.3389/fncel.2021.703810.
7. Pekny, Milos et al. "The dual role of astrocyte activation and reactive gliosis." *Neuroscience letters* vol. 565 (2014): 30-8. doi:10.1016/j.neulet.2013.12.071.
8. O'Brien, Emma R et al. "The role of astrocytes in CNS tumors: pre-clinical models and novel imaging approaches." *Frontiers in cellular neuroscience* vol. 7 40. 16 Apr. 2013, doi:10.3389/fncel.2013.00040.
9. Katsouri L, Birch AM, Renziehausen AWJ, Zach C, Aman Y, Steeds H, Bonsu A, Palmer EOC, Mirzaei N, Ries M, Sastre M. Ablation of reactive astrocytes exacerbates disease pathology in a model of Alzheimer's disease. Glia. 2020 May;68(5):1017-1030. doi: 10.1002/glia.23759. Epub 2019 Dec 4. PMID: 31799735; PMCID: PMC738362.

10. Cheng, Y., Franco-Barraza, J., Wang, Y. *et al.* Sustained hedgehog signaling in medulloblastoma tumoroids is attributed to stromal astrocytes and astrocyte-derived extracellular matrix. *Lab Invest* 100, 1208–1222 (2020). https://doi.org/10.1038/s41374-020-0443-2
11. Louis DN, Perry A, Reifenberger G, von Deimling A, Figarella-Branger D, Cavenee WK, et al. The 2016 World Health Organization Classification of Tumors of the central nervous system: a summary. Acta Neuropathol (2016) 131:803–820. doi: 10.1007/s00401-016-1545-1
12. Ostrom QT, Bauchet L, Davis FG, Deltour I, Fisher JL, Langer CE, et al. The epidemiology of glioma in adults: A state of the science review. Neuro Oncol (2014) 16:896–913. doi: 10.1093/neuonc/nou087
13. Singh, Raj et al. “Dose Escalated Radiation Therapy for Glioblastoma Multiforme: An International Systematic Review and Meta-Analysis of 22 Prospective Trials.” *International journal of radiation oncology, biology, physics* vol. 111,2 (2021): 371-384. doi:10.1016/j.ijrobp.2021.05.001
14. Ferlay J, Ervik M, Lam F, Colombet M, Mery L, Piñeros M, Znaor A, Soerjomataram I, Bray F (2020). Global Cancer Observatory: Cancer Today. Lyon, France: International Agency for Research on Cancer. Available from: https://gco.iarc.fr/today, accessed [DD Month YYYY].
15. Sung H, Ferlay J, Siegel RL, Laversanne M, Soerjomataram I, Jemal A, Bray F. Global cancer statistics 2020: GLOBOCAN estimates of incidence and mortality worldwide for 36 cancers in 185 countries. CA Cancer J Clin. 2021 Feb 4. doi: 10.3322/caac.21660. Epub ahead of print. PMID: 33538338.
16. Ferlay J, Colombet M, Soerjomataram I, Parkin DM, Piñeros M, Znaor A, Bray F. Cancer statistics for the year 2020: An overview. Int J Cancer. 2021 Apr 5. doi: 10.1002/ijc.33588. Epub ahead of print. PMID: 33818764.
17. Instituto Nacional de Câncer José Alencar Gomes da Silva. Estimativa 2020 : incidência de câncer no Brasil / Instituto Nacional de Câncer José Alencar Gomes da Silva. – Rio de Janeiro : INCA, 2019.
18. Louis DN, Ohgaki H, Wiestler OD, Cavenee WK, Burger PB, Jouvet A, et al. The 2007 WHO classification of tumours of the central nervous system. Acta Neuropathol (2007) 114:97–109. doi: 10.1007/s00401-007-0243-4

19. 6. Lima FRS, Kahn SA, Soletti RC, Biasoli D, Alves T, da Fonseca ACC, et al. Glioblastoma: therapeutic challenges, what lies ahead. Biochim Biophys Acta Rev Cancer (2012) 2:338–349. doi: 10.1016/j.bbcan.2012.05.004.
20. 27. Perry A, Wesseling P. “Histologic classification of gliomas,”. In: Handbook of Clinical Neurology, Cambridge, MA: Academic Press (2016). pp. 71–95. doi: 10.1016/B978-0-12-802997-8.00005-0
21. Martinez-Lage M, Sahm F. Practical implications of the updated WHO classification of brain tumors. Semin Neurol (2018) 38:11–18. doi: 10.1055/s-0038-1641162
22. Fedele M, Cerchia L, Pegoraro S, Sgarra R, Manfioletti G. Proneural-mesenchymal transition: phenotypic plasticity to acquire multitherapy resistance in glioblastoma. Int J Mol Sci (2019) 20:2746. doi: 10.3390/ijms20112746.
23. Wesolowski JR, Rajdev P, Mukherji SK. Temozolomide (Temodar). AJNR Am J Neuroradiol (2010) 31:1383–1384. doi: 10.3174/ajnr.A2170
24. Strobel H, Baisch T, Fitzel R, Schilberg K, Siegelin MD, Karpel-Massler G, et al. Temozolomide and other alkylating agents in glioblastoma therapy. Biomedicines (2019) 7:69. doi: 10.3390/biomedicines7030069
25. Umans RA, Sontheimer H. Combating malignant astrocytes: strategies mitigating tumor invasion. Neurosci Res (2018) 126:22–30. doi: 10.1016/j.neures.2017.09.010
26. Gerstner, Elizabeth R et al. “Bevacizumab Reduces Permeability and Concurrent Temozolomide Delivery in a Subset of Patients with Recurrent Glioblastoma.” *Clinical cancer research : an official journal of the American Association for Cancer Research* vol. 26,1 (2020): 206-212. doi:10.1158/1078-0432.CCR-19-1739
27. Champeaux C, Weller J. Implantation of carmustine wafers (Gliadel ®) for high-grade glioma treatment. A 9-year nationwideretrospective study. *J Neurooncol* 2020;147:159-69.
28. Ashby LS, Smith KA, Stea B. Gliadel wafer implantation combined with standard radiotherapy and concurrent followed by adjuvanttemozolomide for treatment of newly diagnosed high-grade glioma: a systematic literature review. *World J Surg Oncol* 2016;14:225.
29. Wang H, Ran J, Jiang T. “Urea,”. In: Yang B, Sands JM, eds. Urea Transporters. Heidelberg, Germany: Springer (2014). pp. 7–29. doi: 10.1007/978-94-017-9343-8

30. Maugeri R, Schiera G, Di Liegro CM, Fricano A, Iacopino DG, Di Liegro I. Aquaporins and brain tumors. Int J Mol Sci (2016) 17:1029. doi: 10.3390/ijms17071029.
31. Saadoun S, Papadopoulos MC, Davies DC, Krishna S, Bell BA. Aquaporin-4 expression is increased in oedematous human brain tumours. J Neurol Neurosurg Psychiatry (2002) 72, 262–265. doi: 10.1136/jnnp.72.2.262.
32. 11. Yang, B. (2017). LIBRO: Aquaporins. In *Advances in Experimental Medicine and Biology* (Vol. 969). https://doi.org/10.1007/978-94-024-1057-0
33. Yang B, Brown D, Verkman AS.The mercurial insensitive water channel (AQP-4) forms orthogonal arrays in stably transfected chinese hamster ovary cells. J Biol Chem (1996) 271:4577–4580.
34. Nesverova, Veronika, and Susanna Törnroth-Horsefield. “Phosphorylation-Dependent Regulation of Mammalian Aquaporins.” *Cells* vol. 8,2 82. 23 Jan. 2019, doi:10.3390/cells8020082
35. 16. Mestre H, Hablitz LM, Xavier AL, Feng W, Zou W, Pu T, et al. Aquaporin-4-dependent glymphatic solute transport in the rodent brain. Elife (2018) 7:e40070. doi: 10.7554/eLife.40070.
36. Smith AJ, Yao X, Dix JA, Jin BJ, Verkman AS. Test of the ‘glymphatic’ hypothesis demonstrates diffusive and aquaporin-4-independent solute transport in rodent brain parenchyma. eLife (2017) 6:1–16. doi: 10.7554/eLife.27679.
37. Hubbard JA, Szu JI, Binder DK. The role of aquaporin-4 in synaptic plasticity, memory and disease. Brain Res Bull (2018) 136:118–129. doi: 10.1016/j.brainresbull.2017.02.011
38. Isoardo G, Morra I, Chiarle G, Audrito V, Deaglio S, Melcarne A, et al. Different aquaporin-4 expression in glioblastoma multiforme patients with and without seizures. Mol Med (2012) 18:1147–1151. doi: 10.2119/molmed.2012.00015.
39. Saadoun S, Papadopoulos MC, Davies DC, Krishna S, Bell BA. Aquaporin-4 expression is increased in oedematous human brain tumours. J Neurol Neurosurg Psychiatry (2002) 72, 262–265. doi: 10.1136/jnnp.72.2.262
40. Sadana P, Coughlin L, Burke J, Woods R, Mdzinarishvili A. Anti-edema action of thyroid hormone in MCAO model of ischemic brain stroke: possible association with AQP4 modulation. J Neurol Sci (2015) 354:37–45. doi: 10.1016/j.jns.2015.04.042

41. Mader S, Brimberg L. Aquaporin-4 water channel in the brain and its implication for health and disease. Cells (2019) 8:90. doi: 10.3390/cells8020090.
42. Ximenes-da-Silva A. Metal ion toxins and brain aquaporin-4 expression: An overview. Front Neurosci (2016) 10:233. doi: 10.3389/fnins.2016.00233.
43. Costa LES, Clementino-Neto, J, Mendes, CB, Franzon, NH, Costa, EDO, Moura-Neto V, Ximenes-da-Silva, A. Evidence of aquaporin 4 regulation by thyroid hormone during mouse brain development and in cultured human glioblastoma multiforme cells. Front Neurosci (2019) 13:137. doi: 10.3389/fnins.2019.00317.
44. Ding T, Ma Y, Li W, Liu X, Ying G, Fu L, et al. Role of aquaporin-4 in the regulation of migration and invasion of human glioma cells. Int J Oncol (2011) 38:1521–1531. doi: 10.3892/ijo.2011.983
45. Lan YL, Wang X, Lou JC, Ma XC. Zhang, B. The potential roles of aquaporin 4 in malignant gliomas. Oncotarget (2017) 8:32345–32355. doi: 10.18632/oncotarget.16017
46. Dubois LG, Campanati L, Righy C, D'Andrea-Meira I, Spohr TC, Porto-Carreiro I, et al. Gliomas and the vascular fragility of the blood brain barrier. Front Cell Neurosci (2014) 8:1–13. doi: 10.3389/fncel.2014.00418
47. 4. Maugeri R, Schiera G, Di Liegro CM, Fricano A, Iacopino DG, Di Liegro I. Aquaporins and brain tumors. Int J Mol Sci (2016) 17:1029. doi: 10.3390/ijms17071029.
48. Ding T, Ma Y, Li W, Liu X, Ying G, Fu L, et al. Role of aquaporin-4 in the regulation of migration and invasion of human glioma cells. Int J Oncol (2011) 38:1521–1531. doi: 10.3892/ijo.2011.983
49. Ding T, Gu F, Fu L, Ma YJ. Aquaporin-4 in glioma invasion and an analysis of molecular mechanisms. J Clin Neurosci (2010) 17, 1359–1361. doi: 10.1016/j.jocn.2010.02.014.
50. Cheng Y, Gao F, Jiang R, Lui H, Hou J, Yi Y, et al. Down-regulation of AQP4 expression via p38 MAPK signaling in temozolomide-induced glioma cells growth inhibition and invasion impairment. J Cell Biochem (2017) 118:4905–4913. doi: 10.1002/jcb.26176.
51. Simone L, Pisani F, Mola MG, De Bellis M, Merla G, Micale L, et al. AQP4 aggregation state is a determinant for glioma cell fate. Cancer Res (2019) 79:2182–2194. doi: 10.1158/0008-5472.CAN-18-2015.

52. Li J, Jia M, Chen G, et al. Involvement of p38 mitogen-activated protein kinase in altered expressions of AQP1 and AQP4 after carbon monoxide poisoning in rat astrocytes. Basic Clin Pharmacol Toxicol (2019) 125(4):394-404. doi:10.1111/bcpt.13247.
53. Giammanco M, Di Liegro CM, Schiera G, Di Liegro I. Genomic and Non-Genomic Mechanisms of Action of Thyroid Hormones and Their Catabolite 3,5-Diiodo-L-Thyronine in Mammals. Int J Mol Sci. 2020 Jun 10;21(11):4140. doi: 10.3390/ijms21114140. PMID: 32532017; PMCID: PMC7312989.
54. Lohela TJ, Lilius TO, Nedergaard M. The glymphatic system: implications for drugs for central nervous system diseases. Nat Rev Drug Discov. 2022 Aug 10. doi: 10.1038/s41573-022-00500-9. Epub ahead of print. PMID: 35948785.
55. Huang, Shifang et al. “Targeting AQP4 localization as a novel therapeutic target in CNS edema.” *Acta biochimica et biophysica Sinica* vol. 53,2 (2021): 269-272. doi:10.1093/abbs/gmaa158.
56. Yasui M, Hazama A, Kwon TH, Nielsen S, Guggino WB, Agre P. Rapid gating and anion permeability of an intracellular aquaporin. Nature 1999;402:184–187.
57. Soveral G, Prista C, Moura TF, Loureiro-Dias MC. Yeast water channels: an overview of orthodox aquaporins. Biol Cell. 2010 Jan;103(1):35-54. doi: 10.1042/BC20100102. PMID: 21143194.

Figure Legends

Figure 1 - Differential expression AQPs mRNAs in gliomas samples from TCGA and GTEx dataset. AQP1 and AQP4 genes in normal (N=163; blue box for AQP1 data and green box for AQP4 data) and tumor (N=207; purple box) samples. Tumor samples are divided into LGG and GBM groups (X axis of both graphs). TPM: transcripts per kilobase million; LGG: low-grade glioma; GBM: glioblastoma multiforme. *$p < 0.05$. Graphs A and B were derived by the GEPIA2 webserver in January 2021.

Figure 2. Differential expression AQPs mRNAs in gliomas samples from TCGA and GTEx dataset. AQP1 and AQP4 genes. Tumor samples are divided into LGG and GBM subtypes groups. A and B represents both AQP1 and AQP4 profiles of expression in LGG subtypes. C and D represents both AQP1 and AQP4 profiles of expression in GBM subtypes. LGG: low-grade glioma; GBM: glioblastoma multiforme. *p < 0.05. All graphs were derived by the GEPIA database in January 2021

Figure 3. Representative immunohistochemical staining distribution of AQP1 and AQP4 expressions in normal and glioma patient samples. Plates A-F are captured in 100 µm; superimposed thumbnails in 200 µm. All data were extracted from the Human Protein Atlas (https://www.proteinatlas.org/).

Figure 4 – Figure 4 – Expression matrix graphs based on a list of genes considered biomarkers of glioma and AQP1 and AQP4. A) Heat Map derived from GEPIA2. The color density in each block represents the median value of gene expression in tumor tissue (GBM and LGG, separately) normalized by the maximum median value of the expression in all blocks. These data were transformed for plotting (linear to log2(TPM + 1)). Graphs B and C were created from the values provided by the heap map for each gene with a subsequent comparison with both AQP1 and AQP4, respectively. For this, one-way ANOVA was performed followed by Tukey's multiple comparisons tests using GraphPad Prism version 8.0. p-value < 0,05 *; p< 0,01 **; p< 0,001 *** and p< 0,0001 ****. TP53: Tumor Protein P53, IDH1: Isocitrate Dehydrogenase (NADP(+)) 1, EGFR: Epidermal Growth Factor Receptor, ATRX: ATRX Chromatin Remodeler, TERT: Telomerase Reverse Transcriptase, and GFAP: Glial Fibrillary Acidic Protein.

Figure 5. Kaplan–Meier survival analysis. (A and C) Patients with GBM and (B and D) patients with LGG. The Cox proportional hazard ratio (HR) and the 95% confidence interval were used in the Kaplan–Meier survival analysis. GBM, N = 523 patients with 448 dying. LGG, N = 514 patients with 125 dying. Log-rank P values ≤ 0.05 were considered statistically significant. All graphs were derived by the TIMER database in September 2021.

Figure 6. Schematic representation of cell processes involving AQPs activity in glioma state (already demonstrated by prior studies), resulting in better or worse outcome for a patient. The overall survival in human patient with LGG is shown in Figure 4.

Tables

Table 1. AQP's Differential Expression in Gliomas Samples from TCGA and GTEx dataset

GENE ID	LogFC	P-Value	Adjusted P-value
***AQP1**	1.42	1.66E-40	3.15E-40
***AQP4**	1.02	8.82E-26	1.48E-25
***AQP5**	-2.18	1.15E-100	3.51E-100
***AQP7**	-3.11	1.1E-114	3.76E-114
***AQP8**	-2.19	7.71E-124	2.83E-123

Note: * Orthodox aquaporins: functional division of AQPS. This group is permeable to water, but not to small neutral solutes. Other members of the family of these proteins are aquaglyceroporins (Yasui et al., 1999; Soveral et al., 2010).

Table 2 – Correlation analysis between genes involved in the Tyrosine Metabolism pathway and AQP's genes

Gliomas (LGG and GBM)				
	AQP1		***AQP4***	
Gene ID	**Coefficient**	**P-Value**	**Coefficient**	**P-Value**
PNMT	0.25	4.5e−17	0.31	4.5e−17
ALDH1A3	0.31	5.3e−17	0.17	5.3e−17
TPO	0.056	0.14	0.0062	0.87
AOC2	-0.21	3.7e−08	-0.15	3.7e−08
GOT1	−0.076	0.046	0.055	0.15
HGD	0.41	6.5e−29	0.14	6.5e−29
ADH1B	−0.063	0.1	0.079	0.039
TYRP1	0.12	0.0017	0.17	1.2e−05
TH	−0.01	0.79	−0.033	0.39

Table 3 – Correlation analysis between genes involved in the Thyroid Hormones Synthesis pathway and AQP's genes

Gliomas (LGG and GBM)

	AQP1		*AQP4*	
Gene ID	**Coefficient**	**P-Value**	**Coefficient**	**P-Value**
PRKCG	−0.075	0.049	0.17	4.8e−06
ADCY1	0.12	0.0023	0.18	1.2e−06
ATP1B1	0.23	1.2e−09	0.35	5.9e−21
ADCY5	-0.32	2.9e−17	0.0065	0.86
TPO	0.056	0.14	0.0062	0.87
PLCB4	-0.3	8.9e−16	−0.096	0.012
TG	0.18	4.3e−06	0.16	3.2e−05
CREB3L3	−0.082	0.033	0.1	0.0076
IYD	0.048	0.21	0.056	0.14
GPX2	−0.065	0.088	0.045	0.24
PRKCB	-0.18	1.3e−06	0.11	1.3e−06
ADCY4	0.068	0.076	−0.037	0.33
ITPR1	0.23	2.6e−09	0.26	2.6e−09
ATP1A3	-0.31	1.2e−16	-0.12	1.2e−16
LRP2	0.16	3.4e−05	0.22	3.4e−05

Table 4 – Correlation analysis between genes involved in the Thyroid Hormones Signaling pathway and AQP's genes

Gliomas (LGG and GBM)				
	AQP1		***AQP4***	
Gene ID	**Coefficient**	**P-Value**	**Coefficient**	**P-Value**
SIN3A	-0.14	0.00041	0.14	0.00024
HDAC1	0.44	3.6e−34	0.15	7.6e−05
MED24	-0.24	2.1e−10	-0.22	5e−09
ATP2A2	-0.15	0.00013	0.16	3.5e−05
MTOR	0.27	3.3e−13	0.26	8e−12
ACTG1	0.096	0.012	0.029	0.45
ACTB	0.35	1e−20	0.038	0.32

Table 5 – Genes involved in thyroid hormone and tyrosine pathways and their function

Official Symbol	Official Full Name
PRKCG	Protein kinase C gamma
ADCY1	Adenylate cyclase 1
ATP1B1	Atpase Na+/k+ transporting subunit beta 1
ADCY5	Adenylate cyclase 5
TPO	Thyroid peroxidase
PLCB4	Phospholipase C beta 4
TG	Thyroglobulin
CREB3L3	Camp responsive element binding protein 3 like 3
IYD	Iodotyrosine deiodinase
GPX2	Glutathione peroxidase 2
PRKCB	Protein kinase C beta type
ADCY4	Adenylate cyclase 4
ITPR1	Inositol1,4,5 – triphosphate receptor type 1
ATP1A3	Atpase Na+/k+ transporting subunit alfa 3
LRP2	LDL receptor related protein 2
SIN3A	Transcription regulator Family member A
HDAC1	Histone deacetylase 1
MED24	Mediator complex subunit 24
ATP2A2	Atpase Na+/k+ transporting subunit alfa 2
MTOR	Mechanistic Target of Rapamaycin kinase
ACTG1	Actin gamma 1
ACTB	Actin beta
PNMT	Phenylethanolamine N-methyltranferase
ALDH1A3	Aldehyde dehydrogenase 1 family member A3
AOC2	Amine Oxidase Copper Containing 2
HGD	Homogentisate 1,2 - dioxygenase
ADH1B	Alcohol dehydrogenase 1B
TYRP1	Tyrosinase-related protein 1
TH	Tyrosine Hydroxilase

Note: All information was derived from the National Center for Biotechnology Information (NCBI) database. Available in: https://www.ncbi.nlm.nih.gov/guide/genes-expression/.

5 CONSIDERAÇÕES FINAIS

O tecido cerebral é sabidamente plástico e heterogêneo. Fatores como idade e sexo, por exemplo, podem influenciar sua composição genética. É possível que as características dos diferentes graus de malignidade dos gliomas (bem como o comportamento molecular das células derivados deste) também mudem dependendo da região cerebral de ocorrência do tumor.

Nosso estudo mostra pela primeira vez uma relação funcional entre a AQP1 e as vias ligadas à síntese e sinalização do hormônio tireoidiano em neoplasias malignas intracranianas. A expressão dos genes das AQP1 e AQP4 está significativamente relacionada a um pior prognóstico em pacientes com glioma de baixo grau. Talvez estes transportadores de água exerçam papei significativos na progressão e na recorrência dos gliomas. A possível interação entre as vias moleculares analisadas neste trabalho e os genes AQP1 e AQP4 podem ser úteis para o diagnóstico molecular de gliomas e para a triagem de novas drogas antitumorais para esses tumores malignos.

6 REFERÊNCIA BIBLIOGRÁFICAS

Warth A, Simon P, Capper D, et al. Expression pattern of the water channel aquaporin-4 in human gliomas is associated with blood-brain barrier disturbance but not with patient survival. J Neurosci Res (2007) 85(6)

Honasoge A, Sontheimer H. Involvement of tumor acidification in brain cancer pathophysiology. Front Physiol (2013) 4:316.

Ashby LS, Smith KA, Stea B. Gliadel wafer implantation combined with standard radiotherapy and concurrent followed by adjuvanttemozolomide for treatment of newly diagnosed high-grade glioma: a systematic literature review. *World J Surg Oncol* 2016;14:225.

ASSINCK, P. et al. “Myelinogenic Plasticity of Oligodendrocyte Precursor Cells following Spinal Cord Contusion Injury.” The Journal of neuroscience: the official journal of the Society for Neuroscience. v. 37, n. 36, 2017

Bartlett, Andrew et al. “Generations of interdisciplinarity in bioinformatics.” New genetics and society vol. 35,2 (2016): 186-209. doi:10.1080/14636778.2016.1184965

Bhat, P., Honson, D. & Guttman, M. Nuclear compartmentalization as a mechanism of quantitative control of gene expression. *Nat Rev Mol Cell Biol* 22, 653–670 (2021)

Brad T Sherman, Ming Hao, Ju Qiu, Xiaoli Jiao, Michael W Baseler, H Clifford Lane, Tomozumi Imamichi, Weizhong Chang, DAVID: a web server for functional enrichment analysis and functional annotation of gene lists (2021 update), *Nucleic Acids Research*, Volume 50, Issue W1, 5 July 2022, Pages W216–W221

Carmeliet P, Jain RK. Molecular mechanisms and clinical applications of angiogenesis. Nature 2011;473:298–307

Champeaux C, Weller J. Implantation of carmustine wafers (Gliadel ®) for high-grade glioma treatment. A 9-year nationwideretrospective study. *J Neurooncol* 2020;147:159-69.

Cheng Y, Gao F, Jiang R, Lui H, Hou J, Yi Y, et al. Down-regulation of AQP4 expression via p38 MAPK signaling in temozolomide-induced glioma cells growth inhibition and invasion impairment. J Cell Biochem (2017) 118:4905–4913.

Cheng, Y., Franco-Barraza, J., Wang, Y. *et al.* Sustained hedgehog signaling in medulloblastoma tumoroids is attributed to stromal astrocytes and astrocyte-derived extracellular matrix. *Lab Invest* 100, 1208–1222 (2020).

Chinnappan, J., Ramu, A., V., V.R. *et al.* Integrative Bioinformatics approaches to therapeutic gene target selection in various cancers for Nitroglycerin. *Sci Rep* 11, 22036 (2021).

Costa LES, Clementino-Neto, J, Mendes, CB, Franzon, NH, Costa, EDO, Moura-Neto V, Ximenes-da-Silva, A. Evidence of aquaporin 4 regulation by thyroid hormone during mouse brain development and in cultured human glioblastoma multiforme cells. Front Neurosci (2019) 13:137.

Davis, N., Mota, B.C., Stead, L. *et al.* Pharmacological ablation of astrocytes reduces Aβ degradation and synaptic connectivity in an ex vivo model of Alzheimer's disease. *J Neuroinflammation* 18, 73 (2021).

Ding T, Gu F, Fu L, Ma YJ. Aquaporin-4 in glioma invasion and an analysis of molecular mechanisms. J Clin Neurosci (2010) 17, 1359–1361.

Ding T, Ma Y, Li W, Liu X, Ying G, Fu L, et al. Role of aquaporin-4 in the regulation of migration and invasion of human glioma cells. Int J Oncol (2011) 38:1521–1531.

Ding T, Ma Y, Li W, Liu X, Ying G, Fu L, et al. Role of aquaporin-4 in the regulation of migration and invasion of human glioma cells. Int J Oncol (2011) 38:1521–1531.

Dubois LG, Campanati L, Righy C, D'Andrea-Meira I, Spohr TC, Porto-Carreiro I, et al. Gliomas and the vascular fragility of the blood brain barrier. Front Cell Neurosci (2014) 8:1–13.

Fedele M, Cerchia L, Pegoraro S, Sgarra R, Manfioletti G. Proneural-mesenchymal transition: phenotypic plasticity to acquire multitherapy resistance in glioblastoma. Int J Mol Sci (2019) 20:2746.

Ferlay J, Colombet M, Soerjomataram I, Parkin DM, Piñeros M, Znaor A, Bray F. Cancer statistics for the year 2020: An overview. Int J Cancer. 2021 Apr 5. doi: 10.1002/ijc.33588. Epub ahead of print.

Ferlay J, Ervik M, Lam F, Colombet M, Mery L, Piñeros M, Znaor A, Soerjomataram I, Bray F (2020). Global Cancer Observatory: Cancer Today. Lyon, France: International Agency for Research on Cancer.

Galán-Cobo, Ana et al. “Aquaporin-1 plays important role in proliferation by affecting cell cycle progression.” *Journal of cellular physiology* vol. 231,1 (2016): 243-56.

Gerstner, Elizabeth R et al. “Bevacizumab Reduces Permeability and Concurrent Temozolomide Delivery in a Subset of Patients with Recurrent Glioblastoma.” *Clinical cancer research : an official journal of the American Association for Cancer Research* vol. 26,1 (2020): 206-212.

Gu, Yuhang et al. “Cerebral edema after ischemic stroke: Pathophysiology and underlying mechanisms.” *Frontiers in neuroscience* vol. 16 988283. 18 Aug. 2022

Giammanco M, Di Liegro CM, Schiera G, Di Liegro I. Genomic and Non-Genomic Mechanisms of Action of Thyroid Hormones and Their Catabolite 3,5-Diiodo-L-Thyronine in Mammals. Int J Mol Sci. 2020 Jun 10;21(11):4140.

GOMES, F. C. A; TORTELLI, V. P; DINIZ, L. Glia: dos velhos conceitos às novas funções de hoje e as que ainda virão citação. Neurociências • Estud. av. v. 27, n. 77, 2013.

Hayashi Y, Edwards NA, Proescholdt MA, Oldfield EH, Merrill MJ. Regulation and function of aquaporin-1 in glioma cells. Neoplasia (2007) 9:777–787.

Hubbard JA, Szu JI, Binder DK. The role of aquaporin-4 in synaptic plasticity, memory and disease. Brain Res Bull (2018) 136:118–129.

Instituto Nacional de Câncer José Alencar Gomes da Silva. Estimativa 2020 : incidência de câncer no Brasil / Instituto Nacional de Câncer José Alencar Gomes da Silva. – Rio de Janeiro : INCA, 2019.

Isoardo G, Morra I, Chiarle G, Audrito V, Deaglio S, Melcarne A, et al. Different aquaporin-4 expression in glioblastoma multiforme patients with and without seizures. Mol Med (2012) 18:1147–1151.

Jäkel S, Dimou L. Glial Cells and Their Function in the Adult Brain: A Journey through the History of Their Ablation. Front Cell Neurosci. v. 11, n. 24, 2017.

Kamaraj, B. & Purohit, R. Computational screening of disease-associated mutations in OCA2 gene. Cell Biochem. Biophys. 68(1), 97–109 (2014).

Katsouri L, Birch AM, Renziehausen AWJ, Zach C, Aman Y, Steeds H, Bonsu A, Palmer EOC, Mirzaei N, Ries M, Sastre M. Ablation of reactive astrocytes exacerbates disease pathology in a model of Alzheimer's disease. Glia. 2020 May;68(5):1017-1030..

Lan YL, Wang X, Lou JC, Ma XC. Zhang, B. The potential roles of aquaporin 4 in malignant gliomas. Oncotarget (2017)

Lan YL, Wang X, Lou JC, Ma XC. Zhang, B. The potential roles of aquaporin 4 in malignant gliomas. Oncotarget (2017) 8:32345–32355. doi:

Li J, Jia M, Chen G, et al. Involvement of p38 mitogen-activated protein kinase in altered expressions of AQP1 and AQP4 after carbon monoxide poisoning in rat astrocytes. Basic Clin Pharmacol Toxicol (2019) 125(4):394-404.

Li, Taiwen et al. “TIMER2.0 for analysis of tumor-infiltrating immune cells.” *Nucleic acids research* vol. 48,W1 (2020): W509-W514. doi:10.1093/nar/gkaa407

Lima FRS, Kahn SA, Soletti RC, Biasoli D, Alves T, da Fonseca ACC, et al. Glioblastoma: therapeutic challenges, what lies ahead. Biochim Biophys Acta Rev Cancer (2012) 2:338–349.

Lohela TJ, Lilius TO, Nedergaard M. The glymphatic system: implications for drugs for central nervous system diseases. Nat Rev Drug Discov. 2022 Aug 10. doi: 10.1038/s41573-022-00500-9.

Lonsdale, J., Thomas, J., Salvatore, M. *et al.* The Genotype-Tissue Expression (GTEx) project. *Nat Genet* 45, 580–585, 2013.

Louis DN, Ohgaki H, Wiestler OD, Cavenee WK, Burger PB, Jouvet A, et al. The 2007 WHO classification of tumours of the central nervous system. Acta Neuropathol (2007) 114:97–109

Louis DN, Perry A, Reifenberger G, von Deimling A, Figarella-Branger D, Cavenee WK, et al. The 2016 World Health Organization Classification of Tumors of the central nervous system: a summary. Acta Neuropathol (2016) 131:803–820.

Mader S, Brimberg L. Aquaporin-4 water channel in the brain and its implication for health and disease. Cells (2019) 8:90.

Martinez-Lage M, Sahm F. Practical implications of the updated WHO classification of brain tumors. Semin Neurol (2018) 38:11–18.

Mason, Shayne. “Lactate Shuttles in Neuroenergetics-Homeostasis, Allostasis and Beyond.” *Frontiers in neuroscience* vol. 11 43. 2 Feb. 2017,

Maugeri R, Schiera G, Di Liegro CM, Fricano A, Iacopino DG, Di Liegro I. Aquaporins and brain tumors. Int J Mol Sci (2016) 17:1029.

Maugeri R, Schiera G, Di Liegro CM, Fricano A, Iacopino DG, Di Liegro I. Aquaporins and brain tumors. Int J Mol Sci (2016) 17:1029..

Mestre H, Hablitz LM, Xavier AL, Feng W, Zou W, Pu T, et al. Aquaporin-4-dependent glymphatic solute transport in the rodent brain. Elife (2018) 7:e40070.

Moulson, Aaron J et al. “Diversity of Reactive Astrogliosis in CNS Pathology: Heterogeneity or Plasticity?.” *Frontiers in cellular neuroscience* vol. 15 703810. 26 Jul. 2021,

Nesverova, Veronika, and Susanna Törnroth-Horsefield. “Phosphorylation-Dependent Regulation of Mammalian Aquaporins.” *Cells* vol. 8,2 82. 23 Jan. 2019,

O'Brien, Emma R et al. “The role of astrocytes in CNS tumors: pre-clinical models and novel imaging approaches.” *Frontiers in cellular neuroscience* vol. 7 40. 16 Apr. 2013,

Ostrom QT, Bauchet L, Davis FG, Deltour I, Fisher JL, Langer CE, et al. The epidemiology of glioma in adults: A state of the science review. Neuro Oncol (2014) 16:896–913.

Pekny M, Pekna M, Messing A, Steinhäuser C, Lee JM, Parpura V, Hol EM, Sofroniew MV, Verkhratsky A. Astrocytes: a central element in neurological diseases. Acta Neuropathol. 2016 Mar;131(3):323-45. doi: 10.1007/s00401-015-1513-1. Epub 2015

Pekny, Milos et al. “The dual role of astrocyte activation and reactive gliosis.” *Neuroscience letters* vol. 565 (2014): 30-8.

Pellerin, L et al. “Evidence supporting the existence of an activity-dependent astrocyte-neuron lactate shuttle.” *Developmental neuroscience* vol. 20,4-5 (1998): 291-9.

Perry A, Wesseling P. “Histologic classification of gliomas,”. In: Handbook of Clinical Neurology, Cambridge, MA: Academic Press (2016). pp. 71–95.

Saadoun S, Papadopoulos MC, Davies DC, Krishna S, Bell BA. Aquaporin-4 expression is increased in oedematous human brain tumours. J Neurol Neurosurg Psychiatry (2002) 72, 262–265..

Saadoun S, Papadopoulos MC, Davies DC, Krishna S, Bell BA. Aquaporin-4 expression is increased in oedematous human brain tumours. J Neurol Neurosurg Psychiatry (2002) 72, 262–265

Sadana P, Coughlin L, Burke J, Woods R, Mdzinarishvili A. Anti-edema action of thyroid hormone in MCAO model of ischemic brain stroke: possible association with AQP4 modulation. J Neurol Sci (2015) 354:37–45.

Simone L, Pisani F, Mola MG, De Bellis M, Merla G, Micale L, et al. AQP4 aggregation state is a determinant for glioma cell fate. Cancer Res (2019) 79:2182–2194.

Singh, Raj et al. “Dose Escalated Radiation Therapy for Glioblastoma Multiforme: An International Systematic Review and Meta-Analysis of 22 Prospective Trials.” *International journal of radiation oncology, biology, physics* vol. 111,2 (2021): 371-384.

Smith AJ, Yao X, Dix JA, Jin BJ, Verkman AS. Test of the ‘glymphatic’ hypothesis demonstrates diffusive and aquaporin-4-independent solute transport in rodent brain parenchyma. eLife (2017) 6:1–16.

Strobel H, Baisch T, Fitzel R, Schilberg K, Siegelin MD, Karpel-Massler G, et al. Temozolomide and other alkylating agents in glioblastoma therapy. Biomedicines (2019) 7:69.

Sung H, Ferlay J, Siegel RL, Laversanne M, Soerjomataram I, Jemal A, Bray F. Global cancer statistics 2020: GLOBOCAN estimates of incidence and mortality worldwide for 36 cancers in 185 countries. CA Cancer J Clin. 2021 Feb 4.

Suzuki Y, Nakamura Y, Yamada K, Kurabe S, Okamoto K, Aoki H, et al. Aquaporin positron emission tomography differentiates between grade III and IV human astrocytoma. Neurosurgery (2018) 82:842–846.

Tang, Zefang et al. “GEPIA2: an enhanced web server for large-scale expression profiling and interactive analysis.” *Nucleic acids research* vol. 47,W1 (2019): W556-W560.

The Cancer Genome Atlas Research Network., Weinstein, J., Collisson, E. *et al.* The Cancer Genome Atlas Pan-Cancer analysis project. *Nat Genet* 45, 1113–1120 (2013)

Tognatta, Reshmi et al. “Astrocytes Are Required for Oligodendrocyte Survival and Maintenance of Myelin Compaction and Integrity.” *Frontiers in cellular neuroscience* vol. 14 74. 2 Apr. 2020,.

Trillo-Contreras, José Luis et al. “AQP1 and AQP4 Contribution to Cerebrospinal Fluid Homeostasis.” *Cells* vol. 8,2 197. 24 Feb. 2019,

Ulgen, Ege et al. “pathfindR: An R Package for Comprehensive Identification of Enriched Pathways in Omics Data Through Active Subnetworks.” *Frontiers in genetics* vol. 10 858. 25 Sep. 2019,

Umans RA, Sontheimer H. Combating malignant astrocytes: strategies mitigating tumor invasion. Neurosci Res (2018) 126:22–30.

Wang H, Ran J, Jiang T. “Urea,”. In: Yang B, Sands JM, eds. Urea Transporters. Heidelberg, Germany: Springer (2014). pp. 7–29.

Wang, K. et al. Integrated bioinformatics analysis the function of RNA binding proteins (RBPs) and their prognostic value in breast cancer. Front. Pharmacol. 10(140), 1–11 (2019).

Wesolowski JR, Rajdev P, Mukherji SK. Temozolomide (Temodar). AJNR Am J Neuroradiol (2010) 31:1383–1384.

Wurm, Julian et al. “Astrogliosis Releases Pro-Oncogenic Chitinase 3-Like 1 Causing MAPK Signaling in Glioblastoma.” *Cancers* vol. 11,10 1437. 26 Sep. 2019,

Ximenes-da-Silva A. Metal ion toxins and brain aquaporin-4 expression: An overview. Front Neurosci (2016) 10:233.

Yang B, Brown D, Verkman AS.The mercurial insensitive water channel (AQP-4) forms orthogonal arrays in stably transfected chinese hamster ovary cells. J Biol Chem (1996) 271:4577–4580.

Yang, B. (2017). LIBRO: Aquaporins. In *Advances in Experimental Medicine and Biology* (Vol. 969).

Zhangsen Huang, Lik-Wei Wong, Yixun Su, Xiaomin Huang, Nan Wang, Hui Chen, Chenju Yi, Blood-brain barrier integrity in the pathogenesis of Alzheimer’s disease, Frontiers in Neuroendocrinology, Volume 59, 2020,

7 APÊNDICES

A

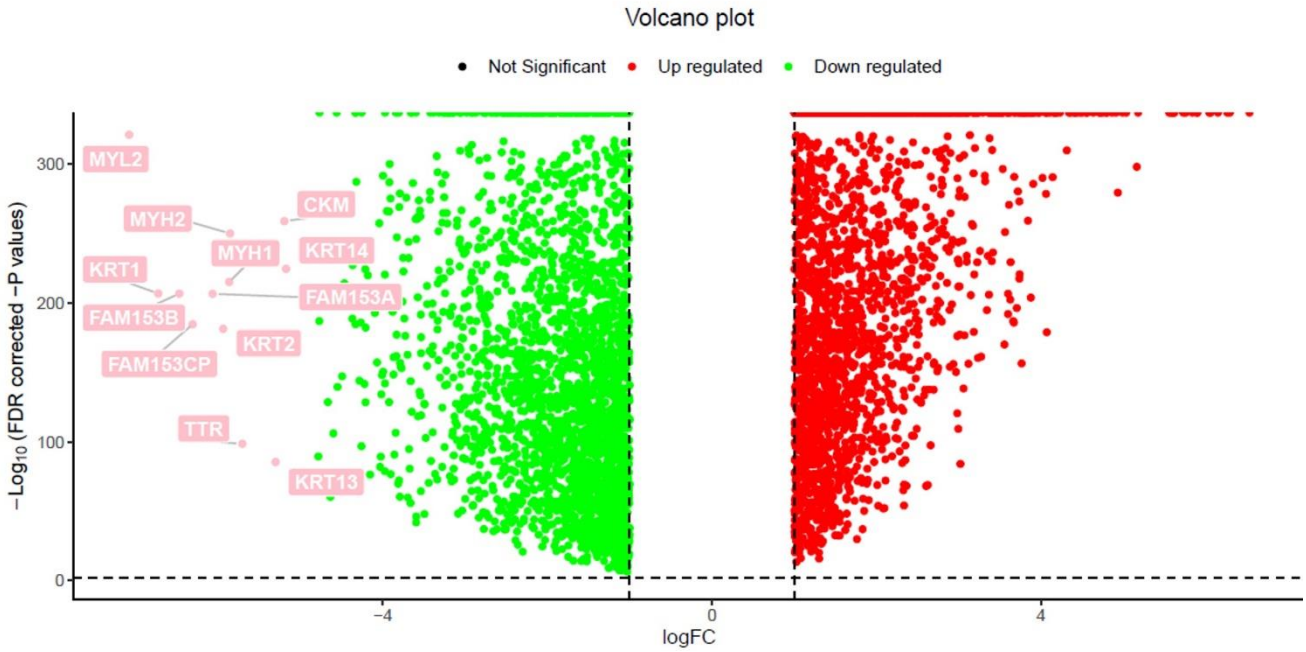

B

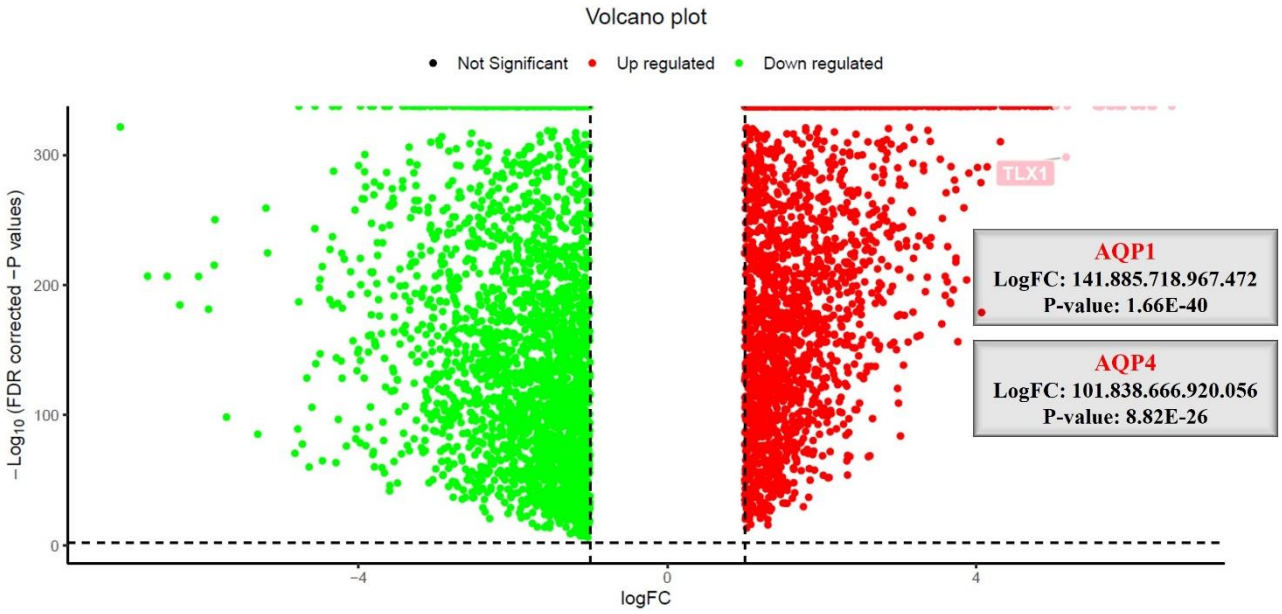

Figure 1 Supplementary – Volcano plots from differential analysis. **A)** represents the distribution of the overexpressed genes in gliomas (among them, *AQP1* and *AQP4*) and **B)** represents the down-regulated genes.

Table 2 Suplemmentary - Dysregulated pathways identified from up-regulated genes in gliomas by the DAVID tool

Term	Count	PValue	Genes	Fold Enrichment
hsa05150:Staphylococcus aureus infection	37	0.00	C1QB, C1QA, SELPLG, ITGAM, C1R, C5AR1, PTAFR, CFI, ITGB2, FPR1, FPR3, ITGAL, C2, ICAM1, C3, C4B, C4A, HLA-DMA, FCGR3A, HLA-DMB, FCGR3B, C3AR1, FCGR1A, HLA-DOA, HLA-DQA2, HLA-DQA1, HLA-DPA1, IL10, HLA-DRB5, FCGR2A, HLA-DPB1, HLA-DRA, MASP1, FCGR2B, HLA-DRB1, C1QC, HLA-DQB1	5.826.191.457.217.410
hsa05166:HTLV-I infection	69	168377.51	RB1, CDKN1A, SPI1, ITGB2, BUB1B, TNFRSF13C, CD3E, ITGAL, ETS1, TNF, PIK3CG, ICAM1, CDC20, CCND2, PTTG1, MYC, CHEK2, CHEK1, TSPO, HLA-DOA, HLA-DPA1, PDGFRA, MSX2, WNT5A, HLA-B, WNT9B, HLA-C, HLA-A, HLA-G, TGFBR1, HLA-E, TNFRSF1A, LCK, TP53, HLA-DQB1, PCNA, RELB, PIK3R5, HLA-DMA, HLA-DMB, POLD1, TP53INP1, POLD2, E2F2, MSX1, HLA-DQA2, HLA-DQA1, EGR1, CDKN2B, EGR2, HLA-DRB5, TGFB1, CDKN2C, FZD2, VCAM1, CDKN2A, NFATC2, FOSL1, CDK4, POLE2, IL2RA, IL2RB, HLA-DPB1, HLA-DRA, BAX, TCF3, CALR, HLA-DRB1, MAD2L1	2.309.894.591.359.020
hsa04514:Cell adhesion molecules (CAMs)	47	37134.10	NLGN3, CD86, NLGN1, SELPLG, ITGAM, SDC3, ITGB2, ITGAL, ICAM1, SPN, HLA-DMA, ALCAM, HLA-DMB, CDH2, ITGB8, ITGAV, TIGIT, HLA-DOA, HLA-DQA2, CD99, HLA-DQA1, MPZL1, JAM2, HLA-DPA1, CD276, HLA-DRB5, VCAM1, HLA-B, HLA-C,	28.144.031.059.036.500

			HLA-A, PDCD1LG2, HLA-G, HLA-E, CD2, CD4, VCAN, PTPRC, CD40LG, SELL, CLDN7, HLA-DPB1, SDC1, HLA-DRA, SIGLEC1, HLA-DRB1, NECTIN2, HLA-DQB1	
hsa05140:Leishmaniasis	31	62440.10	ITGAM, NCF1, NCF2, NCF4, ITGB2, TNF, C3, HLA-DMA, FCGR3A, HLA-DMB, FCGR3B, IRAK1, FCGR1A, HLA-DOA, HLA-DQA2, HLA-DQA1, HLA-DPA1, IL10, MARCKSL1, HLA-DRB5, TGFB1, CYBA, IL1A, FCGR2A, IL1B, HLA-DPB1, HLA-DRA, PTPN6, HLA-DRB1, HLA-DQB1, TLR2	3.712.616.863.106.940
hsa05332:Graft-versus-host disease	20	2861413.61	CD86, HLA-DRB5, HLA-B, HLA-C, HLA-A, TNF, HLA-G, HLA-E, IL1A, HLA-DMA, HLA-DMB, IL1B, HLA-DPB1, HLA-DRA, HLA-DOA, HLA-DQA2, HLA-DQA1, HLA-DRB1, HLA-DPA1, HLA-DQB1	5.153.388.021.125.960
hsa04145:Phagosome	47	2986563.62	ITGAM, NCF1, C1R, NCF2, NCF4, ITGB2, THBS2, CTSS, C3, MRC2, SEC61A1, TUBA1C, HLA-DMA, FCGR3A, HLA-DMB, FCGR3B, SEC61G, MRC1, OLR1, ITGAV, CD14, FCGR1A, HLA-DOA, HLA-DQA2, HLA-DQA1, HLA-DPA1, MSR1, HLA-DRB5, ATP6V0E1, HLA-B, HLA-C, TAP1, CYBA, HLA-A, HLA-G, HLA-E, FCGR2A, HLA-DPB1, HLA-DRA, TLR6, CALR, RAB7B, FCGR2B, HLA-DRB1, ATP6V1B1, HLA-DQB1, TLR2	26.643.016.069.221.200
hsa04110:Cell cycle	41	833806.90	RB1, CDKN1A, PCNA, BUB1B, TTK, CDC20, CCNB2, CCNB1, CDC45, CCND2, ORC1, PTTG1, CHEK2, MYC, CHEK1, E2F2, BUB1, CDKN2B, TGFB1, CDKN2C, CDKN2A, CDC6,	281.150.564.217.074

			CDC25C, CDC25A, GADD45G, WEE1, WEE2, RBL1, DBF4, CDK6, ESPL1, CDK4, CDK2, MCM3, CDK1, MCM4, MCM5, MCM6, TP53, MCM2, MAD2L1	
hsa04612:Antigen processing and presentation	30	235255.88	IFI30, TNF, CTSS, HLA-DMA, HLA-DMB, KLRC1, HLA-DOA, HLA-DQA2, B2M, HLA-DQA1, HLA-DPA1, CD74, HLA-DRB5, KLRC2, KLRC3, KLRC4, HLA-B, HLA-C, TAP1, RFXANK, HLA-A, HLA-G, HLA-E, CD4, HLA-DPB1, HLA-DRA, CALR, HLA-DRB1, LGMN, HLA-DQB1	33.564.829.874.438.800
hsa05330:Allograft rejection	20	3893534.63	IL10, CD86, HLA-DRB5, HLA-B, HLA-C, HLA-A, TNF, HLA-G, HLA-E, HLA-DMA, HLA-DMB, CD40LG, HLA-DPB1, HLA-DRA, HLA-DOA, HLA-DQA2, HLA-DQA1, HLA-DRB1, HLA-DPA1, HLA-DQB1	4.596.264.991.815.050
hsa05152:Tuberculosis	48	33737630.16	ITGAM, ITGB2, LSP1, NOD2, TNF, CTSS, C3, MRC2, CYP27B1, HLA-DMA, FCGR3A, HLA-DMB, FCGR3B, IRAK1, MRC1, FADD, CD14, FCGR1A, HLA-DOA, CTSD, HLA-DQA2, HLA-DQA1, HLA-DPA1, IL10, CD74, HLA-DRB5, TGFB1, FCER1G, SYK, RIPK2, IL10RA, SPHK1, IL18, RFXANK, TNFRSF1A, TLR1, IL1A, FCGR2A, IL1B, HLA-DPB1, BAX, HLA-DRA, TLR6, CLEC4E, FCGR2B, HLA-DRB1, HLA-DQB1, TLR2	2.305.922.775.554.670
hsa04940:Type I diabetes mellitus	20	55331490.20	CD86, HLA-DRB5, HLA-B, HLA-C, HLA-A, TNF, HLA-G, HLA-E, IL1A, HLA-DMA, HLA-DMB, IL1B, HLA-DPB1, HLA-DRA, HLA-DOA, HLA-DQA2, HLA-DQA1, HLA-DRB1, HLA-DPA1, HLA-DQB1	4.049.090.588.027.540

hsa04060:Cytokine-cytokine receptor interaction	59	55489878.51	CXCL9, CSF1, CCL4L2, TNFRSF13C, IL1RAP, CXCL13, CXCL3, TNF, EDA2R, TNFSF13B, CXCL16, TNFRSF8, CCR5, CCR2, IL13RA1, IL10, TNFRSF12A, TNFRSF19, IL18, LIFR, TNFRSF1B, TGFBR1, TNFRSF1A, IL1A, IL1B, TNFRSF21, CX3CR1, CSF1R, CXCR4, CSF2RB, CSF2RA, CCL8, CCL5, CCL4, CCL3, CCL2, IL12RB1, CCL18, TNFSF18, CCR1, NGFR, TGFB1, CCL20, IL10RA, LIF, OSM, TNFRSF10C, INHBB, GDF5, BMP7, CXCL10, BMP2, CD40LG, IL2RA, CLCF1, IL2RB, ACKR3, TNFSF8, IL7R	2.064.536.312.167.130
hsa04380:Osteoclast differentiation	39	57699283.12	CSF1R, SPI1, CSF1, NCF1, NCF2, NCF4, TREM2, LILRA1, LILRA2, TNF, PIK3CG, LILRA4, RELB, PIK3R5, FCGR3A, FCGR3B, BLNK, ACP5, FCGR1A, TGFB1, SYK, CYBB, NFATC2, LILRB1, CYBA, LILRB2, LILRB4, TGFBR1, TNFRSF1A, OSCAR, FOSL1, IL1A, TYROBP, FCGR2A, LCK, IL1B, BTK, LCP2, FCGR2B	25.314.543.447.286.700
hsa05323:Rheumatoid arthritis	30	1069577145.78	CD86, CSF1, ITGB2, ITGAL, TNF, TNFSF13B, ICAM1, HLA-DMA, HLA-DMB, CCL5, CCL3, CCL2, ACP5, HLA-DOA, HLA-DQA2, HLA-DQA1, HLA-DPA1, HLA-DRB5, TGFB1, ATP6V0E1, CCL20, IL18, IL1A, IL1B, HLA-DPB1, HLA-DRA, HLA-DRB1, ATP6V1B1, HLA-DQB1, TLR2	28.987.807.618.833.500
hsa05416:Viral myocarditis	23	1615144724.26	CD86, HLA-DRB5, ITGB2, HLA-B, HLA-C, HLA-A, ITGAL, HLA-G, ICAM1, HLA-E, HLA-DMA, HLA-DMB, CD40LG, DAG1, HLA-DPB1, RAC2,	3.431.071.498.275.970

			HLA-DRA, HLA-DOA, HLA-DQA2, HLA-DQA1, HLA-DRB1, HLA-DPA1, HLA-DQB1	
hsa05310:Asthma	16	2780113630.45	IL10, HLA-DRB5, FCER1G, RNASE3, TNF, HLA-DMA, HLA-DMB, CD40LG, HLA-DPB1, HLA-DRA, HLA-DOA, HLA-DQA2, HLA-DQA1, HLA-DRB1, HLA-DPA1, HLA-DQB1	45.349.814.585.908.500
hsa05320:Autoimmune thyroid disease	20	29956958768.70	IL10, CD86, HLA-DRB5, HLA-B, HLA-C, HLA-A, HLA-G, TSHR, HLA-E, HLA-DMA, HLA-DMB, CD40LG, HLA-DPB1, HLA-DRA, HLA-DOA, HLA-DQA2, HLA-DQA1, HLA-DRB1, HLA-DPA1, HLA-DQB1	3.270.419.321.099.170
hsa04672:Intestinal immune network for IgA production	18	116389922885.73	IL10, CD86, HLA-DRB5, TGFB1, CXCR4, TNFRSF13C, TNFSF13B, HLA-DMA, HLA-DMB, CD40LG, HLA-DPB1, HLA-DRA, HLA-DOA, HLA-DQA2, HLA-DQA1, HLA-DRB1, HLA-DPA1, HLA-DQB1	32.565.026.431.370.400
hsa04640:Hematopoietic cell lineage	26	129952506953.39	CSF1R, ITGAM, CSF1, CD1D, CD3E, TNF, CSF2RA, CD38, CD37, CD14, FCGR1A, CD33, HLA-DRB5, FLT3LG, CD2, IL1A, CD4, IL1B, IL2RA, CD7, CD9, HLA-DRA, CD24, IL7R, CD44, HLA-DRB1	25.411.534.035.207.300
hsa04115:p53 signaling pathway	22	148341039620.31	CDKN1A, STEAP3, RRM2, CD82, CDKN2A, IGFBP3, SERPINE1, GADD45G, CCNB2, CCNB1, TP53I3, CDK6, CCND2, CDK4, CHEK2, CHEK1, CDK2, CDK1, BAX, TP53, GTSE1, RPRM	27.920.594.801.025.700
hsa05144:Malaria	18	21966504696.61	IL10, TGFB1, VCAM1, KLRB1, GYPC, CD81, ITGB2, IL18, ITGAL, THBS2, TNF, ICAM1, KLRK1, CD40LG, IL1B, CCL2, SDC1, TLR2	31.235.841.679.069.600
hsa05321:Inflammatory bowel disease (IBD)	21	248189148745.64	IL10, HLA-DRB5, TGFB1, IL18, NOD2, TNF, IL1A, HLA-DMA, HLA-	27.900.764.833.127.300

			DMB, IL1B, HLA-DPB1, HLA-DRA, HLA-DOA, IL12RB1, TLR5, HLA-DQA2, HLA-DQA1, HLA-DRB1, HLA-DPA1, HLA-DQB1, TLR2	
hsa04610:Complement and coagulation cascades	21	82473825633.46	C1QB, C1QA, SERPINA1, C1R, PROS1, CFI, F2R, C5AR1, SERPINE1, TFPI, F5, C2, C3, C4B, C4A, PLAU, C9, C3AR1, MASP1, A2M, C1QC	2.587.897.028.000.210
hsa03030:DNA replication	14	1276909925467.54	PRIM2, FEN1, RNASEH2A, PCNA, RFC2, PRIM1, POLD1, POLE2, POLD2, MCM3, MCM4, MCM5, MCM6, MCM2	330.675.731.355.583
hsa05169:Epstein-Barr virus infection	30	1324570612929.74	RB1, CDKN1A, ITGAL, PIK3CG, RELB, PIK3R5, ICAM1, SPN, IRAK1, MYC, HLA-DQA2, HLA-DQA1, HLA-DPA1, LYN, HLA-DRB5, SYK, HLA-B, HLA-C, HLA-A, HLA-G, HLA-E, NEDD4, CDK2, HLA-DPB1, HLA-DRA, VIM, TP53, CD44, HLA-DRB1, HLA-DQB1	20.909.238.282.437.300
hsa05133:Pertussis	21	288430555372.25	IL10, C1QB, C1QA, ITGAM, C1R, ITGB2, LY96, TNF, C2, GNAI2, C3, C4B, PYCARD, IL1A, C4A, IRAK1, IL1B, CASP1, IRF8, CD14, C1QC	2.380.865.265.760.190
hsa04666:Fc gamma R-mediated phagocytosis	22	532956114349.05	LYN, MARCKSL1, SYK, MYO10, NCF1, SPHK1, ARPC1B, INPPL1, WAS, PIK3CG, VAV1, PIK3R5, VAV2, HCK, MARCKS, FCGR2A, SCIN, PTPRC, RAC2, FCGR1A, DOCK2, FCGR2B	2.226.999.823.415.150
hsa05322:Systemic lupus erythematosus	30	715069487424.81	C1QB, CD86, C1QA, C1R, TNF, C2, C3, C4B, C4A, HLA-DMA, FCGR3A, HLA-DMB, FCGR3B, C9, FCGR1A, HLA-DOA, TRIM21, HLA-DQA2, HLA-DQA1, HLA-DPA1, IL10, HLA-DRB5, FCGR2A, CD40LG, HLA-DPB1, HLA-	1.903.676.918.251.750

			DRA, HLA-DRB1, C1QC, SNRPB, HLA-DQB1	
hsa05142:Chagas disease (American trypanosomiasis)	25	776320293761.67	C1QB, C1QA, SERPINE1, CD3E, TNF, PIK3CG, GNAI2, PIK3R5, C3, GNA15, IRAK1, CCL5, CCL3, CCL2, FADD, IL10, TGFB1, TGFBR1, TNFRSF1A, PLCB3, IL1B, TLR6, CALR, C1QC, TLR2	20.440.120.756.869.800
hsa05200:Pathways in cancer	68	859980148785.33	RB1, CDKN1A, SPI1, BRCA2, ETS1, PIK3CG, GLI2, EDNRA, GNGT2, EDNRB, MYC, RAC2, ITGAV, PDGFRA, MMP2, WNT5A, F2R, WNT9B, FLT3LG, MMP9, TGFBR1, PGF, RUNX1, AR, PLCB3, COL4A2, TRAF4, SMO, COL4A1, COL4A6, CKS2, RARA, BIRC5, BIRC7, TP53, PTGER4, CSF1R, GSTP1, CXCR4, LPAR4, HIF1A, CSF2RA, RASGRP4, EGFR, GNAI2, PIK3R5, GNG2, E2F2, FADD, CDKN2B, TCF7L1, TGFB1, FZD2, CDKN2A, EGF, LAMB2, FN1, BMP4, BMP2, RAD51, CDK6, LPAR5, CDK4, CDK2, GNB4, BAX, FGF11, F2RL3	14.712.726.106.115.300
hsa04064:NF-kappa B signaling pathway	22	876391040021.25	LYN, VCAM1, SYK, BCL2A1, CCL4L2, LY96, TNFRSF13C, TNF, TNFSF13B, RELB, ICAM1, TNFRSF1A, CD40LG, IRAK1, PLAU, LCK, IL1B, CCL4, BLNK, BTK, CD14, CARD11	21.502.067.260.560.000
hsa05164:Influenza A	36	884605161171.64	NXT1, NLRX1, TMPRSS2, NXT2, TNF, PIK3CG, PIK3R5, ICAM1, IFIH1, PYCARD, HLA-DMA, HLA-DMB, CCL5, CASP1, CCL2, HLA-DOA, HLA-DQA2, HLA-DQA1, HLA-DPA1, IL33, HLA-DRB5, IL18, TNFRSF10C, TNFRSF1A, IL1A, CXCL10, OAS1, OAS2, OAS3, IL1B, HLA-DPB1, HLA-	17.592.600.485.912.700

			DRA, TLR7, HLA-DRB1, TLR3, HLA-DQB1	
hsa04350:TGF-beta signaling pathway	21	0.00	SMAD1, CDKN2B, TGFB1, TGIF2, FST, NOG, INHBB, GDF5, BMP7, TNF, LTBP1, TGFBR1, BMP4, BMP2, RBL1, MYC, ID2, ID1, ID4, ID3, LEFTY2	21.257.725.587.144.600
hsa04512:ECM-receptor interaction	21	0.00	LAMB2, TNC, FN1, HMMR, THBS2, COL1A1, COL3A1, COL1A2, COL4A2, IBSP, COL4A1, TNN, DAG1, COL4A6, SPP1, SDC1, ITGB8, ITGAV, ITGB6, AGRN, CD44	20.524.700.566.898.200
hsa05168:Herpes simplex infection	36	0.00	TNF, IFIH1, C3, HLA-DMA, HLA-DMB, CCL5, CCL2, FADD, HLA-DOA, HLA-DQA2, HLA-DQA1, HLA-DPA1, CD74, HLA-DRB5, ALYREF, HLA-B, HLA-C, TAP1, HLA-A, HLA-G, TNFRSF1A, HLA-E, OAS1, OAS2, OAS3, IL1B, CDK2, CDK1, HLA-DPB1, HLA-DRA, TP53, HLA-DRB1, TLR3, NECTIN2, HLA-DQB1, TLR2	16.727.390.625.949.800
hsa04620:Toll-like receptor signaling pathway	24	0.00	CD86, CXCL9, CCL4L2, LY96, TNF, PIK3CG, PIK3R5, TLR1, CXCL10, IRAK1, IL1B, CCL5, CCL4, SPP1, CCL3, TLR8, IRF5, TLR7, CD14, FADD, TLR6, TLR5, TLR3, TLR2	1.925.227.977.703.660
hsa05202:Transcriptional misregulation in cancer	33	0.00	CD86, CSF1R, CDKN1A, SPI1, ITGAM, BCL2A1, TMPRSS2, SIX1, HOXA10, LYL1, CCND2, PLAU, MYC, CD14, FCGR1A, NGFR, SMAD1, CDKN2C, EYA1, IGFBP3, ETV1, PAX5, ETV4, MMP9, ETV6, RUNX1, MYCN, ID2, TLX1, IL2RB, RARA, TCF3, TP53	16.802.513.637.743.000
hsa05145:Toxoplasmosis	24	0.00	IL10, HLA-DRB5, TGFB1, LAMB2, IL10RA, LY96, TNF, GNAI2, TNFRSF1A, HLA-DMA, HLA-DMB, CD40LG, IRAK1, HLA-DPB1, HLA-	1.855.219.687.605.340

			DRA, BIRC7, HLA-DOA, CCR5, HLA-DQA2, HLA-DQA1, HLA-DRB1, HLA-DPA1, HLA-DQB1, TLR2	
hsa05340:Primary immunodeficiency	11	0.00	CD4, PTPRC, CD40LG, LCK, BLNK, BTK, TAP1, RFXANK, TNFRSF13C, CD3E, IL7R	27.509.997.818.657.700
hsa04662:B cell receptor signaling pathway	17	0.01	LYN, SYK, CD81, INPPL1, NFATC2, DAPP1, PIK3CG, VAV1, PIK3R5, VAV2, BLNK, BTK, RAC2, PTPN6, PIK3AP1, FCGR2B, CARD11	2.094.964.260.762.070
hsa05132:Salmonella infection	19	0.01	ARPC1B, CCL4L2, RHOG, IL18, WAS, CXCL3, PYCARD, IL1A, IL1B, CCL4, CASP1, CCL3, FLNA, CD14, FLNC, PKN1, PFN1, RAB7B, TLR5	1.946.490.535.690.350
hsa04670:Leukocyte transendothelial migration	24	0.01	ITGAM, VCAM1, NCF1, NCF2, MMP2, ITGB2, NCF4, CXCR4, RHOH, CYBA, ITGAL, MMP9, PIK3CG, VAV1, PIK3R5, VAV2, GNAI2, ICAM1, CLDN7, RAC2, EZR, CD99, JAM2, SIPA1	17.745.579.620.572.900
hsa05212:Pancreatic cancer	16	0.01	RB1, TGFB1, CDKN2A, EGF, BRCA2, EGFR, TGFBR1, PIK3CG, PIK3R5, RAD51, CDK6, CDK4, RAC2, E2F2, TP53, ARHGEF6	20.930.683.655.034.700
hsa05222:Small cell lung cancer	19	0.01	RB1, CDKN2B, LAMB2, FN1, PIK3CG, PIK3R5, CDK6, COL4A2, TRAF4, COL4A1, CDK4, MYC, CDK2, COL4A6, CKS2, E2F2, ITGAV, BIRC7, TP53	19.006.907.583.799.800
hsa04062:Chemokine signaling pathway	34	0.01	CX3CR1, CXCL9, NCF1, CCL4L2, WAS, CXCR4, CXCL13, CXCL3, PIK3CG, CXCL16, GNAI2, PIK3R5, GRK1, CCL8, GNGT2, GNG2, CCL5, CCL4, CCL3, RAC2, CCL2, CCR5, CCL18, CCR2, CCR1, LYN, CCL20, VAV1, VAV2, CXCL10, HCK, PLCB3, GNB4, DOCK2	15.543.283.225.008.900

hsa05146:Amoebiasis	22	0.01	IL10, TGFB1, ITGAM, LAMB2, ITGB2, FN1, TNF, PIK3CG, PIK3R5, COL1A1, COL3A1, GNA15, PLCB3, COL1A2, COL4A2, COL4A1, IL1B, C9, COL4A6, CD14, RAB7B, TLR2	17.647.923.128.950.200
hsa05020:Prion diseases	10	0.01	C1QB, IL1A, EGR1, C1QA, NOTCH1, CCL5, IL1B, C9, BAX, C1QC	25.009.088.926.052.400
hsa04611:Platelet activation	25	0.02	MYLK2, ITPR2, PIK3CG, GNAI2, PIK3R5, PTGS1, TBXA2R, LYN, P2RY12, FCER1G, SYK, F2R, PLA2G4A, VAMP8, APBB1IP, COL1A1, COL3A1, PLCB3, FCGR2A, COL1A2, TBXAS1, BTK, LCP2, F2RL3, FERMT3	16.352.096.605.495.800
hsa05205:Proteoglycans in cancer	35	0.02	CD63, CDKN1A, TWIST1, ITPR2, HIF1A, TNF, HOXD10, EGFR, PIK3CG, PIK3R5, PLAU, MYC, FLNA, TIMP3, ITGAV, FLNC, TGFB1, FZD2, LUM, MMP2, RDX, WNT5A, IGF2, FN1, WNT9B, MMP9, SMO, SDC1, HCLS1, PTPN6, HPSE, EZR, TP53, CD44, TLR2	14.880.407.911.001.200
hsa05219:Bladder cancer	11	0.02	RB1, CDKN1A, CDKN2A, CDK4, EGF, MYC, MMP2, E2F2, TP53, MMP9, EGFR	2.281.316.892.278.930
hsa04650:Natural killer cell mediated cytotoxicity	23	0.03	FCER1G, SYK, ITGB2, TNFRSF10C, NFATC2, ITGAL, TNF, PIK3CG, VAV1, PIK3R5, VAV2, ICAM1, FCGR3A, KLRK1, FCGR3B, TYROBP, LCK, RAC2, LCP2, CD48, PTPN6, HCST, CD244	1.603.041.601.653.520
hsa04151:PI3K-Akt signaling pathway	53	0.03	CDKN1A, CSF1, TNC, PIK3CG, GNGT2, CCND2, IBSP, TNN, CREB3L4, MYC, ITGB8, ITGAV, ITGB6, PDGFRA, SYK, F2R, PGF, COL4A2, COL4A1, COL4A6, TP53, TLR2, CSF1R, LPAR4, THBS2, EFNA4, EGFR, PIK3R5, BCL2L11,	1.306.271.833.181.060

			GNG2, PDGFC, SPP1, EIF4EBP1, NGFR, EGF, LAMB2, OSM, FN1, COL1A1, COL3A1, EFNA2, CDK6, COL1A2, LPAR5, CDK4, IL2RA, IL2RB, CDK2, GNB4, PKN1, PIK3AP1, IL7R, FGF11	
hsa05143:African trypanosomiasis	9	0.03	IL10, PLCB3, VCAM1, IL1B, IL18, F2RL1, TNF, IDO1, ICAM1	2.319.024.609.506.680
hsa05162:Measles	24	0.04	TNFRSF10C, TACR1, CD3E, PIK3CG, PIK3R5, IFIH1, IL1A, DOK1, CDK6, CCND2, IRAK1, OAS1, OAS2, CDK4, IL1B, IL2RA, OAS3, IL2RB, CDK2, RACK1, TLR7, FCGR2B, TP53, TLR2	15.343.922.228.314.900
hsa04668:TNF signaling pathway	20	0.04	VCAM1, CSF1, CCL20, LIF, NOD2, CXCL3, TNFRSF1B, TNF, MMP9, PIK3CG, PIK3R5, ICAM1, TNFRSF1A, CXCL10, MMP14, CREB3L4, IL1B, CCL5, CCL2, FADD	15.893.626.607.210.900
hsa05134:Legionellosis	12	0.05	PYCARD, C3, ITGAM, IL1B, ITGB2, CASP1, IL18, CD14, CXCL3, TLR5, TNF, TLR2	18.895.756.077.461.800
hsa04810:Regulation of actin cytoskeleton	34	0.05	CYFIP1, MYLK2, ITGAM, ARPC1B, ITGB2, WAS, ITGAL, IQGAP2, IQGAP3, EGFR, PIK3CG, PIK3R5, FGD3, SCIN, PDGFC, RAC2, ITGB8, ITGAV, NCKAP1L, ITGB6, PDGFRA, EGF, RDX, F2R, FN1, VAV1, VAV2, ENAH, DIAPH2, DIAPH3, EZR, PFN1, FGF11, ARHGEF6	1.376.690.799.929.360
hsa04330:Notch signaling pathway	11	0.05	APH1A, LFNG, NOTCH2, NCSTN, NOTCH1, DTX3L, MAML2, MFNG, DLL1, HES5, DLL3	19.486.248.454.882.500
hsa05218:Melanoma	14	0.07	RB1, PDGFRA, CDKN1A, CDKN2A, EGF, EGFR, PIK3CG, PIK3R5, CDK6, CDK4, PDGFC, E2F2, TP53, FGF11	16.766.656.801.128.100

hsa00532:Glycosaminoglycan biosynthesis - chondroitin sulfate / dermatan sulfate	6	0.08	CHST11, CHPF, CHPF2, UST, CHST14, CHST3	25.509.270.704.573.500
hsa05161:Hepatitis B	24	0.08	RB1, CDKN1A, EGR2, TGFB1, PCNA, NFATC2, TNF, MMP9, TGFBR1, PIK3CG, PIK3R5, IFIH1, CDK6, CREB3L4, CDK4, MYC, CDK2, BAX, BIRC5, E2F2, FADD, TP53, TLR3, TLR2	14.074.080.388.730.200
hsa03410:Base excision repair	8	0.08	FEN1, NEIL3, PCNA, PARP4, POLD1, POLE2, APEX1, POLD2	20.613.552.084.503.800
hsa04974:Protein digestion and absorption	16	0.09	COL22A1, ELN, PRCP, SLC3A2, SLC1A5, DPP4, COL1A1, COL3A1, SLC7A7, COL1A2, COL4A2, COL4A1, XPNPEP2, FXYD2, KCNQ1, COL4A6	15.460.164.063.377.900

Table 3 Supplementary - Dysregulated pathways identified from down-regulated genes in gliomas by the DAVID tool

Term	Count	PValue	Genes	Fold Enrichment
hsa04020:Calcium signaling pathway	62	3.9012587933564586E-17	CHRM2, RYR1, RYR2, CALML5, CALML6, CHRM5, ATP2A3, HTR2C, CALML3, HTR4, GRM1, RYR3, SLC8A2, PPP3CA, PPP3CB, HTR6, GRM5, BDKRB1, NOS1, PRKCG, PRKCB, TNNC1, TNNC2, TACR2, PLCB4, ADORA2A, CCKBR, ITPKA, CAMK2B, PDE1C, PDE1B, PDE1A, CAMK2A, CACNA1B, ADCY4, ITPR1, CACNA1A, CACNA1C, ADCY1, CACNA1F, CACNA1E, CACNA1H, CACNA1G, CACNA1I, PPP3R1, GRIN2A, PTK2B, CACNA1S, DRD1, DRD5, ATP2B3, ATP2B2, ATP2B1, HTR5A, GRIN2C, GRIN1, P2RX5, GNAL, CAMK4, CALM3, CALM1, CALM2	3.1558548225979504
hsa04723:Retrograde endocannabinoid signaling	42	8.55103719244701E-15	GABRB3, GABRB2, FAAH, CACNA1B, ADCY4, ITPR1, CACNA1A, CACNA1C, ADCY1, CACNA1F, GRM1, ADCY5, RIMS1, MAPK9, GNG3, GRM5, GNG7, SLC17A7, CACNA1S, GABRE, GABRD, KCNJ3, PRKCG, GABRA2, GABRA1, KCNJ6, SLC32A1, GABRA6, PRKCB, KCNJ9, GABRA5, GABRA4, GABRG3, GABRG2, GABRG1, MAPK13, GNG13, MAPK11, PLCB4, GNB3, GNB5, MGLL	3.788840076060586
hsa04713:Circadian entrainment	40	2.5124667919419938E-14	CAMK2B, RYR1, RYR2, CALML5, CALML6, CAMK2A, ADCY4, ITPR1, CALML3, CACNA1C, ADCY1, CACNA1H, RYR3, CACNA1G, ADCY5, CACNA1I, GRIN2A, GNG3, RPS6KA5, GNG7, PRKG2, NOS1, KCNJ3, PRKCG, KCNJ6, PRKCB, KCNJ9, GRIN2C, GRIN2B, GRIN1, GNG13, ADCY10, PLCB4, PER3, NOS1AP, GNB3, CALM3, GNB5, CALM1, CALM2	3.8363192750087136
hsa04261:Adrenergic signaling in cardiomyocytes	49	5.063919651480798E-14	RYR2, CALML5, CALML6, CALML3, RPS6KA5, CREB3L3, SCN5A, SCN1B, CACNA2D1, TNNC1, PPP2R5B, CACNA2D3, CACNA2D2, ATP1B1, CACNB1, CACNB2, CACNB3, CACNB4, PLCB4, MYL2, TNNT2, SCN4B, MYH6, RAPGEF3, RAPGEF4, CAMK2B,	3.235156924848834

			CAMK2A, ADCY4, ATP1A3, CACNA1C, ADCY1, CACNA1F, ADCY5, CACNG8, TNNI3, CACNA1S, CACNG2, CACNG3, ATP2B3, ATP2B2, ATP2B1, MAPK13, MAPK11, ACTC1, PPP2R2C, PPP1R1A, CALM3, CALM1, CALM2	
hsa05032:Morphine addiction	38	1.6887042121260623E-13	GABRB3, GABRB2, PDE1C, PDE1B, PDE1A, CACNA1B, ADCY4, CACNA1A, ARRB1, ADCY1, ADCY5, GNG3, GNG7, DRD1, GABRE, GABRD, KCNJ3, PRKCG, GABRA2, GABRA1, KCNJ6, SLC32A1, GABRA6, PRKCB, KCNJ9, GABRA5, GABRA4, PDE2A, PDE4C, OPRM1, GABRG3, GABRG2, GABRG1, GNG13, PDE10A, GNB3, PDE7B, GNB5	3.8047012590058946
hsa04080:Neuroactive ligand-receptor interaction	74	1.9899393267325509E-13	GABRB3, CHRM2, GABRB2, VIPR1, PRSS1, NPFFR1, CHRM5, HTR2C, GRIK1, PRL, PTH1R, HTR4, GRM1, MC4R, GRM3, GRM2, HTR6, GRM5, GRM4, GRM7, BDKRB1, PRSS3, PRSS2, PTGDR, CHRNB3, NPY5R, NPY1R, TACR2, OPRM1, ADRA2C, GABRG3, SSTR3, PRLR, GABRG2, GABRG1, ADORA2A, CCKBR, CHRNA2, GIPR, CHRNA4, LPAR1, GPR83, LPAR3, PLG, CRHR1, CRHR2, GLRA2, GRIN2A, HRH3, P2RY2, CHRNE, KISS1R, DRD1, GABRE, S1PR5, DRD2, GABRD, DRD5, NTSR2, GABRA2, GABRA1, HTR1E, GABRA6, GABRA5, GABRA4, HTR1B, OPRK1, TRPV1, HTR5A, GRIN2C, GRIN2B, GRIN1, GH1, P2RX5	2.434054558060583
hsa04921:Oxytocin signaling pathway	50	4.2920917536042913E-13	RYR1, RYR2, CALML5, CALML6, OXT, CALML3, RYR3, PPP3CA, PPP3CB, PRKCG, PRKCB, CACNA2D1, PLA2G4B, CACNA2D3, CACNA2D2, CACNB1, CACNB2, CACNB3, CACNB4, PLCB4, JMJD7-PLA2G4B, PPP1R12B, PPP1R12C, CAMK1G, CAMK2B, CAMK2A, ADCY4, ITPR1, CACNA1C, ADCY1, CACNA1F, CAMKK1, CAMKK2, ADCY5, TRPM2, CACNG8, PPP3R1, CACNA1S, CACNG2, CACNG3, KCNJ3, KCNJ4, KCNJ6, KCNJ9, KCNJ12, NFATC4, CAMK4, CALM3, CALM1, CALM2	3.0370860927152323
hsa04727:GABAergic synapse	36	4.9489198768800935E-13	GABRB3, GABRB2, GLS2, CACNA1B, ADCY4, CACNA1A, CACNA1C, ADCY1, CACNA1F, TRAK2, ADCY5, GLS, GNG3, GNG7, CACNA1S, GABRE, GABRD, PRKCG, NSF, GABRA2, GABRA1,	3.8588858589793533

			GABARAPL1, KCNJ6, SLC32A1, GABRA6, PRKCB, GABRA5, GAD1, GABRA4, GAD2, GABRG3, GABRG2, GABRG1, GNG13, GNB3, GNB5	
hsa04724:Glutamatergic synapse	41	5.002240056842272E-12	GLS2, ADCY4, SLC1A2, ITPR1, CACNA1A, GRIK1, CACNA1C, ADCY1, SLC1A6, GRM1, ADCY5, GLS, GRM3, PPP3CA, GRM2, GRIN2A, PPP3CB, PPP3R1, GNG3, GRM5, GRM4, GRM7, GNG7, SLC17A7, KCNJ3, PRKCG, PRKCB, HOMER2, PLA2G4B, GRIN2C, GRIN2B, GRIN1, GNG13, PLCB4, DLG4, JMJD7-PLA2G4B, GNB3, GNB5, SHANK3, SHANK2, SHANK1	3.2768560474032764
hsa04728:Dopaminergic synapse	43	1.8101489120583214E-11	CAMK2B, CALML5, CALML6, CAMK2A, CACNA1B, ITPR1, CACNA1A, CALML3, CACNA1C, ADCY5, PPP3CA, MAPK9, GRIN2A, PPP3CB, GNG3, CREB3L3, KIF5C, GNG7, KIF5A, DRD1, DRD2, DRD5, KCNJ3, PRKCG, KCNJ6, PRKCB, KCNJ9, PPP2R5B, GRIN2B, MAPK13, GNG13, MAPK11, PLCB4, GNAL, CALY, TH, PPP2R2C, PPP1R1B, GNB3, CALM3, GNB5, CALM1, CALM2	3.0608133278145697
hsa05033:Nicotine addiction	21	8.045143017855053E-10	GABRB3, GABRA2, GABRB2, GABRA1, SLC32A1, GABRA6, CHRNA4, GABRA5, GABRA4, CACNA1B, CACNA1A, GRIN2C, GABRG3, GRIN2B, GABRG2, GABRG1, GRIN1, GRIN2A, SLC17A7, GABRE, GABRD	4.78341059602649
hsa04720:Long-term potentiation	27	1.6310076836841505E-9	CAMK2B, CALML5, CALML6, CAMK2A, ITPR1, CALML3, CACNA1C, ADCY1, GRM1, PPP3CA, RPS6KA6, GRIN2A, PPP3CB, PPP3R1, GRM5, PRKCG, PRKCB, GRIN2C, GRIN2B, GRIN1, PLCB4, PPP1R1A, CAMK4, CALM3, CALM1, CALM2, RAPGEF3	3.7273329319686934
hsa04925:Aldosterone synthesis and secretion	30	2.6131958524040523E-9	CAMK2B, CALML5, KCNK9, CALML6, CAMK2A, ADCY4, ITPR1, CALML3, CACNA1C, ADCY1, CACNA1F, CACNA1H, CACNA1G, ADCY5, CACNA1I, CREB3L3, CYP11A1, CACNA1S, PRKCG, PRKCB, PDE2A, NR4A2, NR4A1, PLCB4, STAR, CAMK4, CALM3, CALM1, CALM2, CAMK1G	3.3745401030169244
hsa04726:Serotonergic synapse	35	1.168135997762124E-8	GABRB3, GABRB2, ALOX15, CACNA1B, ITPR1, CACNA1A, HTR2C, ALOX12B, CACNA1C, CACNA1F, HTR4, ADCY5, GNG3, HTR6, CYP4X1, CYP2D6, GNG7, CACNA1S, KCNJ3, PRKCG, KCNJ6, HTR1E, PRKCB, KCNJ9, PLA2G4B, HTR1B, HTR3A, HTR5A, GNG13,	2.8729192768927874

			CYP2C8, PLCB4, JMJD7-PLA2G4B, GNB3, GNB5, RAPGEF3	
hsa04024:cAMP signaling pathway	50	2.0871016464187502E-8	CHRM2, RYR2, CALML5, CALML6, HHIP, CALML3, HTR4, HTR6, CREB3L3, PDE4C, NPY1R, ATP1B1, TIAM1, ADORA2A, RAPGEF3, RAPGEF4, CNGB1, CAMK2B, GIPR, CAMK2A, ADCY4, ATP1A3, CACNA1C, ADCY1, CACNA1F, ADCY5, MAPK9, PAK1, GRIN2A, TNNI3, CACNA1S, DRD1, DRD2, DRD5, HTR1E, HTR1B, ATP2B3, ATP2B2, ATP2B1, GRIN2C, GRIN2B, GRIN1, ADCY10, CAMK4, PPP1R1B, FXYD1, CALM3, CALM1, CALM2, HCN2	2.3008227975115396
hsa05414:Dilated cardiomyopathy	29	3.0181938083474414E-8	RYR2, ITGA2B, ADCY4, CACNA1C, ADCY1, CACNA1F, TTN, ADCY5, CACNG8, SGCA, TNNI3, CACNA1S, CACNG2, CACNG3, MYBPC3, CACNA2D1, TNNC1, CACNA2D3, CACNA2D2, CACNB1, CACNB2, CACNB3, ACTC1, DES, CACNB4, ITGA10, MYL2, TNNT2, ITGA8	3.1455534531693474
hsa05031:Amphetamine addiction	25	4.408855826237396E-8	CAMK2B, CALML5, CALML6, CAMK2A, CALML3, CACNA1C, ADCY5, PPP3CA, GRIN2A, PPP3CB, PPP3R1, CREB3L3, DRD1, PRKCG, PRKCB, GRIN2C, GRIN2B, GRIN1, TH, CAMK4, PPP1R1B, CALM3, CALM1, CALM2, STX1A	3.451234196267309
hsa04010:MAPK signaling pathway	57	1.3395813087145517E-7	PTPRR, RASGRF2, RASGRF1, ARRB1, FGF3, FGF5, PPP3CA, PPP3CB, RPS6KA6, RPS6KA5, FGF9, PRKCG, DUSP5, MAP4K2, DUSP2, PRKCB, CACNA2D1, PLA2G4B, CACNA2D3, CACNA2D2, DUSP8, MAPK8IP2, MAPK8IP3, CACNB1, CACNB2, CACNB3, CACNB4, JMJD7-PLA2G4B, RASA2, CACNA1B, CACNA1A, CACNA1C, CACNA1F, RASGRP2, CACNA1E, CACNA1H, CACNA1G, CACNA1I, MAPK9, CACNG8, PPP3R1, PAK1, NTF3, CACNA1S, CACNG2, CACNG3, FGF22, MAPK13, FGF17, NR4A1, MAPK11, FGF13, PTPN5, FGFR3, FGFR2, HSPA1B, HSPA1A	2.0527340784755124
hsa04725:Cholinergic synapse	33	1.5421861532251864E-7	CHRM2, CAMK2B, ACHE, CHRNA4, CHRM5, CAMK2A, CACNA1B, ADCY4, ITPR1, CACNA1A, CACNA1C, ADCY1, CACNA1F, ADCY5, GNG3, CREB3L3, GNG7, CACNA1S, KCNJ3, PRKCG, KCNJ4, KCNJ6, PRKCB, KCNJ12, GNG13, SLC5A7, PLCB4, CAMK4, KCNQ2, KCNQ3, GNB3, KCNQ4, GNB5	2.7087524610703424

hsa04972:Pancreatic secretion	29	3.444760955 1463106E-7	PNLIPRP1, CELA3A, PNLIPRP2, RYR2, PRSS1, CELA3B, ADCY4, ATP2A3, ITPR1, ATP1A3, ADCY1, ADCY5, PRSS3, PRSS2, CLCA4, PRKCG, CPA2, CPA1, CELA2A, PRKCB, PLA2G2A, ATP2B3, ATP2B2, CEL, ATP2B1, ATP1B1, PLCB4, KCNMA1, PNLIP	2.84114505447 55392
hsa04721:Synaptic vesicle cycle	23	3.675673392 7991727E-7	NSF, UNC13C, SNAP25, RAB3A, UNC13A, ATP6V1G2, SLC32A1, SYT1, STXBP1, CACNA1B, CACNA1A, CPLX2, CPLX1, CPLX4, DNM1, CPLX3, DNM3, STX1B, RIMS1, SLC17A7, ATP6V0A4, STX3, STX1A	3.32633238725 954
hsa05410:Hypertrophic cardiomyopathy (HCM)	26	3.921539888 9796116E-7	RYR2, ITGA2B, CACNA1C, CACNA1F, TTN, CACNG8, SGCA, TNNI3, CACNA1S, CACNG2, CACNG3, MYBPC3, CACNA2D1, TNNC1, CACNA2D3, CACNA2D2, CACNB1, CACNB2, CACNB3, ACTC1, DES, CACNB4, ITGA10, MYL2, TNNT2, ITGA8	3.03708609271 5232
hsa04911:Insulin secretion	27	6.427201179 07835E-7	CAMK2B, SNAP25, RYR2, RAB3A, CAMK2A, ADCY4, ATP1A3, CACNA1C, ADCY1, CACNA1F, ADCY5, RIMS2, PCLO, CREB3L3, KCNN1, CACNA1S, FFAR1, PRKCG, PRKCB, ABCC8, ATP1B1, GCK, ADCYAP1, PLCB4, KCNMA1, STX1A, RAPGEF4	2.89416439423 45148
hsa04260:Cardiac muscle contraction	25	6.923647915 584343E-7	RYR2, ATP1A3, CACNA1C, CACNA1F, COX7A1, COX6A2, CACNG8, TNNI3, CACNA1S, CACNG2, CACNG3, CACNA2D1, TNNC1, CACNA2D3, CACNA2D2, COX6B2, ATP1B1, CACNB1, CACNB2, CACNB3, ACTC1, CACNB4, MYL2, TNNT2, MYH6	3.03708609271 52323
hsa04970:Salivary secretion	27	8.273438796 912779E-7	CALML5, CALML6, ADCY4, ITPR1, ATP1A3, CALML3, AQP5, ADCY1, RYR3, ADCY5, PRB2, MUC7, PRKG2, NOS1, PRKCG, PRKCB, ATP2B3, ATP2B2, ATP2B1, MUC5B, ATP1B1, PLCB4, TRPV6, KCNMA1, CALM3, CALM1, CALM2	2.86051131988 2951
hsa04924:Renin secretion	22	2.178500068 9363663E-6	PDE1C, CALML5, PDE1B, CALML6, PDE1A, ITPR1, CALML3, CACNA1C, CACNA1F, ADCY5, ADCYAP1, PPP3CA, PPP3CB, PPP3R1, PLCB4, KCNMA1, PRKG2, CALM3, CACNA1S, CALM1, CALM2, CLCA4	3.13199503311 2583
hsa04750:Inflammatory mediator regulation of TRP channels	27	1.205732237 6745372E-5	CAMK2B, CALML5, CALML6, CAMK2A, ADCY4, ITPR1, HTR2C, CALML3, ADCY1, ADCY5, MAPK9, P2RY2, BDKRB1, ASIC2, ASIC3, PRKCG, PRKCB, PLA2G4B, TRPV3, TRPV1, MAPK13, MAPK11, PLCB4, JMJD7-PLA2G4B, CALM3, CALM1, CALM2	2.51024462765 23858

hsa04974:Protein digestion and absorption	25	1.5704816328089596E-5	COL17A1, CELA3A, PRSS1, CELA3B, COL13A1, COL11A2, ATP1A3, SLC8A2, PRSS3, PRSS2, CPA2, CPA1, CELA2A, COL27A1, COL24A1, MME, KCNJ13, ATP1B1, SLC7A9, COL7A1, COL4A3, COL9A1, COL21A1, COL9A3, COL6A6	2.588425647200482
hsa05412:Arrhythmogenic right ventricular cardiomyopathy (ARVC)	21	1.8894909570694973E-5	RYR2, CACNA2D1, ITGA2B, CACNA2D3, CACNA2D2, CACNA1C, CACNA1F, CACNB1, CACNB2, CACNB3, CACNG8, DES, CACNB4, SGCA, ITGA10, ITGA8, PKP2, CTNNA3, CACNA1S, CACNG2, CACNG3	2.8557675200158146
hsa04014:Ras signaling pathway	46	4.209880935150891E-5	FLT1, CALML5, CALML6, RASGRF2, RASGRF1, CALML3, RASAL1, FOXO4, EFNA5, RASGRP2, FGF3, FGF5, MAPK9, PAK1, GRIN2A, GNG3, FGF9, GNG7, PAK6, PAK5, FGF22, PRKCG, PRKCB, PLA2G4B, PLA2G2A, VEGFD, KSR2, GRIN2B, GRIN1, GNG13, FGF17, TIAM1, JMJD7-PLA2G4B, RASA2, GNB3, CALM3, GNB5, RIN1, FGF13, CALM1, RAPGEF5, FGFR3, CALM2, FGFR2, LAT, PLA1A	1.8545038973216 9
hsa04015:Rap1 signaling pathway	43	6.800413970080024E-5	FLT1, RGS14, CALML5, CALML6, ITGA2B, ADCY4, LPAR1, LPAR3, CALML3, ADCY1, EFNA5, RASGRP2, PRKCZ, FGF3, RAP1GAP, ADCY5, FGF5, GRIN2A, SIPA1L1, FGF9, DRD2, FGF22, PRKCG, PRKCB, VEGFD, GRIN2B, GRIN1, MAPK13, FGF17, MAPK11, TIAM1, PLCB4, ADORA2A, CALM3, FGF13, CALM1, RAPGEF5, FGFR3, CALM2, FGFR2, LAT, RAPGEF3, RAPGEF4	1.8656385998107852
hsa04971:Gastric acid secretion	21	7.400428195307851E-5	PRKCG, CAMK2B, CALML5, CALML6, PRKCB, CAMK2A, ADCY4, ITPR1, ATP1A3, CALML3, ADCY1, ATP1B1, ADCY5, ATP4A, PLCB4, CCKBR, SST, CALM3, CALM1, CALM2, KCNJ1	2.6210469019323233
hsa04912:GnRH signaling pathway	24	8.674253350900336E-5	CAMK2B, CALML5, CALML6, PRKCB, PLA2G4B, CAMK2A, ADCY4, ITPR1, CALML3, CACNA1C, ADCY1, CACNA1F, MAPK13, ADCY5, MAPK11, MAPK9, PLCB4, JMJD7-PLA2G4B, PTK2B, GNRH1, CALM3, CACNA1S, CALM1, CALM2	2.4029692162142493
hsa04070:Phosphatidylinositol signaling system	24	2.8663197636574 27E-4	PRKCG, CDS1, DGKE, CALML5, CALML6, PRKCB, ITPR1, CALML3, SYNJ2, DGKZ, MTMR7, INPP5A, PLCB4, PPIP5K1, DGKQ, ITPKA, PI4KA, INPP5J, PIP4K2A, CALM3, PIP5K1B, CALM1, CALM2, DGKH	2.2313285579132316

hsa04022:cGMP-PKG signaling pathway	32	8.369244695115818E-4	CALML5, CALML6, ADCY4, ATP2A3, ITPR1, ATP1A3, CALML3, CACNA1C, ADCY1, CACNA1F, SLC8A2, ADCY5, NPPB, PPP3CA, PPP3CB, PPP3R1, CREB3L3, PRKG2, CACNA1S, PDE2A, ATP2B3, ATP2B2, ATP2B1, ADRA2C, ATP1B1, NFATC4, PLCB4, KCNMA1, CALM3, CALM1, CALM2, CNGB1	1.8453181322826726
hsa04744:Phototransduction	10	0.00164361435283058	RCVRN, CALML5, CALML6, GUCA1A, PDE6B, CALM3, CALML3, CALM1, CALM2, CNGB1	3.3745401030169244
hsa04270:Vascular smooth muscle contraction	25	0.001671098 3605196707	CALML5, CALML6, ADCY4, ITPR1, CALML3, CACNA1C, ADCY1, CACNA1F, ACTG2, ADCY5, CACNA1S, PRKCG, PPP1R14A, PRKCB, PLA2G4B, PLA2G2A, PLCB4, ADORA2A, JMJD7-PLA2G4B, KCNMA1, CALM3, CALM1, PPP1R12B, CALM2, PPP1R12C	1.946850059432841
hsa05014:Amyotrophic lateral sclerosis (ALS)	14	0.002230216 3747677187	SLC1A2, GRIN2C, GRIN2B, MAPK13, GRIN1, MAPK11, PPP3CA, GRIN2A, PPP3CB, PPP3R1, NEFL, NEFM, NOS1, NEFH	2.5511523178807947
hsa04916:Melanogenesis	21	0.005314927109174211	PRKCG, CAMK2B, WNT10B, WNT10A, CALML5, CALML6, PRKCB, TYRP1, CAMK2A, FZD9, ADCY4, CALML3, ADCY1, ADCY5, POMC, PLCB4, CREB3L3, CALM3, CALM1, WNT1, CALM2	1.9133642384105958
hsa05030:Cocaine addiction	13	0.005515852547638167	GRIN2C, GRIN2B, ADCY5, GRIN1, GRM3, GRM2, GRIN2A, TH, CREB3L3, DLG4, PPP1R1B, DRD1, DRD2	2.4172726044006001
hsa00561:Glycerolipid metabolism	14	0.008715666929150611	PNLIPRP1, PNLIPRP2, DGKE, CEL, DGKZ, LIPF, DGKQ, GPAT3, GPAT2, PLPP2, LPIN3, MGLL, PNLIP, DGKH	2.1992692395524096
hsa04915:Estrogen signaling pathway	20	0.010182046 25602056	KCNJ6, HSP90AA1, CALML5, CALML6, KCNJ9, ADCY4, ITPR1, CALML3, ADCY1, OPRM1, GRM1, ADCY5, PLCB4, CREB3L3, CALM3, CALM1, CALM2, HSPA1B, HSPA1A, KCNJ3	1.8406582380092316
hsa04512:ECM-receptor interaction	18	0.012267379737769413	COL27A1, COL24A1, GP1BB, LAMA3, COL11A2, ITGA2B, LAMC2, GP6, COMP, VTN, SV2C, RELN, SV2B, ITGA10, COL4A3, CHAD, ITGA8, COL6A6	1.8850879196163508
hsa04540:Gap junction	18	0.013706411072355838	PRKCG, PRKCB, LPAR1, ADCY4, ITPR1, HTR2C, ADCY1, TUBB4A, TUBA4A, GRM1, ADCY5, GJD2, GRM5, PLCB4, PRKG2, DRD1, DRD2, TUBA8	1.863666465984347
hsa00564:Glycerophospholipid metabolism	19	0.013859757991400615	CDS1, ACHE, DGKE, CHKB, LPGAT1, PNPLA7, PLA2G4B, PLA2G2A, DGKZ, PISD, ETNPPL, LPCAT4, JMJD7-PLA2G4B, DGKQ, GPAT3, GPAT2, PLPP2, LPIN3, DGKH	1.822251655629139

hsa04114:Oocyte meiosis	21	0.016790518783721904	CAMK2B, CALML5, CALML6, CAMK2A, ADCY4, PPP2R5B, ITPR1, CALML3, ADCY1, ADCY5, PPP3CA, RPS6KA6, CPEB1, PPP3CB, PPP3R1, CALM3, PGR, CALM1, CPEB3, CALM2, YWHAH	1.7237515661356722
hsa04918:Thyroid hormone synthesis	15	0.018038460721542724	PRKCG, GPX2, PRKCB, ADCY4, ITPR1, ATP1A3, LRP2, ADCY1, ATP1B1, ADCY5, TPO, PLCB4, TG, CREB3L3, IYD	1.9524124881740779
hsa04360:Axon guidance	23	0.019355476340172994	EPHB6, SEMA6B, SEMA4A, EPHA7, EPHA6, UNC5A, SEMA4D, EPHA8, SEMA3G, UNC5C, L1CAM, EFNA5, NFATC4, PPP3CA, PAK1, PPP3CB, PPP3R1, ABLIM2, PAK6, SLIT3, SLIT2, PAK5, NGEF	1.6500703968295354
hsa04922:Glucagon signaling pathway	19	0.020699059952204973	CAMK2B, CALML5, CALML6, CAMK2A, ITPR1, CALML3, PYGM, ACACB, CPT1B, GCK, PPP3CA, PPP3CB, PPP3R1, PLCB4, CREB3L3, CALM3, CALM1, PCK1, CALM2	1.7486253261087699
hsa04961:Endocrine and other factor-regulated calcium reabsorption	11	0.021405589053569198	DNM3, PRKCG, KL, PLCB4, CALB1, PRKCB, TRPV5, ATP1A3, PTH1R, ATP1B1, DNM1	2.22719646799117
hsa04730:Long-term depression	13	0.027393615240006345	PRKCG, RYR1, PRKCB, PLA2G4B, ITPR1, CACNA1A, CRHR1, GRM1, PLCB4, JMJD7-PLA2G4B, CRH, PRKG2, NOS1	1.9741059602649007
hsa00250:Alanine, aspartate and glutamate metabolism	9	0.032297647934456 97	FOLH1, GOT1, GLS2, GAD1, GAD2, RIMKLA, ASPA, ASS1, GLS	2.3428949858088934
hsa00350:Tyrosine metabolism	9	0.032297647934456 97	PNMT, ALDH1A3, TPO, AOC2, GOT1, HGD, TH, ADH1B, TYRP1	2.3428949858088934
hsa04930:Type II diabetes mellitus	11	0.032571325621289164	MAPK9, PKLR, ABCC8, ADIPOQ, CACNA1B, CACNA1A, CACNA1C, PRKCZ, CACNA1E, GCK, CACNA1G	2.087996688741722
hsa01100:Metabolic pathways	153	0.036713675321721685	PNMT, GALNT12, DGKE, CMAS, AMY2A, HPSE2, GALNT16, AMY2B, OGDHL, ENO2, COX6A2, CNDP1, GLS, LIPF, NDST3, CKMT1B, PTGDS, ATP6V1G2, HGD, AMY1A, AMY1B, GLCE, AMY1C, CEL, MAT1A, COX6B2, UPB1, DGKZ, PISD, FOLH1, DGKQ, PGP, CYP2E1, HPRT1, PLPP2, PNLIP, ACOT4, DGKH, CDS1, ALOX15, AK5, ACACB, AK7, FUT1, ABO, MTMR7, HSD11B1, TPO, INPP5A, CYP11A1, FUT9, INPP5J, ST8SIA5, B4GALNT1, ATP6V0A4, PIP5K1B, RIMKLA, PCK1, PRODH, HMGCLL1, KL, CHKB, GOT1, SYNJ2, QDPR, CYP2C8, DAO, TH, CYP11B1, PI4KA, GALNTL5, GALNTL6,	1.1435787666581554

			PLCH2, DEGS2, PNLIPRP1, PNLIPRP2, ALAS2, PYGM, CSAD, FTCD, SMPD3, CYP26B1, ACADL, AUH, HYAL1, NMRK2, NMRK1, ME1, IDS, UPP2, UPP1, NOS1, GALNT9, IDH3A, ARG1, PLA2G4B, AMT, NME5, BAAT, ALDH1A3, PLCB4, BDH1, NME7, JMJD7-PLA2G4B, ITPKA, ALDH1A1, RGN, ACSBG1, ALDOB, B4GALT6, ASPA, MGLL, ST6GALNAC5, ST6GALNAC6, NDUFB8, ACSS3, GALT, GLS2, ADH1B, HDC, GCNT1, TYRP1, HSD17B3, PDXP, ALOX12B, SGMS2, HSD17B6, CYP17A1, TRAK2, CKMT2, EXTL1, UGP2, MGAT5B, MGAT3, GPAT3, GPAT2, AOC2, GALNT3, GCH1, MDH1, CKM, PKLR, GAD1, CKMT1A, PLA2G2A, GAD2, NMNAT2, GCK, ASS1, ETNPPL, LPCAT4, ALLC, LPIN3	
hsa00330:Arginine and proline metabolism	11	0.041965996204968214	CKMT2, DAO, GOT1, CKM, ARG1, CKMT1A, CARNS1, CKMT1B, NOS1, PRODH, CNDP1	2.004476821192053
hsa05010:Alzheimer's disease	27	0.043002768 56774349	NDUFB8, CALML5, CALML6, ATP2A3, ITPR1, CALML3, CACNA1C, CACNA1F, COX7A1, COX6A2, RYR3, PPP3CA, GRIN2A, PPP3CB, PPP3R1, CACNA1S, NOS1, SNCA, MME, COX6B2, GRIN2C, GRIN2B, GRIN1, PLCB4, CALM3, CALM1, CALM2	1.46430936613 05582
hsa02010:ABC transporters	10	0.046020185 32980556	ABCA2, ABCA10, ABCA5, ABCC8, ABCA6, ABCC5, ABCA9, ABCA7, ABCG4, ABCC12	2.07074051776 03855
hsa04975:Fat digestion and absorption	9	0.057350225 36080559	LIPF, PNLIPRP1, PNLIPRP2, CLPS, PLA2G2A, CEL, APOB, PLPP2, PNLIP	2.10259806418 7468
hsa00220:Arginine biosynthesis	6	0.059981449 213101154	GOT1, GLS2, ARG1, NOS1, ASS1, GLS	2.73337748344 3709
hsa00500:Starch and sucrose metabolism	8	0.062668575 9485468	UGP2, AMY2A, AMY1A, AMY2B, AMY1B, AMY1C, PYGM, GCK	2.20878988561 10777
hsa04611:Platelet activation	21	0.073056021 67413741	FGB, FGA, COL27A1, COL24A1, GP1BB, PLA2G4B, COL11A2, FGG, ITGA2B, ADCY4, ITPR1, ADCY1, GP6, RASGRP2, PRKCZ, MAPK13, ADCY5, MAPK11, PLCB4, JMJD7-PLA2G4B, PRKG2	1.47181864493 12278
hsa00340:Histidine metabolism	6	0.085048230 20805798	ALDH1A3, HDC, CARNS1, ASPA, FTCD, CNDP1	2.48488862131 24626
hsa04530:Tight junction	15	0.090144398 52891201	MYH7B, CGN, PRKCZ, CLDN6, MYH1, CLDN10, MYH2, CLDN3, PPP2R2C, CLDN9, MYL2, CLDN18, MYH11, CLDN16, TJP3	1.57090659968 02924

hsa04964:Proximal tubule bicarbonate reclamation		6	0.0993456803971687 9	MDH1, GLS2, ATP1A3, ATP1B1, PCK1, GLS	2.376849985603225

Table 4 Suplemmentary - Dysregulated pathways identified from up-regulated genes in gliomas by pathfindR

ID	Term_Description	Fold_Enrichment	support	lowest_p	highest_p	Up_regulated	Down_regulated
1	hsa05415	Diabetic cardiomyopathy	10	0.075290698	1.95E+01	NCF4, MMP9, NDUFA1, NDUFB3, UQCRQ, COX6A1, COX7A2, COX7C, GAPDH	ATP2A2, MTOR, PDHA1, PDHB, VDAC1, SLC25A5, PARP1
2	hsa04130	SNARE interactions in vesicular transport	10	0.011835977	8.01E+06	STX6	STX2, BET1L, SNAP23
3	hsa03410	Base excision repair	1	0.005319149	1.24E+07	POLE4	MUTYH, APEX2, POLD2, PARP1
4	hsa04064	NF-kappa B signaling pathway	10	0.050259176	1.26E+07	LY96	PRKCQ, CARD11, TICAM1, IKBKB, PARP1, UBE2I, CSNK2A2
5	hsa03040	Spliceosome	10	0.047745694	2.23E+07	SF3B6, LSM3, BUD31	SNRPB, SF3B2, U2AF2, PUF60, SNU13, DDX23, EIF4A3, HNRNPA1, PCBP1, SRSF8, SRSF5
6	hsa04714	Thermogenesis	10	0.044198222	2.54E+07	NDUFA1, NDUFB3, UQCRQ, COX6A1, COX7A2, COX7C	ADCY7, CREB1, KDM1A, SMARCA4, ACTG1, ACTB, ARID1A, MTOR
7	hsa03013	RNA transport	10	0.018411145	2.65E+07	NUP214	NUP62, NUP93, RANGAP1, UBE2I, SUMO3, GEMIN4, EIF2S3, EIF2B1, EIF4A3, RNPS1, SRRM1
8	hsa00190	Oxidative phosphorylation	10	0.017700501	3.41E+07	NDUFA1, NDUFB3, UQCRQ, COX6A1, COX7A2, COX7C, ATP6V1D, ATP6V0E1	ATP6V0E2
9	hsa05012	Parkinson disease	10	0.053731822	4.78E+07	DDIT3, NDUFA1, NDUFB3, UQCRQ, COX6A1, COX7A2, COX7C, TXN	UBE2G1, PSMD7, CALM3, CALM1,

							VDAC1, SLC25A5, TUBB
10	hsa05020	Prion disease	10	0.042219004	1.00E+08	DDIT3, NDUFA1, NDUFB3, UQCRQ, COX6A1, COX7A2, COX7C, NCF4	VDAC1, SLC25A5, PSMD7, CREB1, CSNK2A2, TUBB
11	hsa04932	Non-alcoholic fatty liver disease	10	0.011661907	1.74E+08	DDIT3, NDUFA1, NDUFB3, UQCRQ, COX6A1, COX7A2, COX7C	IKBKB, FASLG
12	hsa04659	Th17 cell differentiation	10	0.03468324	2.37E+08		MTOR, JAK1, HLA-DPA1, NFATC3, PRKCQ, IKBKB, GATA3, IL27RA, IL2RB
13	hsa03430	Mismatch repair	10	0.016474093	4.54E+08		MLH1, RPA1, POLD2
14	hsa04260	Cardiac muscle contraction	10	0.038864943	4.56E+08	UQCRQ, COX6A1, COX7A2, COX7C	ATP2A2
15	hsa04722	Neurotrophin signaling pathway	10	0.041410245	8.84E+08		SH2B3, CRKL, FASLG, CALM3, CALM1, ABL1, MAGED1, IRAK2, IKBKB
16	hsa05166	Human T-cell leukemia virus 1 infection	10	0.02312216	1.11E+09		TRRAP, NFATC3, IL2RB, JAK1, VDAC1, SLC25A5, ANAPC1, IKBKB, ZFP36, ADCY7, HLA-DPA1, SRF, ETS1, CREB1
17	hsa04630	JAK-STAT signaling pathway	10	0.0115943	1.71E+09		IL2RB, IL10RA, IL27RA, JAK1, PIAS3, MTOR
18	hsa05167	Kaposi sarcoma-associated herpesvirus infection	10	0.03458242	1.71E+09		TICAM1, JAK1, ZFP36, IKBKB, GNB1, MTOR, CALM3, CALM1, NFATC3, CREB1

19	hsa04931	Insulin resistance	10	0.01729121	3.24E+09		MTOR, IKBKB, PRKCQ, CREB1
20	hsa04530	Tight junction	10	0.018018181	3.95E+09	CLDN9, MYL6B, MYL6	ARHGAP17, SCRIB, TJAP1, SLC9A3R1, ACTG1, ACTB, ITGB1
21	hsa04210	Apoptosis	10	0.02312216	4.04E+09	DDIT3	FASLG, ACTG1, ACTB, PARP1, DFFB, IKBKB
22	hsa05163	Human cytomegalovirus infection	10	0.044265101	4.15E+09		MTOR, IKBKB, GNB1, CALM3, CALM1, NFATC3, ADCY7, JAK1, CREB1, CRKL, IL10RA, FASLG
23	hsa05203	Viral carcinogenesis	10	0.03468324	4.46E+09	GTF2B	CREB1, JAK1, SCRIB, RBL2, HDAC1, DNAJA3, SRF
24	hsa05130	Pathogenic Escherichia coli infection	10	0.067814611	9.98E+09	TLR5, GAPDH, CLDN9	ARF1, ACTG1, ACTB, SLC9A3R1, TUBB, ABL1, ITGB1, IKBKB, FASLG
25	hsa04971	Gastric acid secretion	10	0.029154767	0.00010279		ACTG1, ACTB, CALM3, CALM1, ADCY7
26	hsa05131	Shigellosis	10	0.053381459	0.000118195	HK3, TLR5, CBX3, RRAGD	ITGB1, CRKL, ACTG1, ACTB, PFN1, ARF1, VDAC1, IKBKB, PRKCQ, PIK3R4, MTOR, FNBP1
27	hsa05416	Viral myocarditis	10	0.011800334	0.000119758		ABL1, ACTG1, ACTB, HLA-DPA1
28	hsa04658	Th1 and Th2 cell differentiation	10	0.029154767	0.000122713		JAK1, RUNX3, HLA-DPA1, NFATC3, PRKCQ, IKBKB, IL2RB, GATA3

29	hsa04920	Adipocytokine signaling pathway	10	0.01739145	0.000124678		MTOR, IKBKB, PRKCQ
30	hsa05205	Proteoglycans in cancer	10	0.011800334	0.00012498	MMP9	ACTG1, ACTB, MTOR, FASLG, ITGB1
31	hsa04015	Rap1 signaling pathway	10	0.052174351	0.0001312		CALM3, CALM1, ADCY7, CRKL, LCP2, RALGDS, PFN1, EVL, ACTG1, ACTB, ITGB1
32	hsa05235	PD-L1 expression and PD-1 checkpoint pathway in cancer	10	0.040816673	0.000149123		MTOR, IKBKB, JAK1, NFATC3, TICAM1, CSNK2A2, PRKCQ
33	hsa04110	Cell cycle	10	0.011800334	0.000224586		RBL2, ABL1, HDAC1, CDKN1C, ANAPC1
34	hsa04613	Neutrophil extracellular trap formation	10	0.023188601	0.000422758	NCF4, CAMP	ACTG1, ACTB, VDAC1, SLC25A5, MTOR, HDAC1
35	hsa04140	Autophagy - animal	1	0.005235602	0.000439723	IGBP1, RRAGD	MTOR, PIK3R4, UVRAG, PRKCQ
36	hsa04670	Leukocyte transendothelial migration	10	0.011661907	0.000454983	CLDN9, NCF4, MMP9	ITGB1, ACTG1, ACTB
37	hsa05132	Salmonella infection	10	0.077684315	0.000473079	DYNLT1, STX10, TLR6, LY96, TLR5, GAPDH, TXN	DYNC1H1, TUBB, RAB9A, PFN1, ACTG1, ACTB, ARF1, IKBKB
38	hsa04150	mTOR signaling pathway	3	0.005319149	0.000506901	ATP6V1D, RRAGD	WDR59, MTOR, TELO2, LPIN1, IKBKB
39	hsa04660	T cell receptor signaling pathway	10	0.005830953	0.000650819		LCP2, NFATC3, PRKCQ, CARD11, IKBKB
40	hsa04919	Thyroid hormone signaling pathway	10	0.036036361	0.000665961		SIN3A, HDAC1, MED24, ATP2A2,

							MTOR, ACTG1, ACTB
41	hsa03010	Ribosome	9	0.005847953	0.000705762	MRPS18C, RPS24, MRPL33, RPL26, RPL31, RPL39	RPLP2
42	hsa00020	Citrate cycle (TCA cycle)	10	0.017910607	0.0007264		MDH2, PDHA1, PDHB
43	hsa05170	Human immunodeficiency virus 1 infection	10	0.023399015	0.000833352		CRKL, MTOR, CALM3, CALM1, NFATC3, GNB1, CFL1, IKBKB, FASLG
44	hsa05145	Toxoplasmosis	10	0.005830953	0.000983536	LY96	JAK1, HLA-DPA1, IKBKB, ITGB1, IL10RA
45	hsa05135	Yersinia infection	10	0.041775742	0.001030316		ITGB1, CRKL, ACTG1, ACTB, IKBKB, TICAM1, LCP2, NFATC3
46	hsa04218	Cellular senescence	6	0.005763737	0.001034472		RBL2, MTOR, ETS1, CALM3, CALM1, NFATC3, SLC25A5, VDAC1
47	hsa05418	Fluid shear stress and atherosclerosis	10	0.034785239	0.001124468	GSTO1, TXN, MMP9	CALM3, CALM1, KLF2, ACTG1, ACTB, IKBKB, SUMO3
48	hsa00630	Glyoxylate and dicarboxylate metabolism	2	0.00600606	0.001191188		MDH2, SHMT1
49	hsa05215	Prostate cancer	10	0.01487069	0.0011975	MMP9	CREB1, IKBKB, MTOR
50	hsa05100	Bacterial invasion of epithelial cells	10	0.041900492	0.00129969		CRKL, ACTG1, ACTB, ITGB1
51	hsa04922	Glucagon signaling pathway	10	0.023188601	0.001406923		CREB1, CALM3, CALM1, PDHA1, PDHB
52	hsa03050	Proteasome	10	0.011940405	0.001461399		PSMD7, PSMB10

53	hsa03460	Fanconi anemia pathway	10	0.005830953	0.001541354		TELO2, MLH1, RPA1
54	hsa03420	Nucleotide excision repair	10	0.005900167	0.001562648	GTF2H5, POLE4	XPC, RPA1, POLD2
55	hsa04921	Oxytocin signaling pathway	10	0.01749286	0.001566045	MYL6B, MYL6	EEF2K, EEF2, CALM3, CALM1, NFATC3, ACTG1, ACTB, ADCY7
56	hsa04066	HIF-1 signaling pathway	9	0.005847953	0.001770351	HK3, GAPDH	MTOR, PDHA1, PDHB
57	hsa04621	NOD-like receptor signaling pathway	10	0.011940405	0.002024689	CAMP, TXN	IKBKB, VDAC1, JAK1, TICAM1
58	hsa05164	Influenza A	10	0.01749286	0.002088154		IKBKB, TICAM1, JAK1, HLA-DPA1, FASLG, VDAC1, SLC25A5, ACTG1, ACTB
59	hsa04145	Phagosome	10	0.01749286	0.002110463	ATP6V1D, ATP6V0E1, TLR6, NCF4	ACTG1, ACTB, HLA-DPA1, ATP6V0E2, DYNC1H1, TUBB, ITGB1
60	hsa05110	Vibrio cholerae infection	10	0.005970202	0.002296185	ATP6V1D, ATP6V0E1	ATP6V0E2, PDIA4, ARF1, ACTG1, ACTB
61	hsa05225	Hepatocellular carcinoma	10	0.01734162	0.002453432	GSTO1	MTOR, ACTG1, ACTB, ARID1A, SMARCA4, BRD7
62	hsa05017	Spinocerebellar ataxia	9	0.006024096	0.002852214	GTF2B	VDAC1, SLC25A5, PSMD7, ATP2A2, MTOR, PIK3R4
63	hsa00620	Pyruvate metabolism	10	0.017910607	0.002873734		PDHA1, PDHB, ALDH9A1, MDH2
64	hsa05202	Transcriptional misregulation in cancer	10	0.005830953	0.003362108	MMP9, DDIT3	HDAC1, SIN3A, BCL11B, SLC45A3, EWSR1, IL2RB, TAF15, ASPSCR1
65	hsa03030	DNA replication	1	0.005319149	0.0033888	POLE4	RPA1, POLD2

66	hsa05171	Coronavirus disease - COVID-19	2	0.00610119	0.003642738	RPS24, RPL26, RPL31, RPL39	JAK1, RPLP2, IKBKB
67	hsa04728	Dopaminergic synapse	9	0.005813953	0.004068545	PPP2R3C	CALM3, CALM1, CREB1, GNB1, COMT
68	hsa04371	Apelin signaling pathway	9	0.00625	0.004317333		ADCY7, GNB1, CALM3, CALM1, MTOR, PIK3R4, KLF2
69	hsa04910	Insulin signaling pathway	10	0.011661907	0.00457716	HK3	CALM3, CALM1, CRKL, MTOR, IKBKB
70	hsa05412	Arrhythmogenic right ventricular cardiomyopathy	10	0.017700501	0.004664005		ITGB1, ACTG1, ACTB, ATP2A2
71	hsa04510	Focal adhesion	10	0.01749286	0.004690904		ITGB1, ACTG1, ACTB, CRKL
72	hsa05212	Pancreatic cancer	10	0.031664253	0.005815188		IKBKB, RALGDS, MTOR, JAK1
73	hsa03015	mRNA surveillance pathway	10	0.01201212	0.006961323	PPP2R3C	EIF4A3, RNPS1, SRRM1, WDR33, DAZAP1
74	hsa05133	Pertussis	10	0.011940405	0.007138967	LY96	ITGB1, CALM3, CALM1, CFL1, TICAM1, IRF1
75	hsa05410	Hypertrophic cardiomyopathy	10	0.017700501	0.007496811		ITGB1, ACTG1, ACTB, ATP2A2
76	hsa05169	Epstein-Barr virus infection	10	0.023600668	0.007987099		HLA-DPA1, IKBKB, JAK1, PSMD7, SIN3A, HDAC1, RUNX3
77	hsa04810	Regulation of actin cytoskeleton	10	0.01749286	0.008121293		ITGB1, CRKL, ACTG1, ACTB, PFN1, CFL1
78	hsa05214	Glioma	10	0.0115943	0.008309458		CALM3, CALM1, MTOR
79	hsa05220	Chronic myeloid leukemia	10	0.0289027	0.008646719		ABL1, CRKL, IKBKB, HDAC1

80	hsa05414	Dilated cardiomyopathy	10	0.017700501	0.009116295		ITGB1, ACTG1, ACTB, ADCY7, ATP2A2
81	hsa05031	Amphetamine addiction	9	0.011627907	0.009172326		CALM3, CALM1, CREB1, HDAC1
82	hsa05221	Acute myeloid leukemia	10	0.0115943	0.009855441		IKBKB, MTOR
83	hsa05417	Lipid and atherosclerosis	10	0.011661907	0.010206952	NCF4, MMP9, LY96, TLR6, DDIT3, ABCA1	IKBKB, TICAM1, NFATC3, CALM3, CALM1, FASLG
84	hsa04014	Ras signaling pathway	10	0.0115943	0.012413612		GNB1, CALM3, CALM1, RASA3, RASAL3, IKBKB, FASLG, ETS1, RALGDS, ABL1
85	hsa04012	ErbB signaling pathway	10	0.017910607	0.013477445		CRKL, ABL1, MTOR
86	hsa05230	Central carbon metabolism in cancer	10	0.0115943	0.014477071	HK3	PDHA1, PDHB, MTOR
87	hsa04668	TNF signaling pathway	10	0.011661907	0.014519694	BAG4, MMP9	IKBKB, CREB1, IRF1
88	hsa04662	B cell receptor signaling pathway	10	0.0115943	0.015549302		NFATC3, CARD11, IKBKB, CD81
89	hsa00670	One carbon pool by folate	6	0.005763737	0.01595238		SHMT1, ATIC
90	hsa05142	Chagas disease	2	0.005507974	0.017231694	TLR6	TICAM1, IKBKB, FASLG
91	hsa04068	FoxO signaling pathway	1	0.00625	0.017519445		IKBKB, RBL2, FASLG, KLF2, S1PR1
92	hsa04750	Inflammatory mediator regulation of TRP channels	10	0.005830953	0.017949678		CALM3, CALM1, ADCY7, PRKCH, PRKCQ
93	hsa04620	Toll-like receptor signaling pathway	2	0.005507974	0.018259257	TLR6, LY96, TLR5	IKBKB, TICAM1
94	hsa04657	IL-17 signaling pathway	9	0.005847953	0.021008208	S100A8, S100A9, MMP9	IKBKB

95	hsa04520	Adherens junction	9	0.005813953	0.021202609		ACTG1, ACTB, CSNK2A2
96	hsa04120	Ubiquitin mediated proteolysis	10	0.005830953	0.021446866	TRIP12	UBE2G1, UBE2I, HERC1, PIAS3, ANAPC1
97	hsa04390	Hippo signaling pathway	6	0.005830953	0.02855338		SCRIB, SMAD7, ACTG1, ACTB
98	hsa04625	C-type lectin receptor signaling pathway	9	0.005847953	0.028658156	CLEC4D	CALM3, CALM1, NFATC3, IKBKB, IRF1
99	hsa05160	Hepatitis C	10	0.005830953	0.030812107	CLDN9	CD81, TICAM1, IKBKB, JAK1, FASLG
100	hsa05034	Alcoholism	9	0.005847953	0.033083273		HDAC1, GNB1, CREB1, CALM3, CALM1
101	hsa00340	Histidine metabolism	10	0.005830953	0.03359145	HNMT	ALDH9A1, CNDP2
102	hsa05162	Measles	10	0.005830953	0.034539549		IKBKB, CSNK2A2, JAK1, RAB9A, FASLG, IL2RB
103	hsa04141	Protein processing in endoplasmic reticulum	9	0.005813953	0.034631511	CKAP4, DDIT3	DDOST, EDEM1, PDIA4, UBE2G1
104	hsa04611	Platelet activation	10	0.011661907	0.03550691		ADCY7, ACTG1, ACTB, ITGB1, LCP2, SNAP23
105	hsa04270	Vascular smooth muscle contraction	10	0.005830953	0.038158102	MYL6B, MYL6	CALM3, CALM1, PRKCH, PRKCQ, ADCY7
106	hsa04744	Phototransduction	8	0.008872126	0.039277632		GNB1, CALM3, CALM1
107	hsa04211	Longevity regulating pathway	9	0.005813953	0.040455414		ADCY7, CREB1, MTOR
108	hsa04350	TGF-beta signaling pathway	9	0.005813953	0.040455414		SMAD7, TGIF2
109	hsa05210	Colorectal cancer	2	0.005867575	0.041399736		RALGDS, MLH1, MTOR

110	hsa05161	Hepatitis B	10	0.005830953	0.04383446	MMP9	FASLG, IKBKB, NFATC3, JAK1, CREB1, TICAM1
111	hsa04710	Circadian rhythm	1	0.005319149	0.045169642		CRY1, BHLHE40, CREB1
112	hsa04136	Autophagy - other	10	0.005830953	0.048268333	IGBP1	MTOR, PIK3R4
113	hsa04713	Circadian entrainment	9	0.005813953	0.049092202		CALM3, CALM1, CREB1, GNB1, ADCY7